NUREG/CR-5498
BNL-NUREG-51713

TWO-DIMENSIONAL MODELING OF INTRA-SUBASSEMBLY HEAT TRANSFER AND BUOYANCY-INDUCED FLOW REDISTRIBUTION IN LMFBRs

Mohsen Khatib-Rahbar and Erik G. Cazzoli

Date Published — June 1984

CODE DEVELOPMENT, VALIDATION AND APPLICATION GROUP
DEPARTMENT OF NUCLEAR ENERGY, BROOKHAVEN NATIONAL LABORATORY
UPTON, LONG ISLAND, NEW YORK 11973

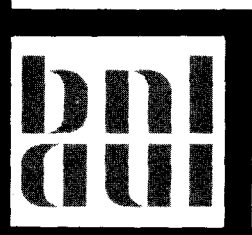

Prepared for the U.S. Nuclear Regulatory Commission
Office of Nuclear Regulatory Research
Contract No. DE-AC02-76CH00016

NUREG/CR--3498

TI85 003877

TWO-DIMENSIONAL MODELING OF INTRA-SUBASSEMBLY HEAT TRANSFER AND BUOYANCY-INDUCED FLOW REDISTRIBUTION IN LMFBRs

Mohsen Khatib-Rahbar and Erik G. Cazzoli

Manuscript Completed — May 1984
Date Published — June 1984

CODE DEVELOPMENT, VALIDATION AND APPLICATION GROUP
DEPARTMENT OF NUCLEAR ENERGY
BROOKHAVEN NATIONAL LABORATORY
UPTON, LONG ISLAND, NEW YORK 11973

PREPARED FOR
UNITED STATES NUCLEAR REGULATORY COMMISSION
WASHINGTON, D.C. 20555
UNDER CONTRACT NO. DE-AC02-76CH00016
NRC FIN NO. A-3015

Available from
GPO Sales Program
Division of Technical Information and Document Control
U.S. Nuclear Regulatory Commission
Washington, D.C. 20555
and
National Technical Information Service
Springfield, Virginia 22161

ABSTRACT

Phenomenological models and numerical techniques for prediction of coolant flow and temperature fields during forced, mixed, and free convection regimes of operation in LMFBR subassemblies are addressed. It is shown that, simplified integral solutions provide an excellent approach to assessing the importance of the intra-subassembly buoyancy induced flow redistribution, and the transverse thermal conduction and mixing effects on the assembly wide peak coolant temperatures. Furthermore, a more detailed steady-state and transient parabolic two-dimensional porous-body model, resulting in the TWIST computer code is developed. Comparison of calculated results and out-of-pile sodium and water test data indicate generally good agreement in cross-assembly temperature profiles. However, the impact of fuel pin distortion and bowing, caused by large transverse power gradients on transverse temperature distributions is found to be significant.

CONTENTS

LIST OF ILLUSTRATIONS

LIST OF TABLES

NOMENCLATURE

Symbol	Definition	Unit
A_d	Duct Wall Heat Transfer Area	m^2
A_p	Porous-Body Area	m^2
A_r	Rod Area	m^2
A_w	Wire Area	m^2
B_o, B_1, B_2	Flow Dependent Variables	-
c_p	Coolant Heat Capacity at Constant Pressure	J/kg·K
C_f	Flow Regime Dependent Constant	-
D_e	Hydraulic Equivalent Diameter	m
D_r	Rod Diameter	m
D_w	Wire Diameter	m
f	Friction Factor	-
F	Nuclear Peak to Average Factor	-
g	Gravitational Acceleration	m/s^2
G	Mass Flux	kg/m^2-s
Gr	Temperature Rise Grashof Number	-
k	Thermal Conductivity	W/m·K
ℓ	Assembly Flat-to-Flat Distance	m
L_h	Rod Heated Length	m
$\overline{L}$	Dimensionless Assembly Length	-
M	Total Number of Axial Nodes	-
M_d	Mass of Duct Wall	kg
M_s	Mass of Interstitial Coolant	kg

Symbol	Definition	Unit
n	Exponent in the Friction Factor Equation	-
N	Total Number of Transverse Nodes	-
p	Rod Pitch	m
P	Pressure	N/m^2
$\overline{P}$	Dimensionless Pressure	-
$\tilde{P}$	Modified Pressure	$N/m^2/kg/m^2$
Pe	Peclet Number (PrRe)	-
Pr	Fluid Prandtl Number	-
Q'''	Volumetric Heat Generation Rate	W/m^3
$\hat{Q}'''$	Average Volumetric Heat Generation Rate	W/m^3
Re	Flow Reynolds Number	-
Ri	Richardson Number (Gr/Re^2)	-
s	Even Number of Subdivisions	-
T	Temperature	k
$\hat{T}$	Average Temperature	k
T*	Reference Inlet Temperature	k
u	Superficial Velocity in the x-Direction	m/s
$\hat{u}$	Superficial Average Velocity in the x-Direction	m/s
U	Dimensionless Velocity in the x-Direction	-
v	Superficial Velocity in the y-Direction	m/s
V	Dimensional Velocity in the y-Direction	-
w	Superficial Velocity in the z-Direction	m/s
W	Weight Factor	-
x	Axial Position	m
X	Dimensionless Axial Direction	-

Symbol	Definition	Unit
y	Transverse Position	m
Y	Dimensionless Transverse Position	-
Y_u	Velocity Shape Factor	-
Y_L	Velocity Shape Factor for Laminar Flow	-

GREEK SYMBOLS

Symbol	Definition	Unit
α_i	Fraction of the Area A_p that is Occupied by Region i of the Rod Bundle	-
α^*	Temperature Peaking Factor	-
α_e	Equivalent Thermal Diffusivity	m^2/s
β	Volumetric Thermal Expansion Coefficient	K-1
δ	Thermal Penetration Distance	m
δ_d	Duct Wall Thickness	m
ε^*	Mixing Parameter	-
ε^*_∞	Maximum Value of ε^*	-
ε_h	Eddy Diffusivity of Heat	m^2/s
η^*	Temperature Rise Hot Channel Factor	-
θ	Dimensionless Temperature	-
κ	Conductivity Shape Factor	-
λ_i	Porosity for Region i	-
λ_a	Bundle Average Porosity	-
μ	Fluid Dynamic Viscosity	Ns/m^2
ν	Fluid Kinematic Viscosity (μ/ρ)	m^2/s
ξ	Dimensionless Axial Distance	-
ρ	Fluid Density	kg/m^3
ψ	Temperature Shape Factor	-
ψ	Flow Intermittency Factor (Table I)	-

SUPERSCRIPT

*	Reference Inlet Condition
k	Previous Time Value
k+1	Current Time Value
^	Average Value

ACKNOWLEDGMENTS

The authors wish to extend their appreciation to many individuals that have been very helpful throughout this project. In particular, they wish to acknowledge the help of I. K. Madni (UPM), W. C. Horak and B. C. Chan, who gave valuable technical advice; R. A. Markley and F. C. Engel of Westinghouse Engineering and Advanced Energy System Division for their help in understanding their experiments; F. Namekawa of Toshiba Nuclear Engineering Laboratory for providing the water test data; J. G. Guppy and R. J. Cerbone for reviewing the manuscript, and Mrs. C. Falkenbach for her excellent typing of the many versions of this manuscript.

Thanks are also due to Akira Watanabe and Nobuo Tanaka of the Power Nuclear and Fuel Development Corporation (PNC) of Japan for their continuing interest in this work and to PNC for providing partial support of this project.

The work reported herein, was also supported in part by the Division of Accident Evaluation, United States Nuclear Regulatory Commission.

1. INTRODUCTION

The liquid metal fast breeder reactor (LMFBR) core consists of fuel, blanket, control and shielding assemblies packed in a hexagonal configuration. The purpose of the blanket assemblies is to increase the conversion of fertile to fissile material by utilizing the neutron leakage from the fuel assemblies. For efficient breeding, a high volume fraction of the fertile material is required.

The fuel and blanket assemblies consist of cylindrical fuel elements enclosed by stainless steel cladding, arranged in a triangular pitch contained in a hexagonal duct. To minimize hot spots and provide adequate cooling, the rods are separated by spacer wires wound helically around each rod. Radial blanket assemblies occupy peripheral locations in the reactor core, and are characterized by steep power gradients; while inner blanket assemblies are located within the fuel assembly region and have higher power levels, but flatter distributions.

It is due to the presence of this radial power gradient that large sodium temperature distributions exist at full power, full flow conditions. However, at low power, low flow natural convection conditions significant heat and flow redistribution take place leading to considerable radial temperature flattening.

The prediction of assembly flow and temperature distributions must consider a wide range of coolant flow and thermal convection regimes which include laminar, transition and turbulent flow [1] during natural, mixed and forced convection conditions of reactor operation.

Analytical studies of heat transfer in rod bundles have been pursued along two separate paths - distributed parameters and lumped parameter methods [2]. In lumped parameter methods, often referred to as subchannel analyses, the rod bundle is divided into a number of subchannels whose boundaries are defined arbitrarily by surfaces of fuel elements and imaginary lines between elements and/or duct walls. Average subchannel parameters are evaluated by solving equations of continuity, momentum, and energy for each subchannel increment. Equations for each subchannel are coupled with those of its neighbors by interchannel transport of mass, momentum and energy which is treated in terms of integral transport coefficients.

Distributed parameter methods solve time-averaged Reynolds equations of momentum and energy transport for velocity and temperature distributions. These methods provide detailed information about thermal characteristics of an idealized array of fuel elements cooled by parallel flow, but have fallen short of providing overall power distribution and thermal behavior of entire fuel assemblies with spacers. Because of numerical and computer complications, as well as the lack of knowledge of local Reynolds shear stresses and turbulent heat fluxes in various directions, the application of distributed parameter methods has been rather restricted. Results of the distributed parameter method can be used to evaluate integral parameters to feed into lumped parameter analysis.

A number of models and computer codes have been developed [2-8]. These models are either limited to steady-state conditions, or are highly complex, thus requiring extensive computer storage and simulation time.

The purpose of the present study is to formulate simple, physically accurate and numerically efficient models supported by experimental data for the study of forced, mixed and natural convection flows through rod bundles using the two-dimensional porous-body approach.

Chapter 2 describes the steady-state two-dimensional porous body equations, related parameters and the governing dimensionless forms. In Chapter 3, approximate integral solutions applicable to the two limiting cases of (1) flow redistribution only; and (2) heat redistribution only are developed and discussed. A finite difference marching technique is developed for the steady-state flows in Chapter 4. The calculated results are then compared with the recent experimental data for sodium and water tests. In Chapter 5 the finite difference formulation is further extended to include transient flows; and the calculated results are also compared with transient sodium data. Finally, important results of this investigation, together with areas of future development are discussed in Chapter 6.

The computer codes and the user's guides are presented in the appendices.

2. STEADY-STATE POROUS-BODY MODEL

2.1 Governing Equations

In the porous-body treatment, the presence of fuel rods is taken into account by inclusion of a volume porosity in the governing equations. The energy generation by the rods is modeled by a continuous volumetric heat source distribution. The energy transfer in the transverse direction is modeled by molecular conduction and an empirically determined effective eddy diffusivity.

A strip section of a rod bundle is shown in Fig. 1. For simplicity, the rod bundle will be approximated by a porous slab of width ℓ and height L_h corresponding to the assembly flat-to-flat and the rod heated length, respectively.

For the simulated channel described above, the following assumptions apply:

(1) steady, two-dimensional flow,
(2) negligible axial conduction,
(3) negligible viscous dissipation, and
(4) uniform pressure at any axial level.

Therefore, the conservation of mass, energy and momentum equations can be written as follows:

a. Conservation of Mass:

The mass continuity requires,

$$\frac{\partial(\rho u)}{\partial x} + \frac{\partial(\rho v)}{\partial y} = 0, \qquad (1)$$

where ρ is the fluid density, u is the superficial velocity in the longitudinal direction and v is the superficial velocity in the transverse direction.

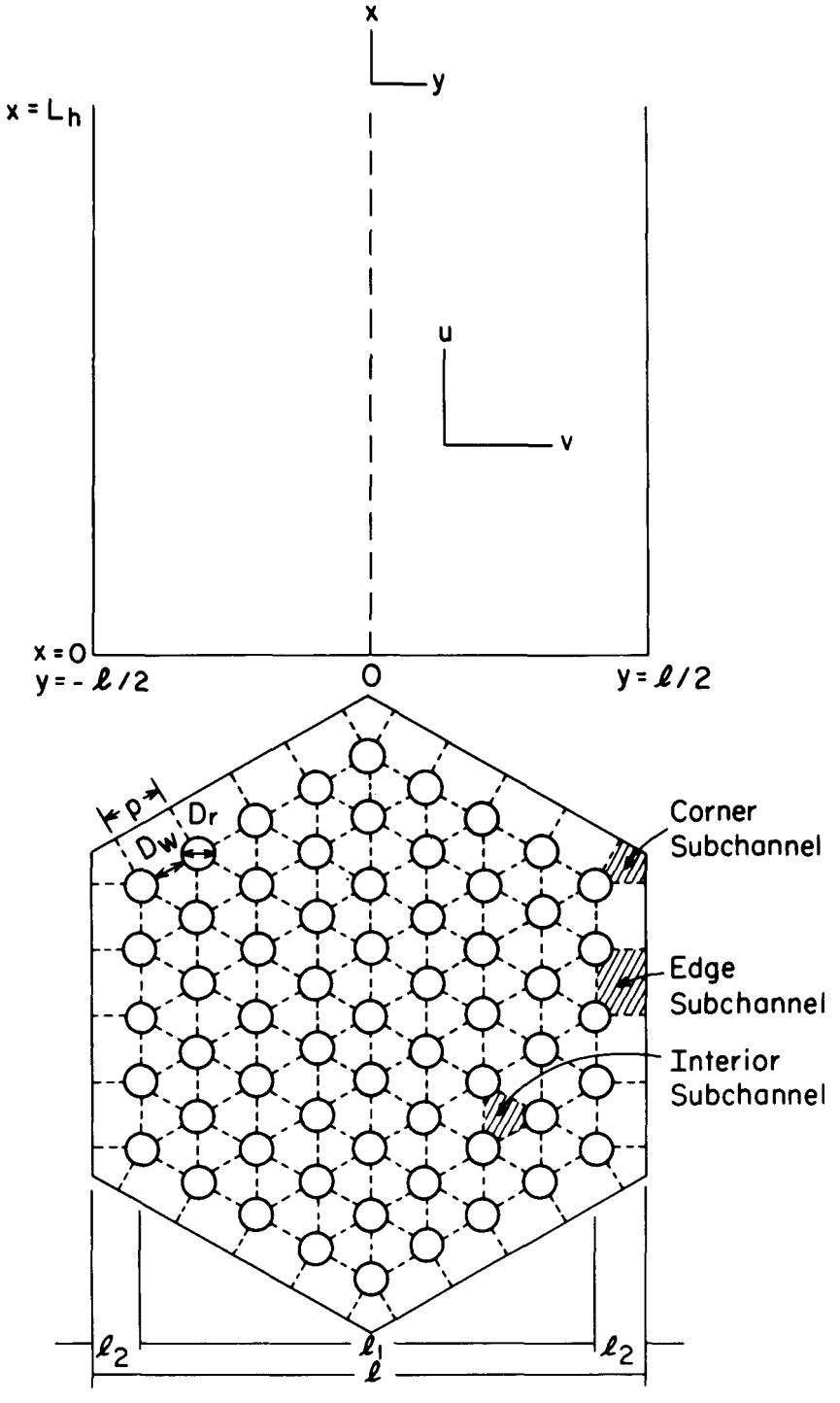

Fig. 1 Schematic of a Typical Rod Bundle and the 2-D Computational Domain

b. Conservation of Energy:

The conservation of energy requires,

$$\rho c_p \left(\frac{\partial(uT)}{\partial x} + \frac{\partial(vT)}{\partial y}\right) = \frac{\partial}{\partial y}\left(k_e \frac{\partial T}{\partial y}\right) + Q'''(x,y) \tag{2}$$

where c_p is the specific heat of sodium at constant pressure, T is the fluid temperature, Q''' is the volumetric heat generation rate and k_e is the effective thermal conductivity defined as:

$$k_e = \rho c_p \varepsilon_h + \kappa k \tag{3}$$

where the eddy diffusivity of heat, ε_h (m^2/s) is defined by;

$$\varepsilon_h = \hat{u} D_e \varepsilon^* \tag{4}$$

Here, ε^* is the mixing parameter empirically determined.

The shape factor κ (also known as tortuosity) for molecular conductivity k is to account for the reduction in thermal conduction due to the presence of the fuel rods inside the sodium and is assumed to be given by* [9];

$$\kappa = \frac{\lambda_a}{1 + 0.5\,(1 - \lambda_a)} \tag{5}$$

c. Conservation of Axial Momentum:

The axial momentum is conserved according to

$$u \frac{\partial u}{\partial x} + v \frac{\partial u}{\partial y} = - \frac{1}{\rho} \frac{dP}{dx} - g \frac{\rho^*}{\rho} [1 - \beta(T-T^*)] + \nu \frac{\partial^2 u}{\partial y^2} - \frac{f}{2D_e \lambda^2} u^2 \tag{6}$$

---

*Eq. (5) is only applicable to liquid metal systems (see discussions in 4.3.2)

where P is the pressure, T* is the reference temperature, ρ^* is the density evaluated at T*, ν is the kinematic viscosity, g is the gravitational acceleration, β is the volumetric thermal expansion coefficient, D_e is the hydraulic equivalent diameter, λ is the axial area fraction occupied by the coolant, and f is the skin friction factor.

The transverse momentum equation need not be formulated, since the pressure is assumed to be uniform in the transverse direction at any axial level.

2.2 Porous-Body Parameters

Figure 1 also shows the schematics of a rod bundle, with the porous-body parameters defined [9] as:

$$A_p = \frac{\sqrt{3}}{2} \ell^2 \tag{7}$$

$$\alpha_1 = (\ell_1/\ell)^2 \tag{8a}$$

$$\alpha_2 = (4\ell_1 \ell_2/\ell^2) \tag{8b}$$

$$\alpha_3 = 4(\ell_2/\ell)^2 \tag{8c}$$

and thus, the axial area fraction occupied by the coolant in any region of the bundle can be defined by:

$$\lambda_1 = 1 - \left[\frac{2}{\sqrt{3}} \frac{A_r + A_w}{p^2}\right] \tag{9a}$$

$$\lambda_2 = 1 - \left[\frac{A_r + A_w}{2\, p\ell_2}\right] \tag{9b}$$

$$\lambda_3 = 1 - \left[\frac{1}{2\sqrt{3}} \frac{A_r + A_w}{\ell_2^2}\right] \tag{9c}$$

Thus,

$$\lambda_a = \sum_{i=1}^{3} (\alpha_i \lambda_i) \tag{10}$$

The hydraulic equivalent diameter in any region of the bundle is also defined by:

$$D_{e_1} = \left[\frac{\frac{2\sqrt{3}}{\pi} p^2 - (D_r^2 + D_w^2)}{(D_r + D_w)} \right] \tag{11a}$$

$$D_{e_2} = \left[\frac{\frac{8p}{\pi} \ell_2 - (D_r^2 + D_w^2)}{(D_r + D_w)} \right] \tag{11b}$$

$$D_{e_3} = \left[\frac{\frac{8\sqrt{3}}{\pi} \ell_2^2 - (D_r^2 + D_w^2)}{(D_r + 3D_w)} \right] \tag{11c}$$

and

$$p = D_r + D_w \tag{12}$$

where D_r is the rod outer diameter, and D_w is the diameter of the wire-wrap. Therefore, the cross-sectional area of the rod and wire can be calculated using,

$$A_r = \pi \left(\frac{D_r}{2} \right)^2 \tag{13}$$

and

$$A_w = \pi \left(\frac{D_w}{2} \right)^2 \tag{14}$$

The friction factor f is some function of the flow Reynolds number;

$$f = f(Re) \tag{15}$$

and the Reynolds number is defined as:

$$Re = \frac{\rho\, u\, D_e}{\lambda\, \mu} \tag{16}$$

2.3 Dimensionless Forms

The conservation of mass, energy and axial momentum equations (Eqs. (1), (2) and (6)) can be transformed into a dimensionless form for constant property fluids, using the following substitutions:

$$\begin{aligned}
X &= \frac{x}{D_e} \\
Y &= \frac{y}{D_e} \\
U &= \frac{u}{\hat{u}} \\
V &= \frac{v}{\hat{u}} \\
\overline{P} &= \frac{p + g\rho^* x}{\frac{\rho^* \hat{u}^2}{\lambda^2}} \\
\theta &= \frac{T(x,y) - T^*}{\hat{T}(L_h) - T^*} \\
Re^* &= \frac{\rho^* \hat{u} D_e}{\lambda \mu^*} \\
Pr^* &= \frac{\mu^* c_p^*}{k_e^*} \\
Gr^* &= \frac{g\, \beta\, \rho^{*2}\, (\hat{T} - T^*)\, D_e^3}{\mu^{*2}}
\end{aligned} \tag{17}$$

Therefore,

$$\frac{\partial U}{\partial X} + \frac{\partial V}{\partial Y} = 0 \tag{18}$$

$$\lambda \overset{*}{Pr}\,\overset{*}{Re}\,(U\frac{\partial \theta}{\partial X} + V\frac{\partial \theta}{\partial Y}) = \frac{\partial^2 \theta}{\partial Y^2} + \frac{D_e^2 Q'''}{k_e(\hat{T} - T^*)} \tag{19}$$

and,

$$U\frac{\partial U}{\partial X} + V\frac{\partial U}{\partial Y} = -\frac{\partial \bar{P}}{\partial X} + \frac{\overset{*}{Gr}}{\overset{*2}{Re}}\theta + \frac{\lambda}{\overset{*}{Re}}\frac{\partial^2 U}{\partial Y^2} - \frac{f}{2}U^2 \tag{20}$$

alternatively,

$$\overset{*}{Ri} = \overset{*}{Gr}/\overset{*2}{Re} \tag{21}$$

where, in arriving at Equation (19), the mass continuity equation was added to the energy equation.

Equations (19) and (20) illustrate that the temperature and velocity fields in the subassembly are dependent on the magnitude of flow Reynolds number, the assembly modified Grashof number and the fluid Prandtl number. They also demonstrate, at high Reynolds number forced convection conditions the frictional forces dominate; however, at low Reynolds number conditions the buoyancy effects become increasingly significant.

3. APPROXIMATE INTEGRAL SOLUTIONS

In this chapter, approximate integral solutions to the conservation equations are developed for two limiting cases; namely, (a) buoyancy-induced flow redistribution in the absence of transverse thermal conduction; and (b) transverse thermal conduction in the absence of flow redistribution.

3.1 Buoyancy-Induced Flow Redistribution

3.1.1 Model Equations

The conservation of mass, energy and momentum equations (Eqs. (1), (2) and (3)) can be simplified assuming:

(1) negligible transverse thermal conduction,

(2) negligible momentum flux terms, and

(3) constant properties.

Thus:

$$\frac{\partial u}{\partial x} + \frac{\partial v}{\partial y} = 0, \tag{22}$$

$$\overset{*}{\rho} c_p^* \left(u \frac{\partial T}{\partial x} + v \frac{\partial T}{\partial y}\right) = Q''' \tag{23}$$

and

$$-\frac{dP}{dx} = \frac{\overset{*}{\rho} f}{2 D_e \lambda_a^2} u^2 + g\rho^* \left[1 - \beta (T - T^*)\right] \tag{24}$$

The solution procedure is an adaptation of the approximate integral solution proposed by Meyer [10].

Equations (22) through (24) must be solved over the slab assembly subject to the conditions:

(a) Inlet Temperature, given as,

$$T(o,y) = T^* \tag{25}$$

(b) Total Flow, the average velocity is a specified value and defined by:

$$\hat{u} = \frac{1}{\ell} \int_{-\ell/2}^{\ell/2} u(x,y)dx \tag{26}$$

(c) Assembly Edge Condition, given by,

$$v\ (x, \pm\ \ell/2) = 0 \tag{27}$$

and,

(d) Transverse Power Generation, is given by a linear distribution of the form:

$$Q'''\ (x,y) = \hat{Q}'''\ (x)\ \left[1 + (F-1)(\frac{2y}{\ell})\right] \tag{28}$$

where F is the nuclear heat input factor, and $\hat{Q}'''$ (x) is the average radial power distribution at a given axial location.

The friction factor can be represented by the Darcy-Weisbach relation of the form:

$$f = C_f\ R_e^{-n} \tag{29}$$

where C_f and n are flow dependent parameters.

Now, let us consider an axial velocity distribution which is linear in

the transverse direction at each axial position. That is,

$$u(x,y) = \hat{u} \left[1 + \left(\frac{2y}{\ell}\right) Y_u(x)\right] \tag{30}$$

where Y_u is the velocity shape factor, and as yet an unknown function of x.

Differentiate Eq. (24) with respect to y to obtain:

$$\frac{\partial T}{\partial y} = \frac{C_f \lambda_a^{n-2} \overset{*}{\mu}^n}{g\beta D_e^{1+n} \overset{*}{\rho}^n} \left(1 - \frac{n}{2}\right) u^{1-n} \frac{\partial u}{\partial y} \tag{31}$$

and using Eq. (30) to find:

$$\frac{\partial T}{\partial y} = \frac{2B_o}{\ell} Y_u(x) \; u^{1-n} \tag{32}$$

where,

$$B_o = \frac{C_f \lambda_a^{n-2} \overset{*}{\mu}^n}{g\beta D_e^{1+n} \overset{*}{\rho}^n} \left(1 - \frac{n}{2}\right) \hat{u} \tag{33}$$

is the flow regime-dependent constant.

Integrate Eq. (32) over the y-direction to obtain:

$$T(x,y) = T_c(x) + \frac{B_o \hat{u}^{1-n}}{(2-n)} \left\{\left[1 + \frac{2y}{\ell} \; Y_u(x)\right]^{2-n} - 1\right\} \tag{34}$$

where $T_c(x)$ is the coolant temperature at the center of the assembly (y=0), and is a function of axial position x only.

Now, substitute Eq. (30) back into the continuity equation (Eq. (22)) and integrate the results with respect to y, and evaluate the constant of integration by the edge condition of Eq. (27), to obtain:

$$v = \left(\frac{\ell}{4}\right) \hat{u} \frac{dY_u}{dx} \left[1 - \left(\frac{2y}{\ell}\right)^2\right] \tag{35}$$

Therefore, equations (32), (34) and (35) can be used to evaluate.

$$u \frac{\partial T}{\partial y} = \frac{1}{2} B_o \hat{u}^{2-n} Y_u \frac{dY_u}{dx} \left[1 + \left(\frac{2y}{\ell}\right) Y_u\right]^{1-n} \left[1 - \left(\frac{2y}{\ell}\right)^2\right] \tag{36}$$

$$u \frac{\partial T}{\partial x} = \hat{u} \left[1 + \left(\frac{2y}{\ell}\right) Y_u\right] \frac{dT_c}{dx} + B_o \hat{u}^{2-n} \frac{dY_u}{dx} \left[1 + \left(\frac{2y}{\ell}\right) Y_u\right]^{2-n} \left(\frac{2y}{\ell}\right) \tag{36b}$$

Equations (32), (34), (35) and (36) provide a complete description of the velocity and temperature fields within the assembly if $T_c(x)$ and $Y_u(x)$ can be determined. This solution is achieved by defining two weight functions, $W_1(y)$ and $W_2(y)$ [10,11], multiplying the energy equation (Eq. (23)) by each and integrating each resulting equation with respect to y across the assembly.

Choose the weight functions such that,

$$W_1(y) = 1 \qquad -\ell/2 \leq y \leq \ell/2 \tag{37a}$$

and

$$W_2(y) = \begin{cases} -1 & -\ell/2 \leq y < 0 \\ +1 & 0 \leq y \leq \ell/2 \end{cases} \tag{37b}$$

Therefore,

$$\rho^* c_p^* \int_{-\ell/2}^{+\ell/2} \left(u \frac{\partial T}{\partial x} + v \frac{\partial T}{\partial y}\right) dy = \int_{-\ell/2}^{+\ell/2} Q'''(x,y) dy \tag{38}$$

and,

$$\overset{*}{\rho}c_p^* \left[- \int_{-\ell/2}^{0} \left(u \frac{\partial T}{\partial x} + v \frac{\partial T}{\partial y}\right) dy + \int_{0}^{+\ell/2} \left(u \frac{\partial T}{\partial x} + v \frac{\partial T}{\partial y}\right) dy \right] \tag{39}$$

$$= - \int_{-\ell/2}^{0} Q^{III}(x,y)\, dy + \int_{0}^{+\ell/2} Q^{III}(x,y)\, dy$$

Thus, integrating Equations (38) and (39); and after simplifications one obtains:

$$\frac{dY_u}{dx} = \left(\frac{\hat{Q}^{III}(x)}{\overset{*}{\rho}c_p^* \hat{u}}\right)\left(\frac{1}{B_0 B_1 \hat{u}^{1-n}}\right)\left(1 - \frac{F-1}{Y_u}\right) \tag{40}$$

and

$$\frac{dT_c}{dx} = \frac{\hat{Q}^{III}(x)}{\overset{*}{\rho}c_p^* \hat{u}} - B_0 B_2 \hat{u}^{1-n} \frac{dY_u}{dx} \tag{41}$$

where,

$$B_1 = \left[\frac{(1+Y_u)^{2-n} - (1-Y_u)^{2-n}}{4(2-n)}\right] + \frac{1}{4Y_u^2}\left[\frac{(1+Y_u)^{4-n} - (1-Y_u)^{4-n}}{(4-n)} - \frac{(1+Y_u)^{2-n} - (1-Y_u)^{2-n}}{(2-n)}\right] + \left(\frac{1}{Y_u^3} - \frac{1}{Y_u}\right)\left[\frac{(1+Y_u)^{2-n} + (1-Y_u)^{2-n} - 2}{2(2-n)}\right] - \left[\frac{(1+Y_u)^{4-n} + (1-Y_u)^{4-n} - 2}{2Y_u^3(4-n)}\right] \tag{42}$$

and

$$B_2 = \left[\frac{(1+Y_u)^{2-n} - (1-Y_u)^{2-n}}{4(2-n)}\right] + \frac{1}{4Y_u^2}\left[\frac{(1+Y_u)^{4-n} - (1-Y_u)^{4-n}}{(4-n)} - \frac{(1+Y_u)^{2-n} - (1-Y_u)^{2-n}}{(2-n)}\right] \tag{43}$$

For laminar flow (n=1), Equations (40) through (43) reduce to the form derived by Meyer [10] that is:

$$\frac{dY_u}{d\xi} = \frac{(F-1) - Y_u}{1 - \frac{2}{3} Y_u^2} \tag{44}$$

and

$$\frac{dT_c}{d\xi} = B_o \left[1 - \frac{Y_u^2 - (F-1)\, Y_u}{Y_u^2 - \frac{3}{2}} \right] \tag{45}$$

where the dimensionless axial distance ξ is defined as,

$$\xi = \frac{\hat{Q}''' x}{B_o \overset{*}{\rho} c \overset{*}{p} \hat{u}} \tag{46}$$

Note that

$$Y_u = 0 \quad \text{at} \quad \xi = 0 \tag{47}$$

and reaches Y_L at the assembly exit, which corresponds to $\xi = \xi_L$, where

$$\xi_L = \frac{\hat{Q}''' L_h}{B_o \overset{*}{\rho} c \overset{*}{p} \hat{u}} \tag{48}$$

Let the average temperature rise in the assembly be $\Delta\hat{T}$, where

$$\Delta\hat{T} = \hat{T} - T^* = \frac{\hat{Q}''' L_h}{\overset{*}{\rho} c \overset{*}{p} \hat{u}} \tag{49}$$

Defining a Grashof number based on this temperature rise by:

$$\overset{*}{Gr} = g\beta D_e^3 \Delta\hat{T} / \overset{*}{\nu}^2 \tag{50}$$

Combining Equations (16), (48), (49) and (50) one obtains:

$$\xi_L = \frac{2}{C_f} \frac{\overset{*}{Gr}}{\overset{*}{Re}} \tag{51}$$

The temperature peaking factor is given by:

$$\alpha^* = (T(L_h, -\ell/2) - T^*)/\Delta\hat{T} \tag{52}$$

The temperature rise hot channel factor is then defined as the fractional reduction in F caused by buoyancy-induced flow redistribution. That is,

$$\eta^* = \frac{\alpha^* - 1}{F - 1} \tag{53}$$

Thus, for laminar flow, a convenient form for η^* can be obtained [10] as:

$$\eta^*_{Laminar} = \frac{Y_L - \frac{1}{3} Y_L^2}{\xi_L (F - 1)} \tag{54}$$

which, in a limit as Y_L approaches $(F - 1)$, becomes:

$$\eta^*_{Laminar} \sim \frac{1 - \frac{1}{3}(F - 1)}{\xi_L} \tag{55}$$

Equations (48) through (55) show that the hot channel factor depends not only on Reynolds number, but also on the average temperature rise (namely, $\overset{*}{Gr}$) and the flow regime characteristics.

Equations (40) and (41), together with appropriate flow-dependent parameters, can be integrated numerically to obtain a complete characteristic of the temperature, and flow field as a function of the radial power factor F, at various average power and flow conditions in the bundle, resulting in the FREDIS code described in Appendix A.

3.1.2 Results

In this section, the influence of the bundle friction factor on the flow redistribution is examined. The model described in the previous sections is then used to investigate the transverse temperature flattening effects due to thermal buoyancy-induced intra-assembly flow redistribution caused by radial power gradients in the Westinghouse Blanket Test Model and the results are compared to the experimental measurements.

3.1.2.1 Influence of the Friction Factor

Because of the importance of the friction factor defined in Eq. (29) previously, we will examine its influence on flow redistribution in this subsection. Table I lists some typical friction factor correlations for both fuel and blanket wire-wrapped assemblies. It is seen that the friction factor is inversely proportional to the Reynolds number in the laminar flow regime, and behaves like the Blasius approximation in the turbulent flow regime, while it is usually interpolated in the transition regime.

Figures 2 and 3 illustrate the influence of the friction factor on flow redistribution for a typical fuel and blanket assembly, respectively. It is clearly evident that a reduction in the frictional drag leads to a significantly enhanced redistribution towards the warmer side of the bundle, and thus, lower peak temperatures. Furthermore, in the transition from laminar to turbulent regime, discontinuities may occur.

In the present study, for conservatism, in the transition flow regime the friction factor is evaluated based on the turbulent flow conditions.

3.1.2.2 Comparison with Experimental Measurements

The Westinghouse Blanket Test section shown schematically in Fig. 4 is a one-to-one scale model of a typical LMFBR 61-pin blanket assembly. The power level, axial and radial power distributions of the assembly are simulated using electrically heated fuel rod simulators.

Table I Friction Factor Parameters for Fuel and Blanket Assemblies

Assembly	Flow Regime	n	C_f	Reference
Fuel	Laminar	1	84	Spencer, [17]
	Transition & Turbulent	-	$f = (1.078 + 0.3 \times 10^6/Re^2)\ f_c$ $1/f_c = -2 \log [2.51/Re\ f_c]$	Spencer, [17]
	Turbulent	0.25	$0.316 \left[\frac{1.034}{(P/D)^{0.124}} + \frac{29.7(P/D)^{6.94}\ Re^{0.086}}{(H/D)^{2.239}} \right]^{0.885}$	Novendstern, [18]
Blanket	Laminar	1	110	Engel, [19]
	Transition	0	$\frac{110}{Re} \sqrt{1-\psi} + \frac{0.48}{Re^{25}} \sqrt{\psi}$; $\psi = \frac{Re - 400}{4600}$	Engle, [19]
	Turbulent	0.25	0.48	Engel, [19]

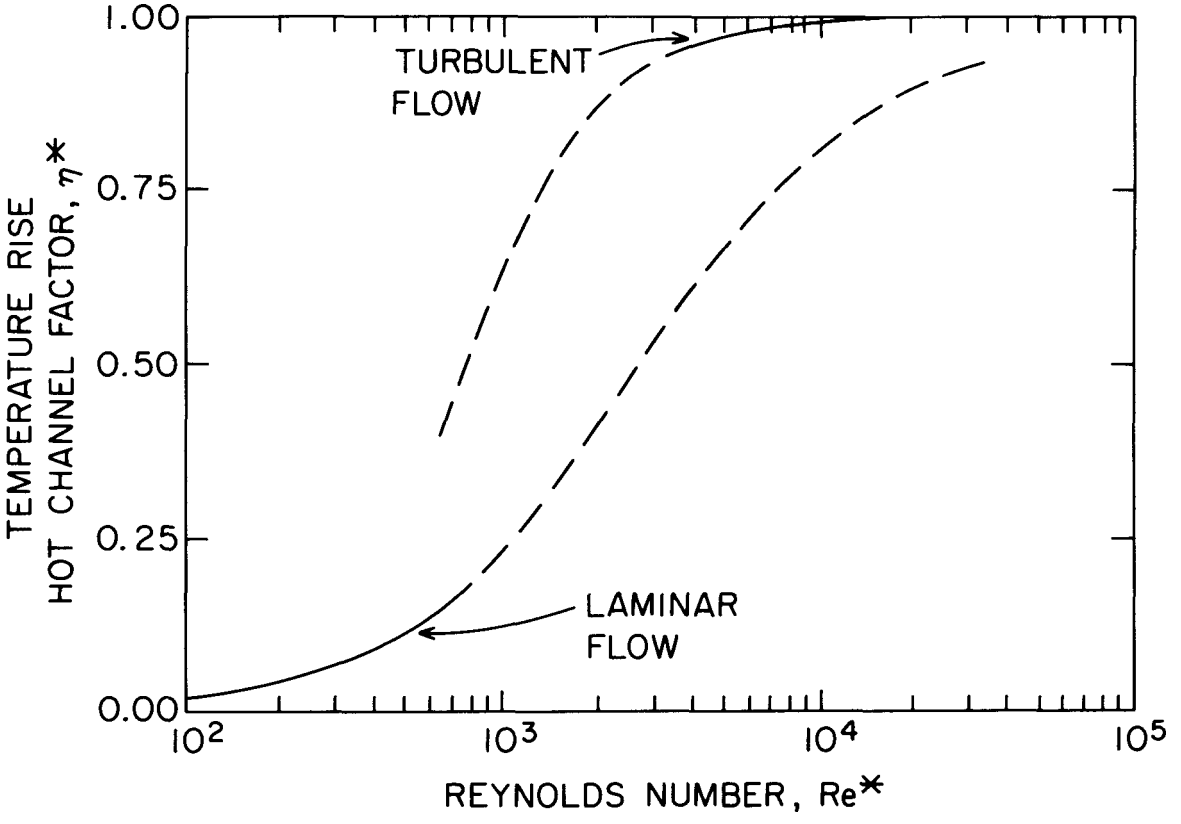

Fig. 2 Impact of Flow Regime on Calculated Fuel Assembly Temperature Rise Hot Channel Factor

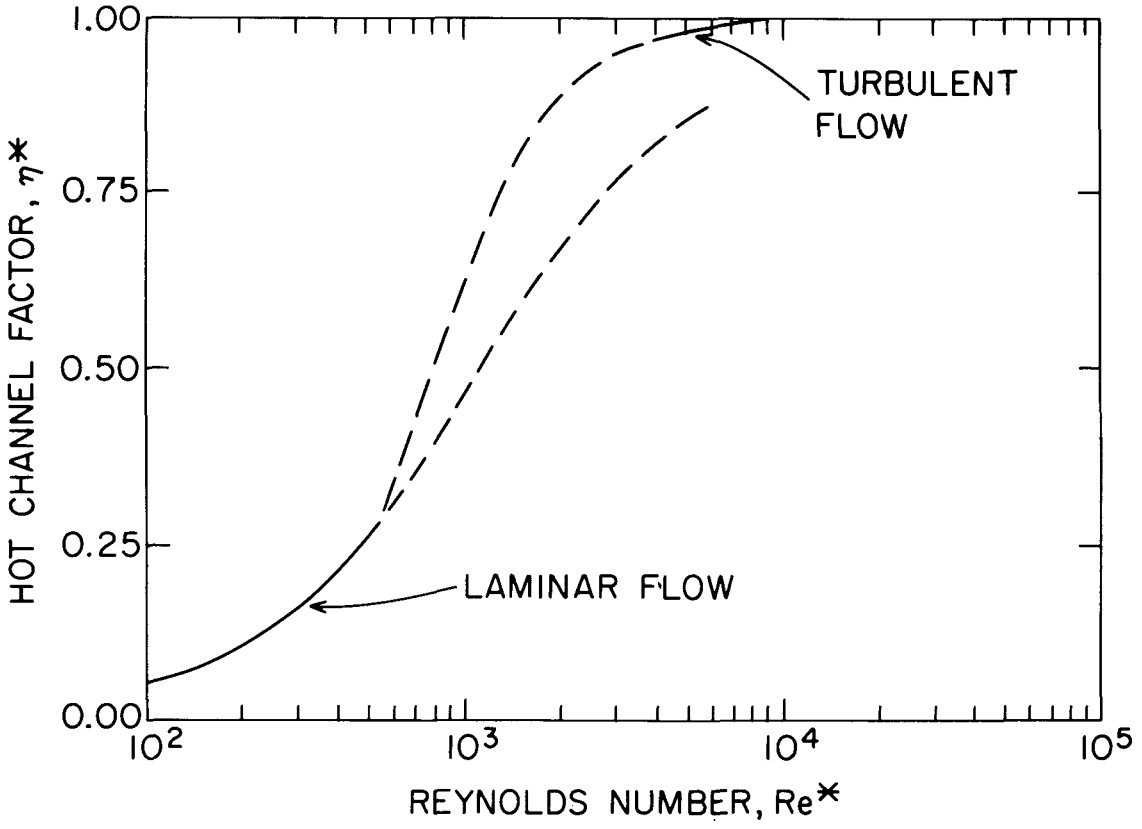

Fig. 3 Impact of Flow Regime on Calculated Blanket Assembly Temperature Rise Hot Channel Factor

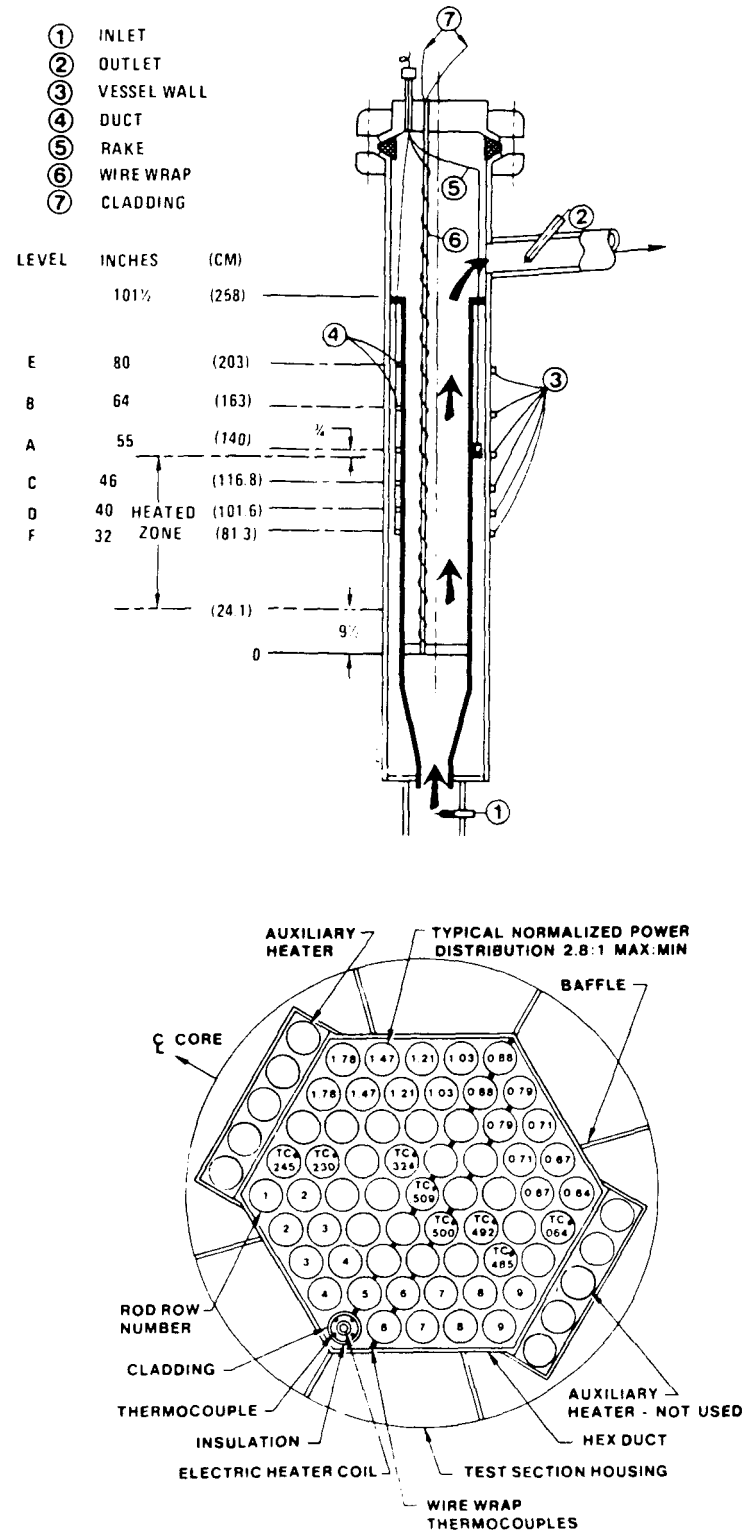

Fig. 4 Schematic of the Westinghouse 61-Pin Blanket Test Model

The test section is vertically mounted, with sodium entering at the bottom and flowing upward through the heated rod bundle, discharging from the duct near the vessel exit nozzle. The space outside the duct contains stagnant sodium and is compartmentalized by numerous horizontal and radial baffles to minimize heat loss by convective transfer in the annular space between the duct and the vessel walls.

Table II summarizes the geometric characteristics of the test section [12-16]. The test section has been used extensively to study thermal-hydraulic characteristics of LMFBR blanket assemblies for steady state, transient, forced, mixed and free convection conditions. Due to the controlled experimental conditions, these tests can serve a very useful purpose for identification of phenomenological heat transfer and fluid dynamics issues applicable to fast reactor cores.

Figures 5 and 6 show typical steady-state transverse temperature profiles at various axial locations corresponding to different levels of power and bundle flow conditions for radial power gradients of (2.79:1) and (2.04:1), respectively. It is seen that the maximum temperature is reached away from the bundle edge in the interior of the assembly, as a result of enhanced cooling at the edge subchannels due to higher sodium flow rate. The temperature flattening at low Reynolds numbers discussed earlier is very clearly evident.

Figure 7 shows the calculated temperature rise hot channel factor as a function of inlet Reynolds number using the present flow redistribution model. Also shown are the measured data of Engel, et al., [14] corresponding to the same conditions.

At high Reynolds number forced convection conditions, the subassembly radial temperature distribution is primarily influenced by transverse thermal conduction and it is unaffected by thermal buoyancy. However, comparison with experimental data seems to indicate that this effect is counterbalanced by the larger magnitude of the velocity as assumed in the present model.

Table II Geometric Characteristics of the Westinghouse 61 Pin Test Model

D_r	(m)	1.318×10^{-2}
D_w	(m)	9.400×10^{-4}
p/D_r	(-)	1.082
ℓ	(m)	0.1140
ℓ_1	(m)	0.0988
ℓ_2	(m)	0.0076
L_h	(m)	1.1430
A_r	(m^2)	1.3643×10^{-4}
A_w	(m^2)	6.9398×10^{-7}
A_p	(m^2)	1.1255×10^{-2}
D_{e1}	(m)	3.5163×10^{-3}
D_{e2}	(m)	7.1810×10^{-3}
D_{e3}	(m)	4.8997×10^{-3}
D_{ea}	(m)	3.7282×10^{-3}
α_1		0.7511
α_2		0.2311
α_3		0.0178
λ_1		0.2214
λ_2		0.3674
λ_3		0.3077
λ_a		0.2567

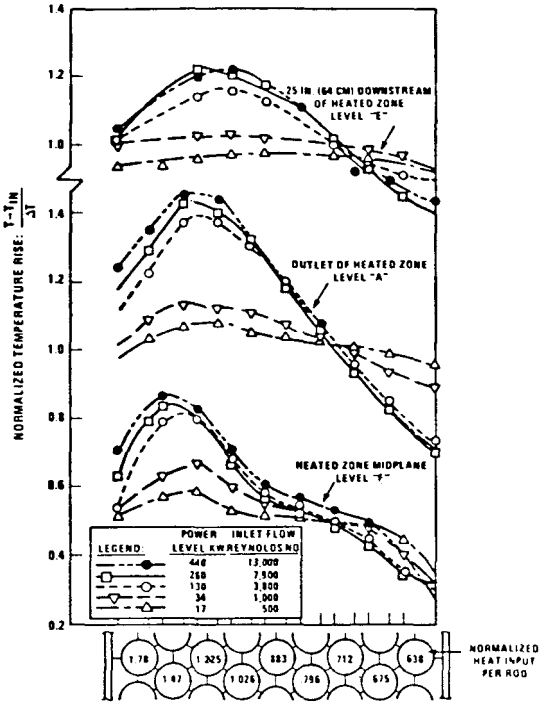

Fig. 5 Measured Transverse Temperature Distribution (2.79:1)

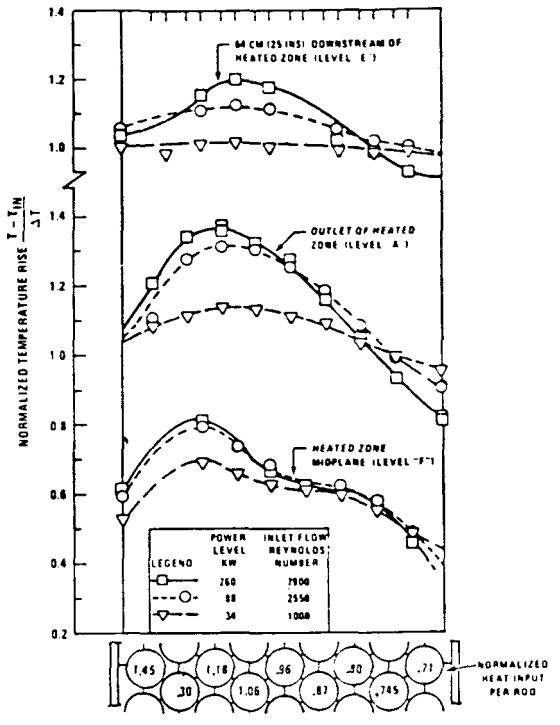

Fig. 6 Measured Transverse Temperature Distribution (2.04:1)

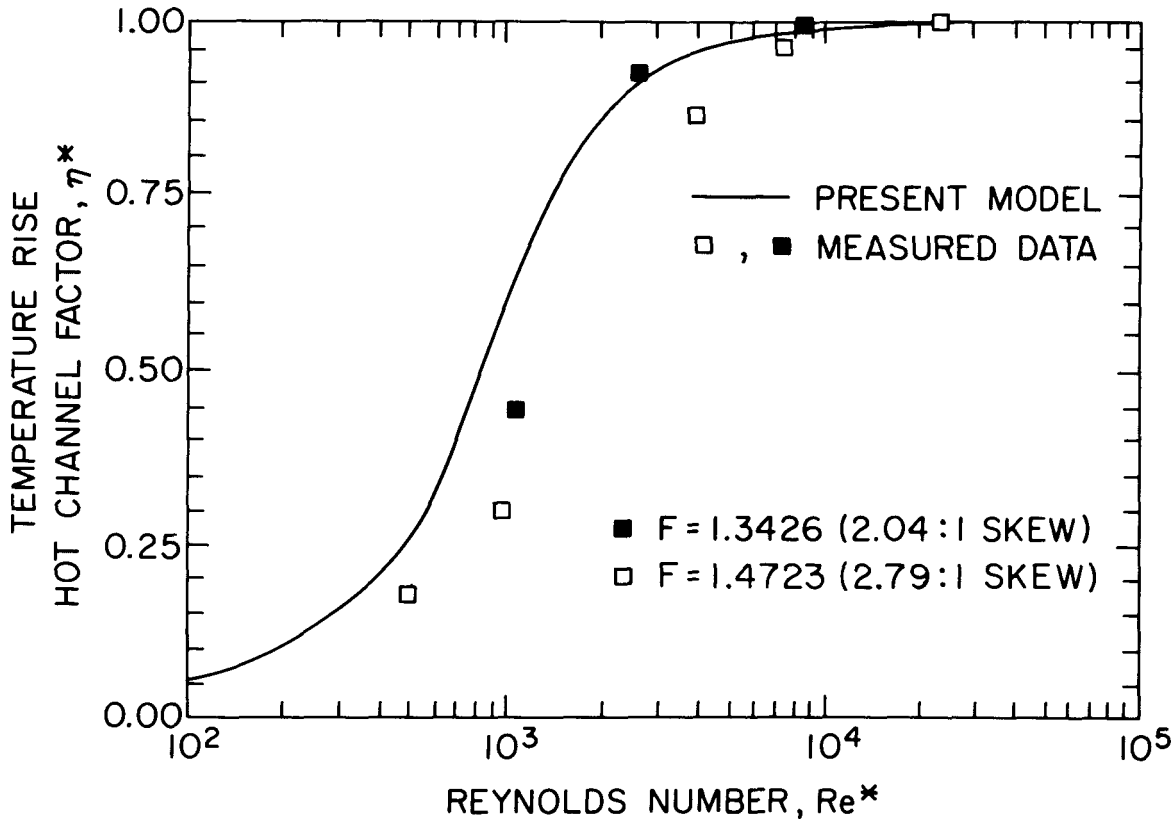

Fig. 7 Comparison of Calculated and Measured Temperature Rise Hot Channel Factors

At lower Reynolds numbers, for mixed and free convection conditions, the influence of thermal buoyancy and transverse thermal conduction become increasingly important, and thus the discrepancy between the measured and calculated values become increasingly significant.

Figure 8 shows the calculated temperature peaking factor as a function of the temperature rise Grashof number to inlet flow Reynolds number ratio ($G\overset{*}{r}/R\overset{*}{e}$) at various radial power gradients. It is seen that the temperature peaking factor remains constant in the forced convection regime, where it is only dependent on the radial power gradient. The initiation of the mixed convection regime is seen to be a unique function of $G\overset{*}{r}/R\overset{*}{e}$ and is found to be independent of the radial power gradient, in excellent agreement with recent experimental observation of Engel, et al., [16]. Furthermore, as the buoyancy effects become more significant, a change in shape becomes apparent beyond which free convection regime is dominant.

These calculations seem to indicate that, even though, buoyancy-induced flow redistribution has a dominant influence on transverse temperature flattening in LMFBR rod bundles, thermal conduction effects must also be included, especially during mixed and free convection regimes. The significance of molecular and turbulent diffusion is further discussed in the following section.

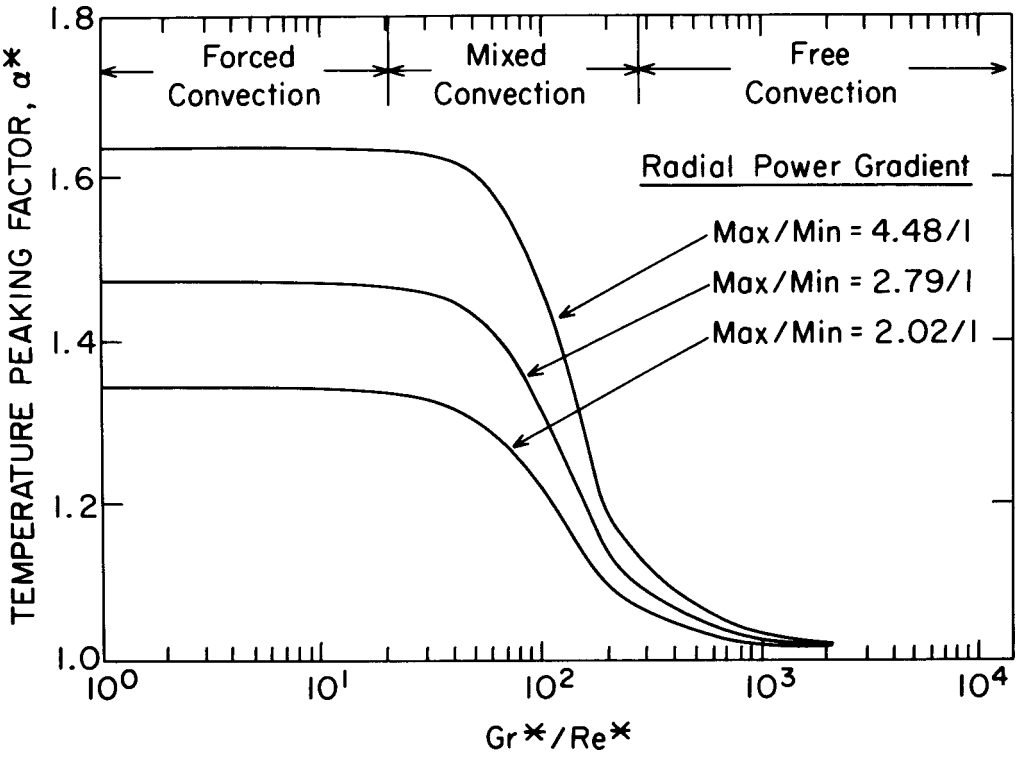

Fig. 8 Calculated Temperature Peaking Factor as a Function of Thermal Buoyancy Parameter

3.2 Transverse Heat Transfer

3.2.1 Meyer's Integral Method

In the absence of buoyancy-induced flow redistribution, the coolant flow is predominantly in the axial direction and is assumed to be independent of axial and transverse positions within the rod bundle. Therefore, the conservation of energy equation (Eq. 2) can be simplified to;

$$\rho c_p \hat{u} \frac{\partial T}{\partial x} = k_e \frac{\partial^2 T}{\partial y^2} + Q''' \tag{56}$$

where k_e is defined in equation (3) as:

$$k_e = \rho c_p \varepsilon_h + \kappa k \tag{57}$$

Subject to the following boundary conditions:

$$\begin{cases} T(o,y) = T^* \\ \frac{\partial T}{\partial y}(x, \pm \ell/2) = 0.0 \end{cases} \tag{58}$$

Meyer [11] has solved this equation using an approximate integral technique. He assumed,

$$T = \hat{T}(x) \left\{ 1 + (F-1)\left(\frac{2y}{\ell}\right) - (F-1)\left(\frac{\delta}{\ell}\right) \psi_1 \right\} \quad \text{for} \quad \delta < \frac{\ell}{2} \tag{59}$$

where, δ is the distance into the assembly that the effect of insulation at the duct wall has penetrated, ψ_1 is a skew symmetric function about $y = 0$; that is:

$$\psi_1(-y,\delta) = -\psi_1(y,\delta) \tag{60}$$

and where, for non-negative values of y,

$$\psi_1 = \begin{cases} 0 & 0 \leq y < \left(\frac{\ell}{2} - \delta\right) \\ \left[\frac{2y + 2\delta - \ell}{2\delta}\right]^2 & \left(\frac{\ell}{2} - \delta\right) \leq y \leq \ell/2 \end{cases} \tag{61}$$

The temperature distribution of Equation (59) was chosen [11] to have the following nature:

- the temperature $\hat{T}$ and the distance δ are functions of x only;
- if at any axial location, the temperature is averaged between y = $-\ell/2$ and y = $\ell/2$, the resulting average is $\hat{T}$;
- The first two terms within the braces of Eq. (59) give the exact solution for the case of zero conductivity;
- The temperature shape of the penetration term (the final term within the braces in Eq. (59)) is parabolic;
- both temperature and heat flux are continuous; and
- the boundary conditions (Eq. (58)) are satisfied both at the inlet and at the duct walls if:

$$\begin{cases} \hat{T}(o) = T^* \\ \delta(o) = o \end{cases} \tag{62}$$

Meyer [11] obtained an integral solution using the following weighted residual technique:

Step (a) Substitute Eq. (59) into Eq. (57); multiply by the weight function $W_1(y)$, where;

$$W_1(y) = 1 \qquad -\ell/2 \leq y \leq +\ell/2 \tag{63}$$

and integrate the resulting equation from $y = -\ell/2$ to $y = +\ell/2$.

Step (b) Again substitute Eq. (59) into Eq. (57); multiply by the weight function $W_2(y)$, where;

$$W_2(y) = \begin{cases} 0 & -\ell/2 \leq y < 0 \\ 1 & 0 \leq y \leq \ell/2 \end{cases} \tag{64}$$

and integrate the resulting equation from $y = \ell/2$ to $y = +\ell/2$.

Equations obtained by completing steps (a) and (b), can, after substituting the boundary conditions from Equation (62), be solved for $\hat{T}$ and δ:

$$\hat{T}(x) = T^* + \frac{\hat{Q}'''}{\rho c_p \hat{u}} x \tag{65}$$

and

$$\delta(x) = \sqrt{\frac{3 k_e x}{\rho c_p \hat{u}}} \tag{66}$$

Equation (66) ceases to apply if the value of δ calculated is greater than $(\ell/2)$. That is, Eq. (66) applies only if $x \leq x_{max}$; where x_{max} is given by:

$$x_{max} = \left[\frac{\rho c_p \hat{u} \ell^2}{12 k_e}\right] \tag{67}$$

An alternative equation that is equivalent to Eq. (66) is then:

$$\frac{\delta}{\ell} = \frac{1}{2}\sqrt{\frac{x}{x_{max}}} \qquad \text{for } x \leq x_{max} \tag{68}$$

For values of x larger than x_{max}, another integral equation for temperature was employed. Meyer [11] chose the following:

$$T(x,y) = \hat{T}(x) + T_d(x)\ \psi_2(y) \tag{69}$$

where $\hat{T}$ and T_d are functions of x and ψ_2 is a skew symmetric function about y = 0; that is:

$$\psi_2(-y) = -\psi_2(y) \tag{70}$$

and where,

$$\psi_2(y) = 1 - \left[\frac{2y - \ell}{\ell}\right]^2 \qquad 0 \leq y \leq \ell/2 \tag{71}$$

The temperature distribution of Eq. (69) has the following nature:

- if at any level, the temperature is averaged between y = -ℓ/2 and y = ℓ/2, the resulting average is $\hat{T}$;
- both temperature and heat flux are continuous;
- the boundary conditions (Equation (58)) are satisfied at the duct wall; and
- the temperature can be made to match with Equation (59) at x = x_{max}

The integral equation was solved using the same steps performed earlier to obtain:

$$T_d(x) = \frac{1}{4}\ \hat{T}(x)\ \left(\frac{x_{max}}{x}\right)\ \left\{3 - \text{Exp}\ [-(x - x_{max})/x_{max}]\right\} \tag{72}$$

Now, define a dimensionless assembly length $\bar{L}$ as:

$$\bar{L} = L_h/x_{max} \tag{73}$$

or using Eq. (67),

$$\bar{L} = \left[\frac{12 k_e\ L_h}{\rho c_p\ \hat{u}\ \ell^2}\right] \tag{74}$$

and then by using Eqs. (59), (65), (68), (72) and the definition of the temperature rise hot channel factor (Eq. (53)), one obtains:

$$\eta^* = \begin{cases} 1 - \frac{1}{2}\sqrt{\bar{L}} & \text{for } \bar{L} \leq 1 \\ \frac{1}{4\bar{L}}\ [3 - \text{Exp}\ (1-\bar{L})] & \text{for } \bar{L} > 1 \end{cases} \tag{75}$$

An alternative form for $\bar{L}$ may be obtained using the definition of Reynolds number and Prandtl number (Eq. (17)) to obtain:

$$\bar{L} = \left(\frac{1}{Re}\right)\ \left(\frac{1}{Pr}\right)\ \left(\frac{k_e}{k}\right)\ \left(\frac{12\ D_e L_h}{\lambda_a \ell^2}\right) \tag{76}$$

where according to Eqs. (3) and (4),

$$\left(\frac{k_e}{k}\right) = \kappa + Re\ Pr\ \lambda_a \varepsilon^* \tag{77}$$

and Meyer [11] suggests the following approximation to Chiu's results [20]:

$$\left(\varepsilon^*/\varepsilon^*_\infty\right) = \begin{cases} 1 & Re \geq 7000 \\ 1 - \left[1 - \frac{Re}{7000}\right]^2 & Re < 7000 \end{cases} \tag{78}$$

where ε_∞^* is usually chosen to match the experimental data.

Therefore, Eqs. (75), (76) and (77) relate the temperature rise hot channel factor to the coolant Reynolds number, Prandtl number and the assembly geometry.

Meyer [11] also found a high flow and a low flow asymptote for $\overline{L}$ as:

$$(\overline{L})_{\text{high flow}} \simeq \left[\frac{12\, D_e\, L_h\, \varepsilon_\infty^*}{\ell^2}\right] \tag{79}$$

and

$$(\overline{L})_{\text{low flow}} \simeq \left(\frac{1}{Re}\right)\left(\frac{1}{Pr}\right)\left[\frac{12\, D_e\, L_h\, \kappa}{\lambda_a\, \ell^2}\right] \tag{80}$$

Note, that at high flow $\overline{L}$ and thus η^* is independent of the flow rate.

A useful approximation to η^* can be obtained by taking the larger of $\overline{L}_{\text{high flow}}$ and $\overline{L}_{\text{low flow}}$ for a given value of Reynolds number.

3.2.2 Results

Results of Meyer's [11] calculations are presented in Figure 9 for CRBRP fuel and blanket assemblies. It is seen that major reduction in temperature rise hot channel factors occur below full flow values (Re < 3000 for fuel assemblies and Re < 1500 for blanket assemblies). However, full flow transverse thermal conduction is more significant in the blanket assemblies (η^* = 0.68) as compared to the fuel assemblies (η^* = 0.90). Figure 9 also shows that the asymptotic results supply an excellent representation of the complete solution.

It is therefore evident that the thermal conduction effect is quite significant at high flow forced convection; however, its influence becomes more pronounced at low Reynolds numbers, where it is of the same order as the flow redistribution observed in the previous section.

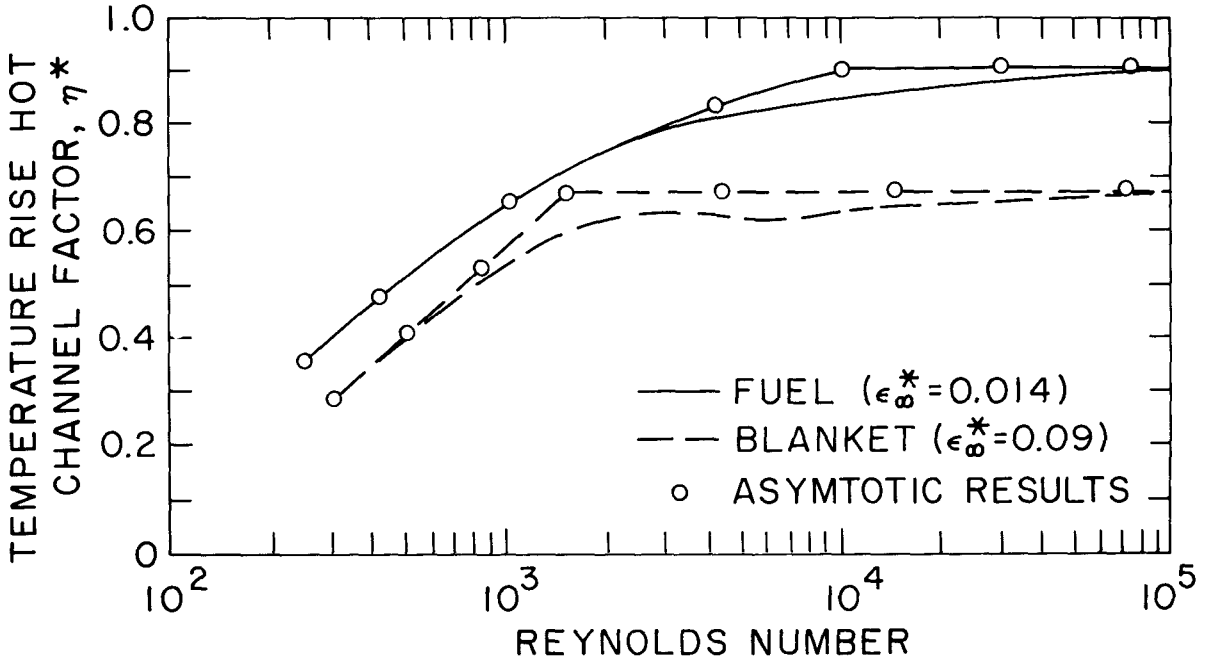

Fig. 9 Impact of Transverse Conduction and Mixing on Temperature Rise Hot Channel Factor

4. FINITE DIFFERENCE SOLUTION

In the previous chapter, approximate integral solutions to the conservation equations were developed. It was also demonstrated that both thermal buoyancy and transverse conduction can significantly reduce the transverse temperature gradient within an LMFBR subassembly subject to a radial power gradient.

In this chapter, finite difference solutions to a more detailed form of the conservation equations are developed, which retain both the buoyancy-induced redistribution and the transverse thermal conduction effects in the same two-dimensional slab geometry. Finally, calculated results are compared to experimental measurements for model validation.

4.1 Steady-State Two-Dimensional Parabolic Flow Model

In LMFBR subassemblies, the flow is predominantly in the axial direction and can therefore be treated as a two-dimensional parabolic flow. Under these conditions, convection in the axial direction dominates the axial diffusion. It is this feature that imparts the one-way character to the streamwise direction. Obviously, no reverse flow in the axial direction would be acceptable.

The solution for two-dimensional parabolic flows is obtained by starting with a known distribution of temperature and velocity at an upsteam station and marching in the streamwise direction. For every forward step, the distribution of temperature and velocity in the cross-stream coordinate is calculated at one streamwise station. Thus, computationally only a one-dimensional problem needs to be solved.

Recall the conservation of mass, energy and momentum equations (Eqs. (1), (2) and (6)) of Chapter 2 where,

$$\frac{\partial(\rho u)}{\partial x} + \frac{\partial(\rho v)}{\partial y} = 0 \tag{81}$$

$$\left(u \frac{\partial T}{\partial x} + v \frac{\partial T}{\partial y}\right) = \alpha_e \frac{\partial^2 T}{\partial y^2} + \frac{Q'''}{\rho c_p} \tag{82}$$

$$u \frac{\partial u}{\partial x} + v \frac{\partial u}{\partial y} = - \frac{1}{\rho} \frac{dP}{dx} - g \frac{\rho^*}{\rho} [1 - \beta(T-T^*)] + \nu \frac{\partial^2 u}{\partial y^2} - \frac{f}{2D_e \lambda^2} u^2 \tag{83}$$

where α_e is the effective thermal diffusivity and is defined as;

$$\alpha_e = k_e/\rho c_p \tag{84}$$

Equations (81) through (83) must be solved subject to the following boundary conditions (see Fig. 10):

(1) Inlet Velocity and Temperature are specified as;

$$\begin{cases} u(o,y) = F(u_{in}) \\ T(o,y) = T^* \end{cases} \tag{85}$$

(2) No Slip at the duct walls requires,

$$\begin{cases} u(x,o) = u(x,\ell) = 0 \\ v(x,o) = v(x,\ell) = 0 \end{cases} \tag{86}$$

(3) Adiabatic Duct requires,

$$\frac{\partial T}{\partial x}(x,o) = \frac{\partial T}{\partial x}(x,\ell) = 0 \tag{87}$$

4.2 Method of Solution

4.2.1 Finite Difference Equations

In finite difference form, Eqs. (81) through (83) can be expressed as follows:

Mass Continuity

$$\left[\frac{(\rho u)_{i+1,j} + (\rho u)_{i+1,j+1} - (\rho u)_{i,j} - (\rho u)_{i,j+1}}{2\Delta x}\right] + \left[\frac{(\rho v)_{i+1,j+1} - (\rho v)_{i+1,j}}{\Delta y}\right] = 0 \tag{88}$$

$$i = 1,2,3,\ldots\ldots, M$$

$$j = 2,3,4,\ldots\ldots, N-2$$

Note, the somewhat unusual representation of Eq. (88) is chosen for a reason which will become clear shortly.

Now, add all of the velocities in the transverse direction, and substitute the boundary conditions of Eq. (86) to obtain:

$$\sum_{j=3}^{N-2} (\rho u)_{i+1,j} = \sum_{j=3}^{N-2} (\rho u)_{i,j} \tag{89}$$

If both sides of Eq. (89) are multiplied by Δy, it can be seen to be the trapezoidal rule integration form of the equation, i.e.,

$$\left[\int_0^{\ell} \rho u \, dy\right]_{i+1} = \left[\int_0^{\ell} \rho u \, dy\right]_i \tag{90}$$

Subsequently, dividing both sides of Eq. (90) by ℓ, one obtains;

$$G = \langle \rho u \rangle_{i+1} = \langle \rho u \rangle_i \tag{91}$$

which indicates that the mass flux is constant throughout the axial location. Equation (91) is often [21] referred to as the "equation of constraint".

Energy

$$u_{ij}\left[\frac{T_{i+1,j}-T_{i,j}}{\Delta x}\right]+v_{i,j}\left[\frac{T_{i+1,j+1}-T_{i+1,j-1}}{2\Delta y}\right] \tag{92}$$

$$=\alpha_e\left[\frac{T_{i+1,j+1}-2T_{i+1,j}+T_{i+1,j-1}}{(\Delta y)^2}\right]+\left[\frac{Q'''_{i,j}}{\rho c_p}\right]$$

and Axial Momentum

$$u_{ij}\left[\frac{u_{i+1,j}-u_{i,j}}{\Delta x}\right]+v_{i,j}\left[\frac{u_{i+1,j+1}-u_{i+1,j-1}}{2\Delta y}\right]$$

$$=-\frac{\Delta\tilde{P}}{\Delta x}-\frac{f_{i,j}}{2D\lambda^2_{i,j}}u_{i,j}u_{i+1,j}+g\beta\,(T_{i+1,j}-T^*) \tag{93}$$

$$+\nu_{i,j}\left[\frac{u_{i+1,j+1}-2u_{i+1,j}+u_{i+1,j-1}}{(\Delta y)^2}\right]$$

for i=1, 2, 3,..., M

j=3, 4, 5,..., N-2

where i and j denote x and y, respectively. The mesh points of the rectangular grid structure superimposed on the channel flow field is shown in Fig. 10. The points j=1 and j=N designate the duct wall, while i=1 and i=M represent the subassembly inlet and exit, respectively.

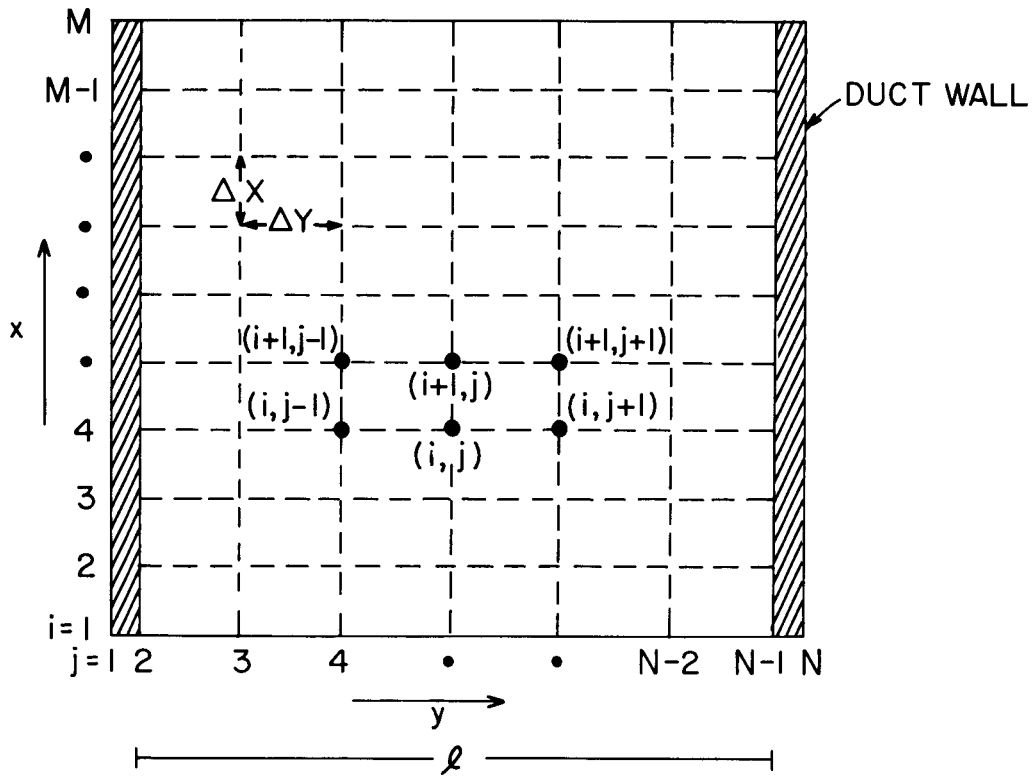

Fig. 10 Coordinate System for the Finite Difference Equations

The energy equation (Eq. (92)) together with the boundary conditions of Eq. (87) yield;

$$\begin{bmatrix} \phi_{i,3} & \sigma_{i,4} & 0 & 0 & \cdots & 0 \\ \xi_{i,3} & \phi_{i,4} & \sigma_{i,5} & 0 & \cdots & 0 \\ 0 & \xi_{i,4} & \phi_{i,5} & \sigma_{i,6} & & \\ & \ddots & \ddots & \ddots & \ddots & \sigma_{i,N-2} \\ 0 & \cdots & 0 & \xi_{i,N-3} & \phi_{i,N-2} & \end{bmatrix} \begin{bmatrix} T_{i+1,3} \\ T_{i+1,4} \\ \vdots \\ T_{i+1,N-2} \end{bmatrix} = \begin{bmatrix} C_{i,3} \\ C_{i,4} \\ \vdots \\ C_{i,N-2} \end{bmatrix} \tag{94a}$$

and,

$$T_{i+1,1} = T_{i+1,2} = T_{i+1,3} \tag{94b}$$

where

$$\phi_{i,j} = \left[\frac{u_{i,j}}{\Delta x} + \frac{2\alpha_e}{(\Delta y)^2} \right] \tag{95a}$$

$$\sigma_{i,j} = \left[\frac{v_{i,j-1}}{2\Delta y} - \frac{\alpha_e}{(\Delta y)^2} \right] \tag{95b}$$

$$\xi_{i,j} = \left[\frac{v_{i,j+1}}{2\Delta y} + \frac{\alpha_e}{(\Delta y)^2} \right] \tag{95c}$$

$$C_{i,j} = \left[\frac{Q'''_{i,j}}{\rho c_p} + \frac{T_{i,j}\, u_{i,j}}{\Delta x} \right] \tag{95d}$$

Similarly, Eqs. (89) and (93) can be written as:

$$
\begin{bmatrix}
\rho_{i+1,3} & \rho_{i+1,4} & \rho_{i+1,5} & \rho_{i+1,6} & \rho_{i+1,7} & \cdots & \rho_{i+1,N-2} & 0 \\
\gamma_{1+1,3} & \Omega_{1+1,4} & 0 & 0 & 0 & \cdots & 0 & \frac{1}{\Delta x} \\
\Gamma_{i+1,3} & \gamma_{i+1,4} & \Omega_{i+1,5} & 0 & 0 & \cdots & & \\
0 & \Gamma_{i+1,4} & \gamma_{i+1,5} & \Omega_{i+1,6} & 0 & \cdots & & \\
0 & 0 & \ddots & \ddots & \ddots & \ddots & 0 & \frac{1}{\Delta x} \\
0 & 0 & \cdots & 0 & \Gamma_{i+1,N-4} & \gamma_{i+1,N-3} & \Omega_{i+1,N-2} & \frac{1}{\Delta x}
\end{bmatrix}
\begin{bmatrix}
u_{i+1,3} \\ u_{i+1,4} \\ \\ \\ u_{i+1,N-2} \\ \Delta\tilde{P}_{i+1}
\end{bmatrix}
$$

$$
= \begin{bmatrix}
S_{i+1} \\ C_{i+1,3} \\ C_{i+1,4} \\ \\ \\ \\ \\ C_{i+1,N-2}
\end{bmatrix} \tag{96a}
$$

and

$$
u_{i+1,1} = u_{i+1,2} = u_{i+1,N-1} = u_{i+1,N} = 0 \tag{96b}
$$

where:

$$v_{i+1,j} = \left[\frac{u_{i,j}}{\Delta x} + \frac{f_{i,j}\, u_{i,j}}{2D_{i,j}\lambda^2_{i,j}} + \frac{2\nu_{i,j}}{(\Delta y)^2}\right] \tag{97a}$$

$$\Omega_{i+1,j} = \left[\frac{v_{i,j}}{2\Delta y} - \frac{\nu_{i,j}}{(\Delta y)^2}\right] \tag{97b}$$

$$\Gamma_{i+1,j} = -\left[\frac{v_{i,j}}{2\Delta y} + \frac{\nu_{i,j}}{(\Delta y)^2}\right] \tag{97c}$$

$$S_{i+1} = \sum_{j=3}^{N-2} (\rho_{i,j}\, u_{i,j}) \tag{97d}$$

$$C_{i+1,j} = \frac{u_{i,j}}{\Delta x} + g\rho\ [T_{i+1,j} - T^*] \tag{97e}$$

and

$$\Delta\widetilde{P}_{i+1} = \left[\frac{\Delta P + g\rho^* \Delta x}{\rho}\right]_{i+1} \tag{97f}$$

4.2.2 Numerical Solution Procedure

The numerical solution procedure is as follows:

(1) Start at row i=1, and solve Eq. (94) for $T_{2,1}$, $T_{2,2}$,....., $T_{2,N}$ using the Gaussian elimination technique [22].

(2) Calculate the physical properties as a function of $T_{i+1,j}$'s.

(3) Solve Eq. (96) for $u_{2,1}$, $u_{2,2}$,....., $u_{2,N}$ and $\Delta\tilde{P}_2$ using the Gauss-Jordan reduction method [22].

(4) Now, back substitute into Eq. (88), together with Eq. (86), to obtain $v_{2,1}$, $v_{2,2}$...., $v_{2,N}$.

(5) March in the stream-wise direction up to row i=M; repeating steps (1) through (4).

4.3 Results and Comparison with Experimental Data

In this section, the two-dimensional parabolic flow model developed in the previous sections is applied to the Westinghouse Blanket Sodium [14] Test data and the Toshiba Water Simulation measurements [25,26].

4.3.1 Comparison with Sodium Test Data

The Westinghouse Blanket Test section described previously in Section 3.1.2.2 is a highly prototypic test section simulating forced, mixed and free convection conditions typical of LMFBR blanket assemblies subject to various power and flow conditions. Table II summarizes the geometric characteristics while Table III lists the experimental conditions as given by Engel, et al., [14].

Figure 11 illustrates the transverse power profiles for the aforementioned experiments as used for the present simulation (see also Appendix B for more details).

The power distribution in the bundle is represented by the following chopped cosine axial distribution; with peak to average of 1.4; that is,

$$Q'''(x,y) = 1.40\,\hat{Q}'''\,\bar{\Psi}(y)\cos\left\{0.8738\,\pi\left(\frac{x}{L_h} - \frac{1}{2}\right)\right\} \qquad (98)$$

Table III Westinghouse Blanket Test Conditions

Power Skew (Max/Min)	Power Level (Kw)	Inlet Reynolds Number
1:1	34	1000
	130	3800
	260	7900
	440	13000
Inner Blanket	22	550
	44	1100
	165	4400
	440	11500
2:1	34	1000
	88	2550
	260	7900
2.8:1	17	500
	34	1000
	130	3800
	260	7900
	440	13000

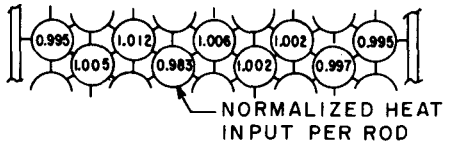

(a) UNIFORM

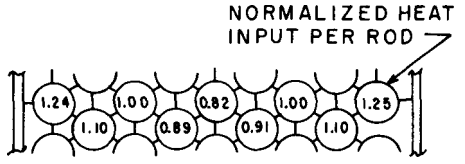

(b) DOUBLE HUMP

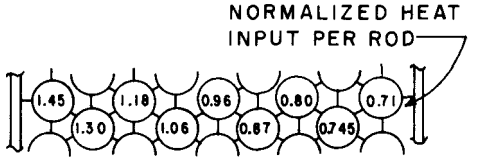

(c) 2/1 SKEW

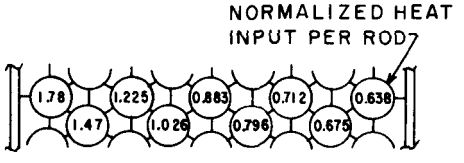

(d) 2.8/1 SKEW

Fig. 11 Normalized Transverse Power Distribution

where $\hat{Q}'''$ is the total average volumetric power generation in the assembly; and $\overline{\psi}(y)$ is the radial shape factor (normalized).

Engel, et al., [14] present their temperature data by normalizing the measured local temperature rise at all elevations with respect to a calculated mixed mean sodium temperature rise at the exit of the heated section. The mixed mean sodium temperatures were calculated by mapping all measured subchannel temperatures at the exit of the heated section plane and filling-in missing subchannels (by interpolation) assuming smooth monotonic temperature profiles. The various subchannel (interior, corner or edge) temperature rises were then weighted to calculate the mixed mean outlet temperatures, using flow area and the blanket assembly flow split obtained from MIT studies as the weighting factors [15] .

In the present study, the mean sodium temperature at the exit is calculated as,

$$\hat{T}(L_h) = \frac{1}{\hat{u}\ell} \int_0^{\ell} T(L_h,y)\, u(L_h,y)\, dy \tag{99}$$

where the integration is carried out numerically by the Simpson's rule:

$$\hat{T}(L_h) \simeq \frac{1}{3\hat{u}s} [(uT)_0 + 4(uT)_1 + 2(uT)_2 + \ldots + 2(uT)_{s-2} + 4(uT)_{s-1} + (uT)_s] \tag{100}$$

where s is an even number of equal subdivisions in the transverse direction.

It must be noted that in the present analysis the effect of heat losses from the test assembly has been neglected.

Parameters which can have significant effects on calculated temperature distributions include, inlet velocity distribution, bundle tolerance and especially the bundle bowing, pin distortion and the bundle housing thermo-mechanical behavior caused by heating effects.

In the present application the effect of bundle bowing and distortion are not taken into account. However, these effects can readily be included through adjustments in the hydraulic diameters and the porosity to match the experimental data.

In a typical fuel and blanket assembly, the flow area of the channels in the wall region is nearly twice as large as the flow area of the interior channels. As a result, the coolant temperature rise in the wall region is lower than in the interior channels. The wall channels act as a heat sink to the interior regions of the assembly. At low Reynold numbers (or at low Peclet number; Pe = Re Pr), the flattening of the transverse temperature profile occurs as a result of the two distinct processes described earlier, namely; first, by energy transport due to increased conduction, combined with wire wrap induced mixing, and secondly, by buoyancy-induced flow redistribution. As the wall channels are cooler than the interior channels, there will be density differences between the wall and the interior regions of the bundle, even in the absence of radial power skew. The effect of higher density, and to a lesser extent the higher viscosity in the wall region compared to the interior region, results in higher frictional forces in the wall channels. The combined effect of frictional and static head forces results in a net diversion of flow from the wall to the interior regions of the bundle. This buoyancy-induced cross flow tends to further flatten the transverse temperature gradient. This cross flow effect can be further enhanced in the presence of radial power skew across the bundle [23].

The following analysis of simulation experiments demonstrates the importance of intra-subassembly processes as they influence the sodium temperatures during forced, mixed and free convection conditions.

A. Uniform Power Distribution

Figure (11a) depicts the normalized transverse power distribution in the assembly. It is seen that the distribution is nearly uniform (flat), thus the expected temperature distribution is inversely proportional to the velocity distribution shown in Figure 12 (high Reynolds number).

Figures 13 through 17 illustrate the calculated transverse coolant temperature distribution corresponding to the power and flow conditions of Table III for two different mixing parameters ($\varepsilon_\infty^* = 0.09$ and $\varepsilon_\infty^* = 0.03$).

Also shown are the experimental data of Engel, et al. [14]. It is seen that the agreement between the calculated and measured data improves in going from the forced to the free convection regime. Furthermore, the quantitative differences in the measured and calculated temperatures are believed to be in part due to the bundle distortions and inlet velocity distribution. Similar observations were made by Juneau and Khan [23] using the ENERGY and COBRA computer codes.

Figures 13 through 17 also demonstrate the influence of the mixing parameter ε_∞^* on the bundle temperature profile calculations. It is seen that a reduction in turbulent mixing reduces the transverse temperature flattening at high Reynolds numbers, leading to higher temperatures in the interior region, and subsequently lower sodium temperatures in the side (wall) region.

Figure 15 illustrates the temperature distribution downstream of the heated section corresponding to the exit of the subassembly. It is seen that significant flattening of the radial temperature distribution occurs as a result of turbulent and molecular diffusion, in close agreement with experimental measurements.

B. Double-Hump Power Distribution

The double-humped power distribution depicted in Fig. (11b) exemplifies the power distribution for LMFBR inner blanket subassemblies.

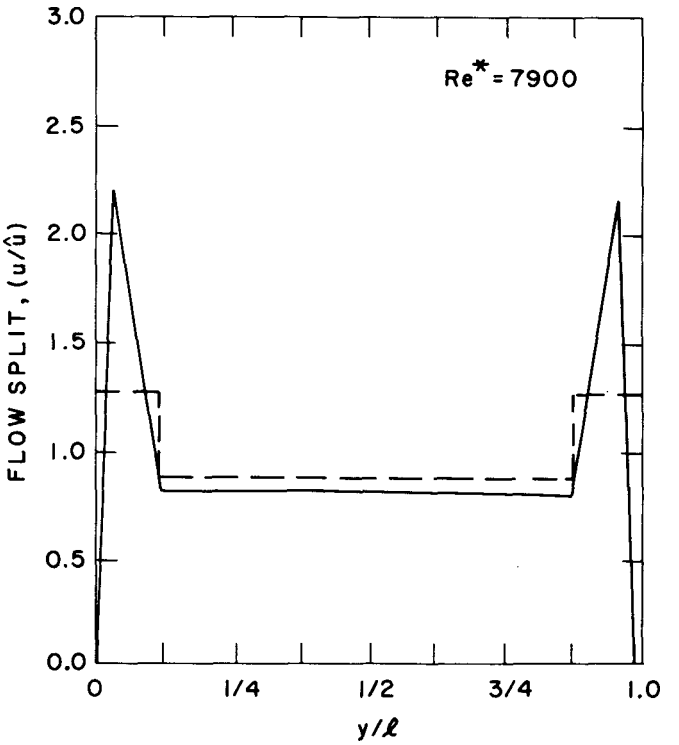

Fig. 12 Calculated Flow Split at the Exit of the Heated Section

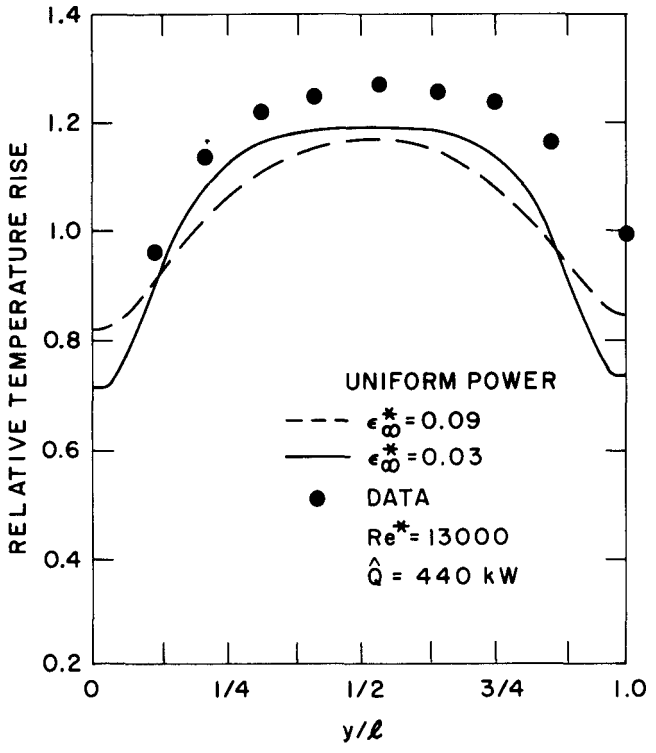

Fig. 13 Comparison of Calculated and Measured Transverse Temperature Distribution (Uniform)

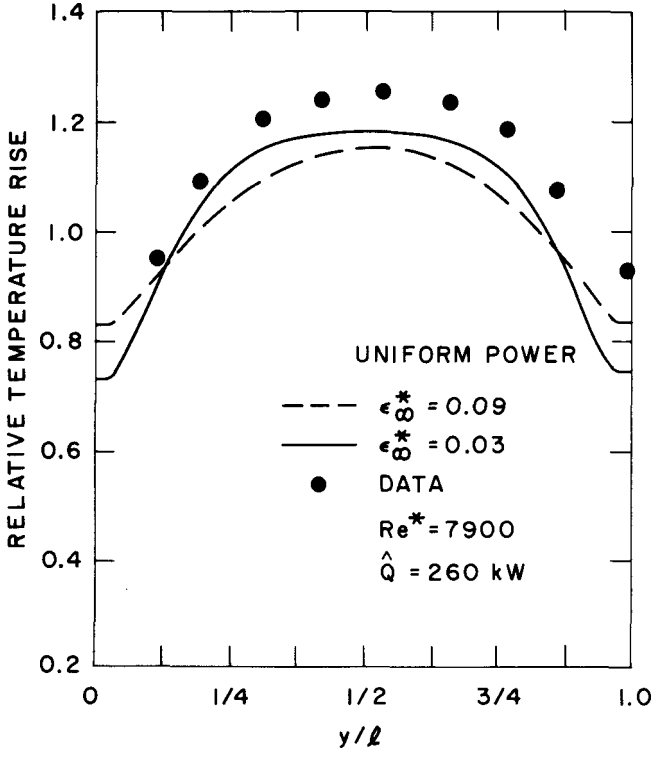

Fig. 14 Comparison of Calculated and Measured Transverse Temperature Distribution (Uniform)

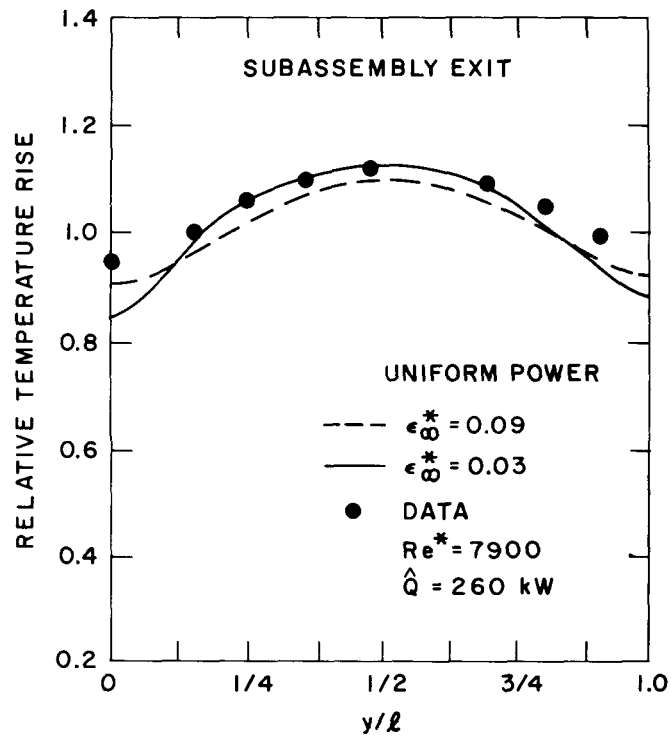

Fig. 15 Comparison of Calculated and Measured Transverse Temperature Distribution at the Subassembly Exit (Uniform)

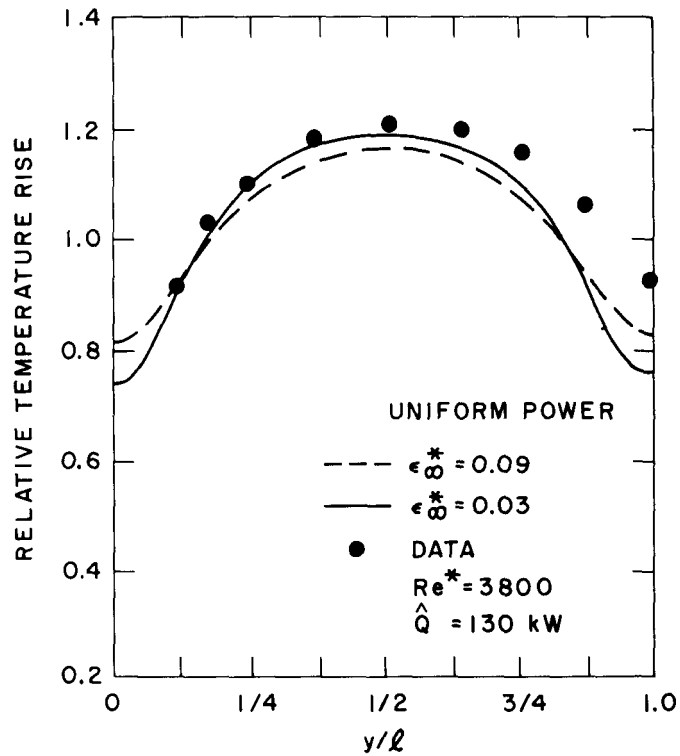

Fig. 16 Comparison of Calculated and Measured Transverse Temperature Distribution (Uniform)

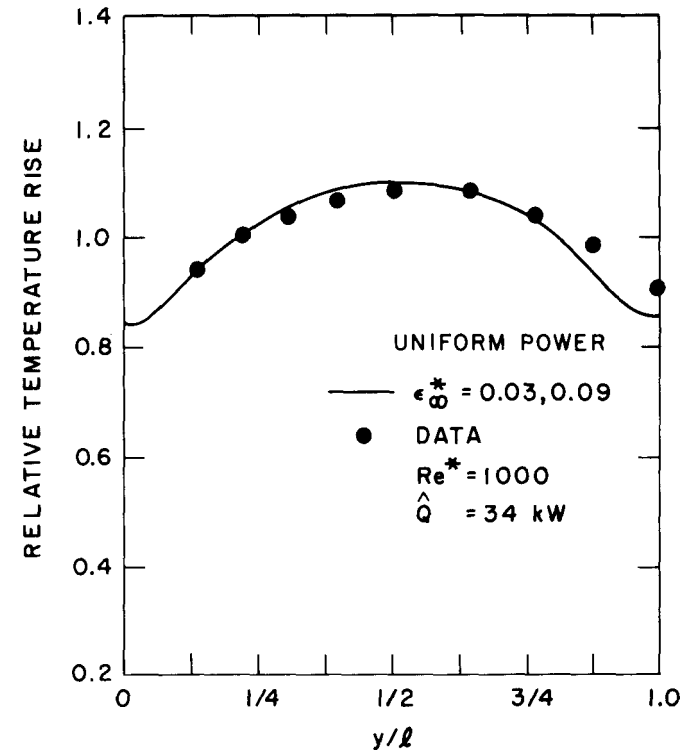

Fig. 17 Comparison of Calculated and Measured Transverse Temperature Distribution (Uniform)

Figures 18 through 21 show the comparison of the measured and calculated temperature distribution at high, intermediate and low Reynolds numbers corresponding to forced, mixed and free convection conditions. The agreement between the calculated and measured values improves at low flow natural convection conditions; a trend also observed for the uniform power distribution case discussed earlier.

C. Steep Power Gradients

Figures (11c) and (11d) show the normalized transverse power gradients corresponding to 2:1 and 2.8:1 power skews, respectively, while Table III summarizes the corresponding test conditions.

Figures 22 through 24 show the calculated and measured transverse temperature distribution at 2:1 power skew across the assembly. It is seen that the calculated results are in agreement with the experimental measurements, especially in the higher power side of the assembly. Again, the agreement between the calculated and measured temperatures improve at lower Reynolds numbers.

The larger discrepancy in the low-power side of the bundle is believed to be influenced by the reduction in the flow area caused by pin distortion and bowing as a result of large transverse power (temperature) gradients. Similar observations have been made using COTEC, ENERGY-II and COBRA-IV computer codes [14,23,24].

Figures 25 through 29 show the calculated and measured transverse temperature distribution at 2.8:1 power skew across the assembly. The behaviors are quite similar to the 2:1 power skew case, however, the maximum temperatures are higher as a consequence of the larger power gradients.

Figures 25 and 29 also show the transverse temperature distribution corresponding to the midplane of the heated section. It is seen that the agreement between the calculated and measured temperature distributions is good. Furthermore, the better agreement with experimental measurements, as compared to the exit of the heated section, suggests that differential bowing seems to be more pronounced towards the top of the assembly.

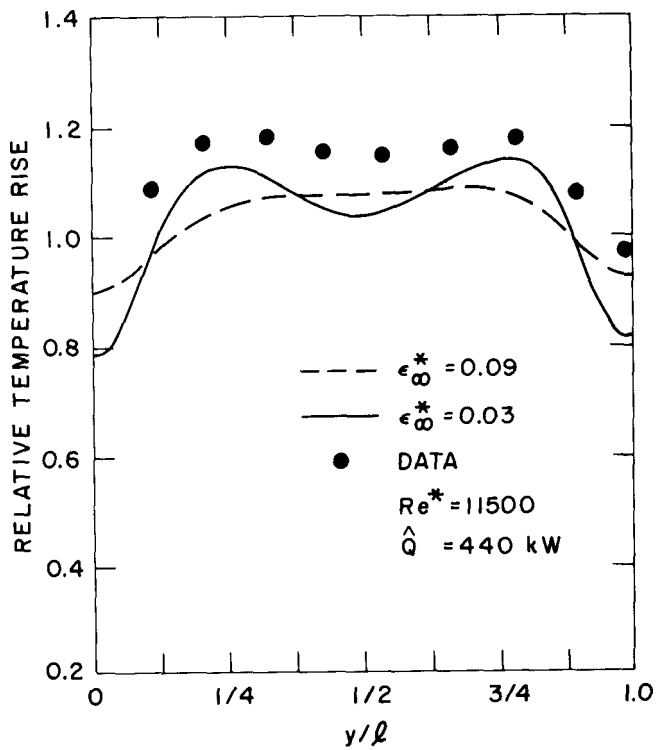

Fig. 18 Comparison of Calculated and Measured Transverse Temperature Distribution (Internal Blanket)

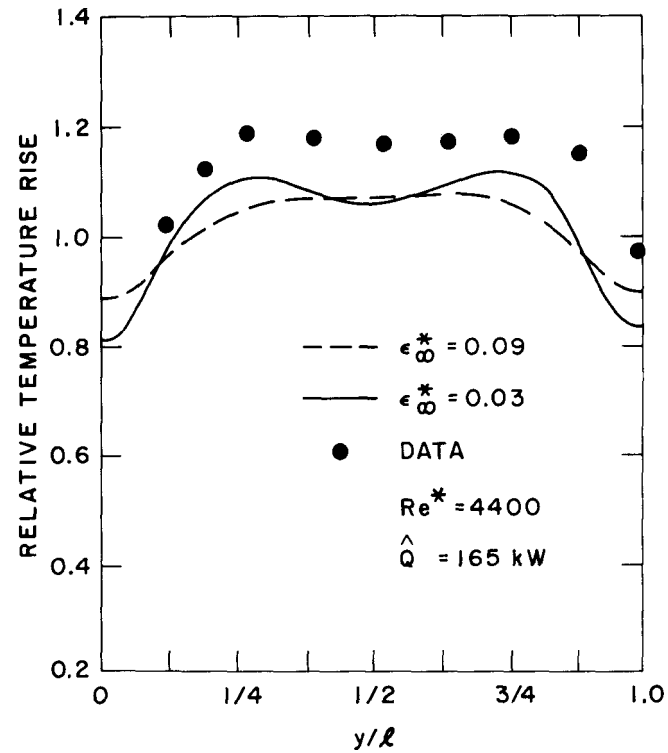

Fig. 19 Comparison of Calculated and Measured Transverse Temperature Distribution (Internal Blanket)

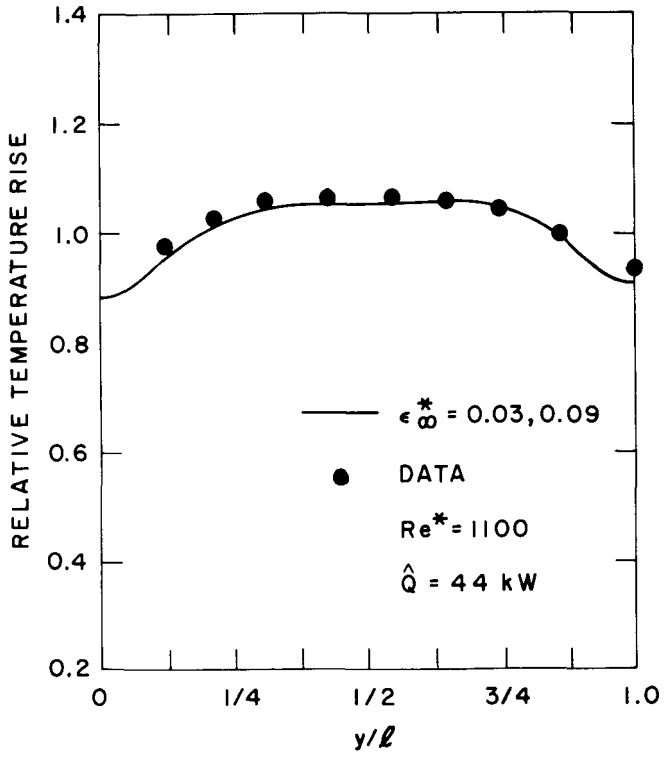

Fig. 20 Comparison of Calculated and Measured Transverse Temperature Distribution (Internal Blanket)

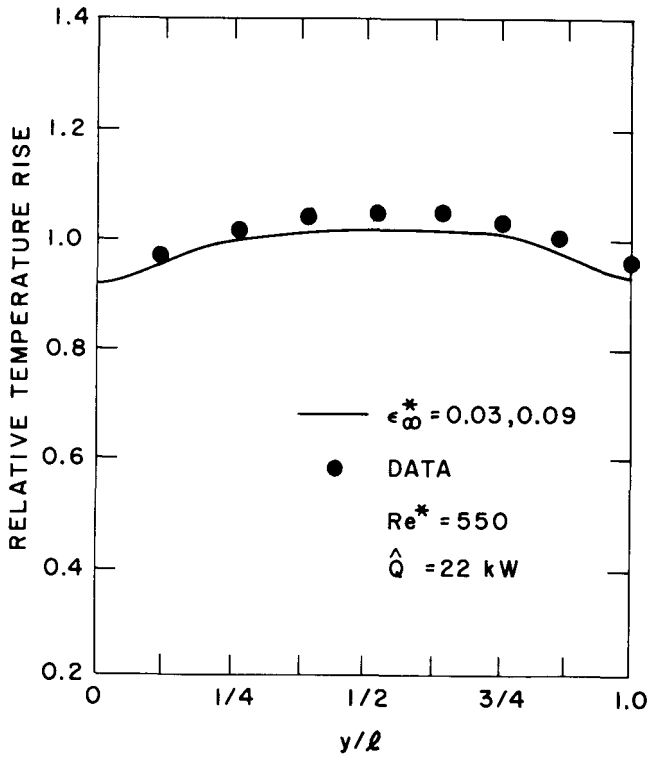

Fig. 21 Comparison of Calculated and Measured Transverse Temperature Distribution (Internal Blanket)

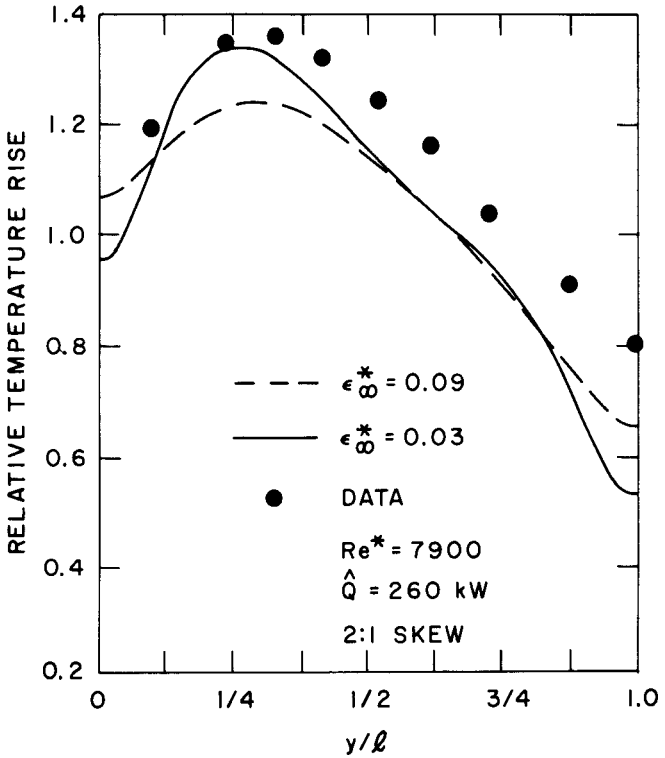

Fig. 22 Comparison of Calculated and Measured Transverse Temperature Distribution (2:1 Skew)

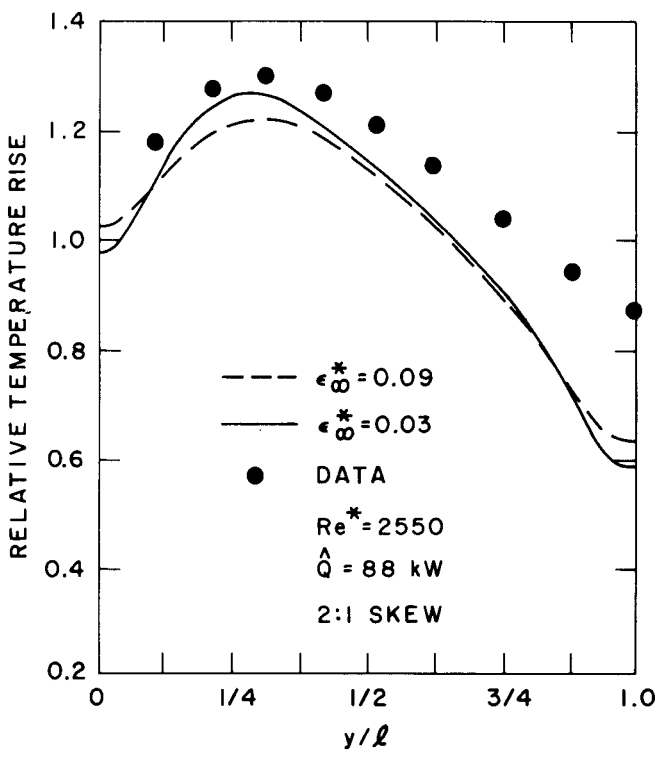

Fig. 23 Comparison of Calculated and Measured Transverse Temperature Distribution (2:1 Skew)

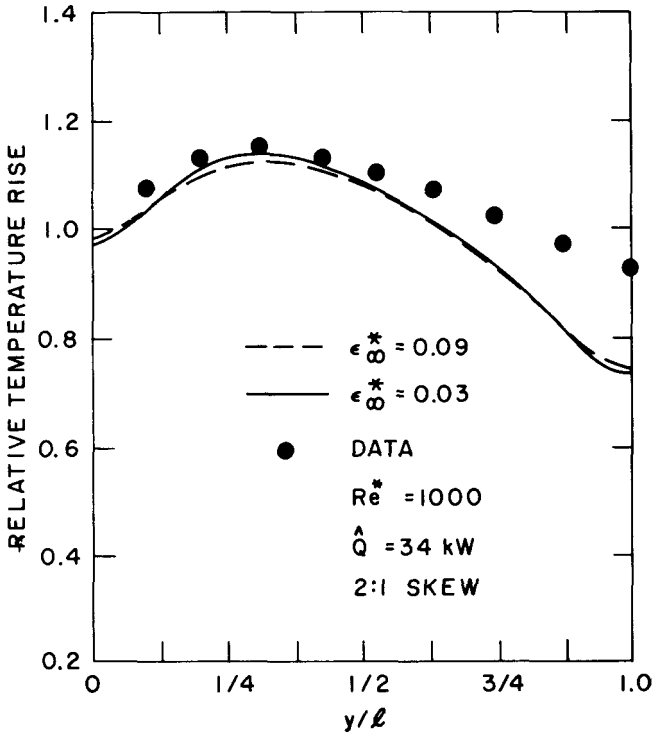

Fig. 24 Comparison of Calculated and Measured Transverse Temperature Distribution (2:1 Skew)

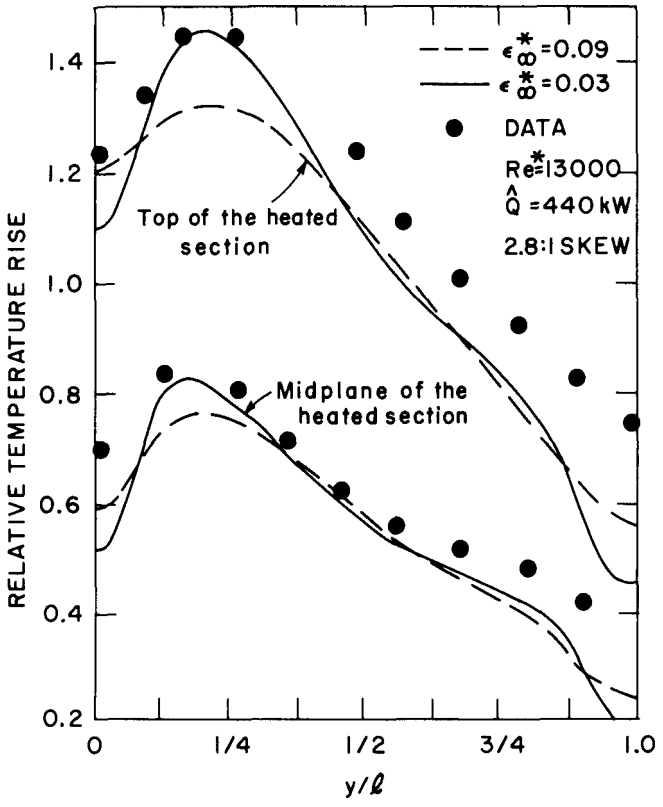

Fig. 25 Comparison of Calculated and Measured Transverse Temperature Distribution (2.8:1 Skew)

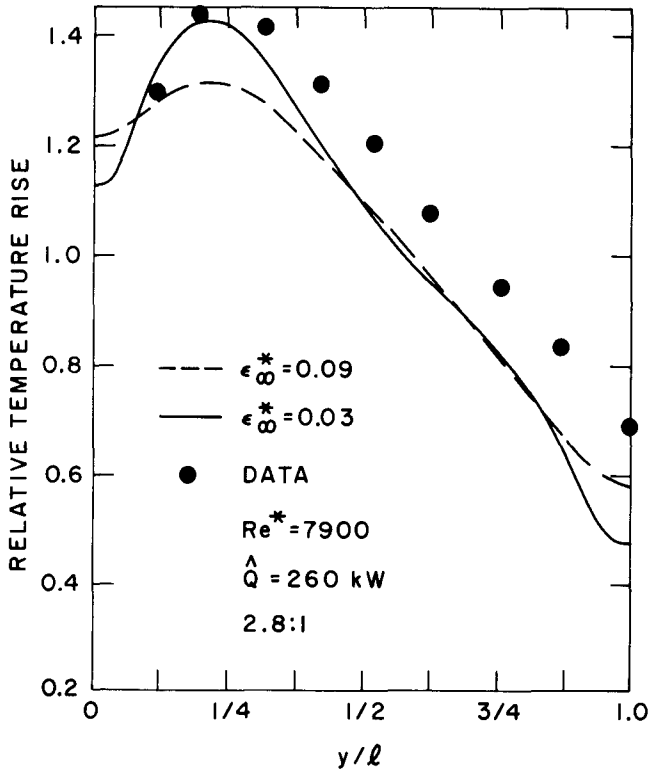

Fig. 26 Comparison of Calculated and Measured Transverse Temperature Distribution (2.8:1 Skew)

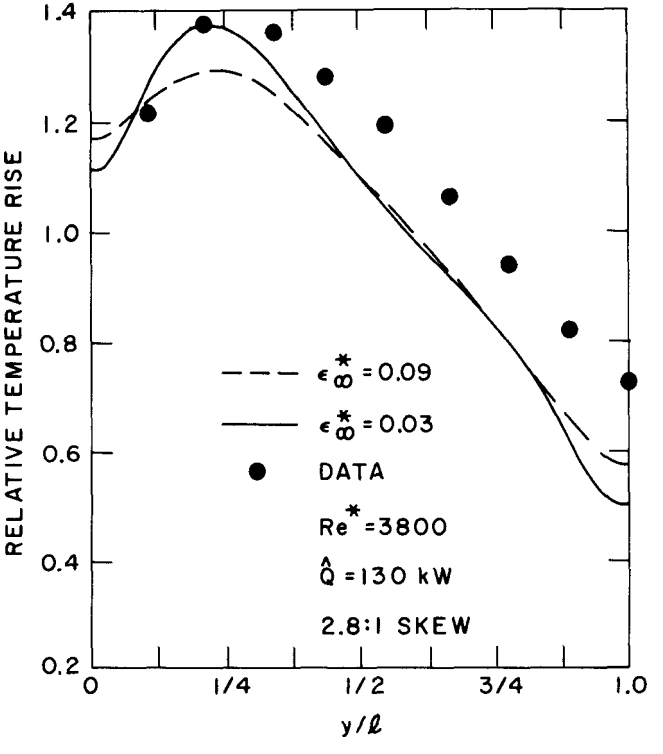

Fig. 27 Comparison of Calculated and Measured Transverse Temperature Distribution (2.8:1 Skew)

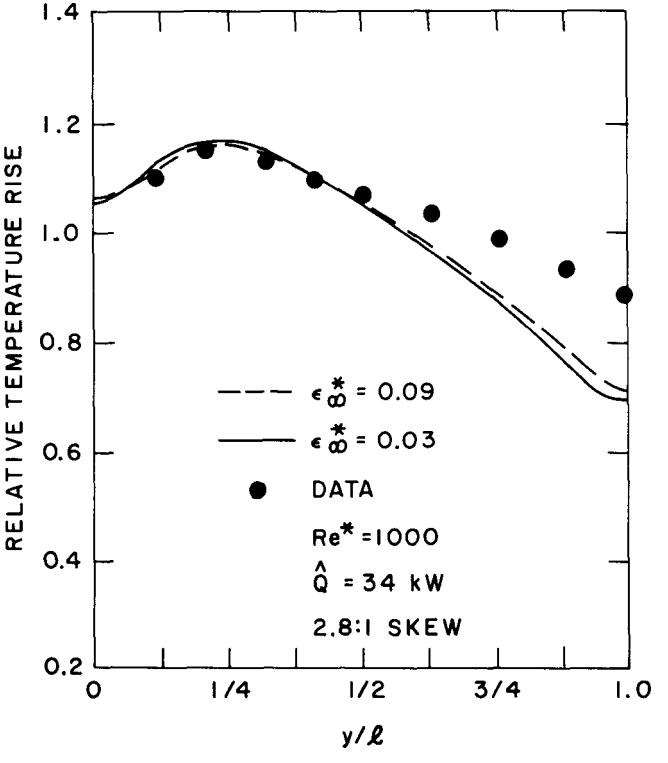

Fig. 28 Comparison of Calculated and Measured Transverse Temperature Distribution (2.8:1 Skew)

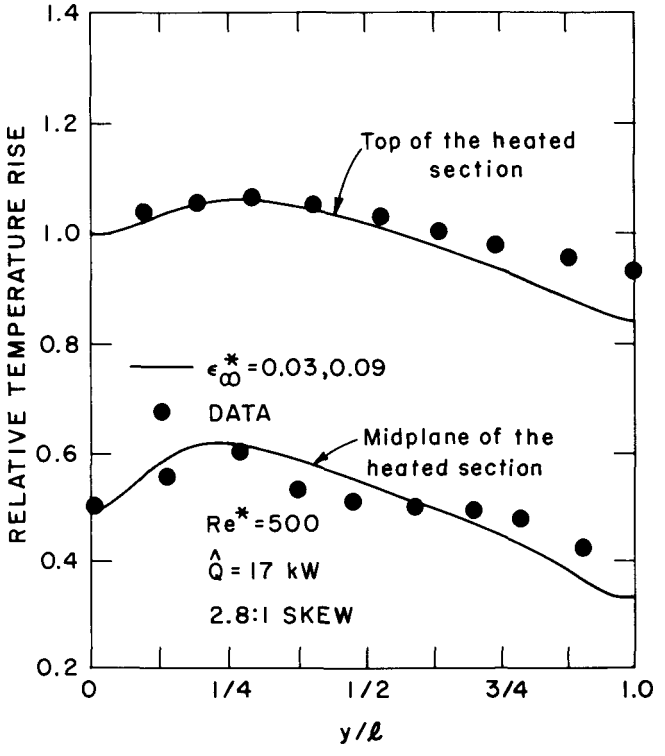

Fig. 29 Comparison of Calculated and Measured Transverse Temperature Distribution (2.8:1 Skew)

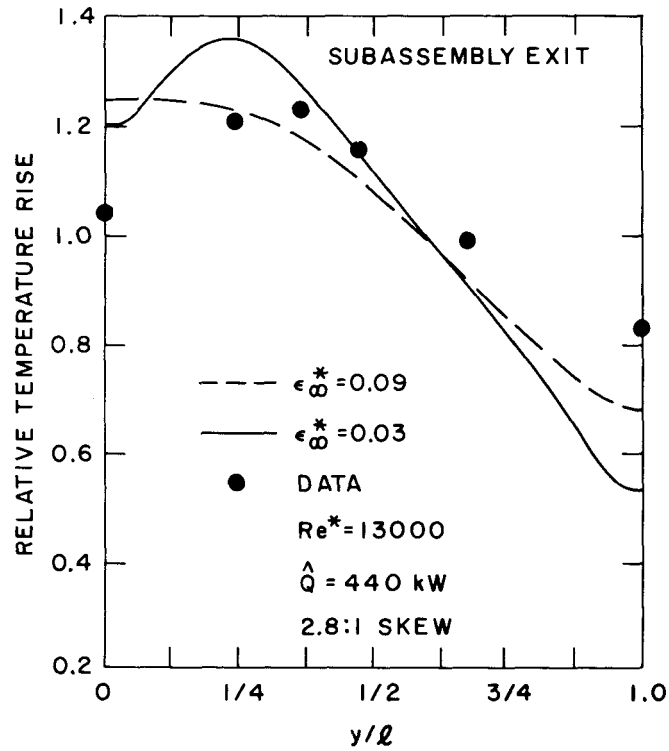

Fig. 30 Comparison of Calculated and Measured Transverse Temperature Distribution at the Subassembly Exit (2.8:1 Skew)

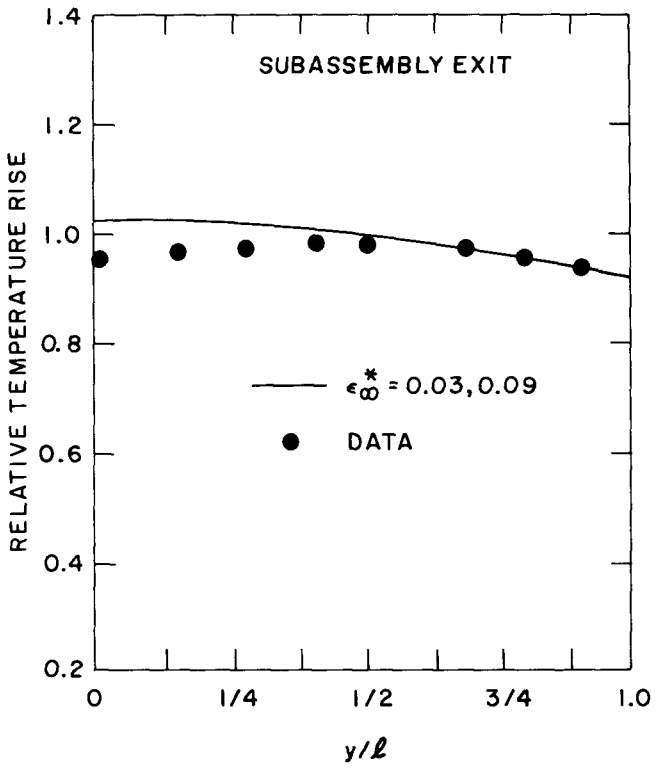

Fig. 31 Comparison of Calculated and Measured Transverse Temperature Distribution at the Subassembly Exit (2.8:1 Skew)

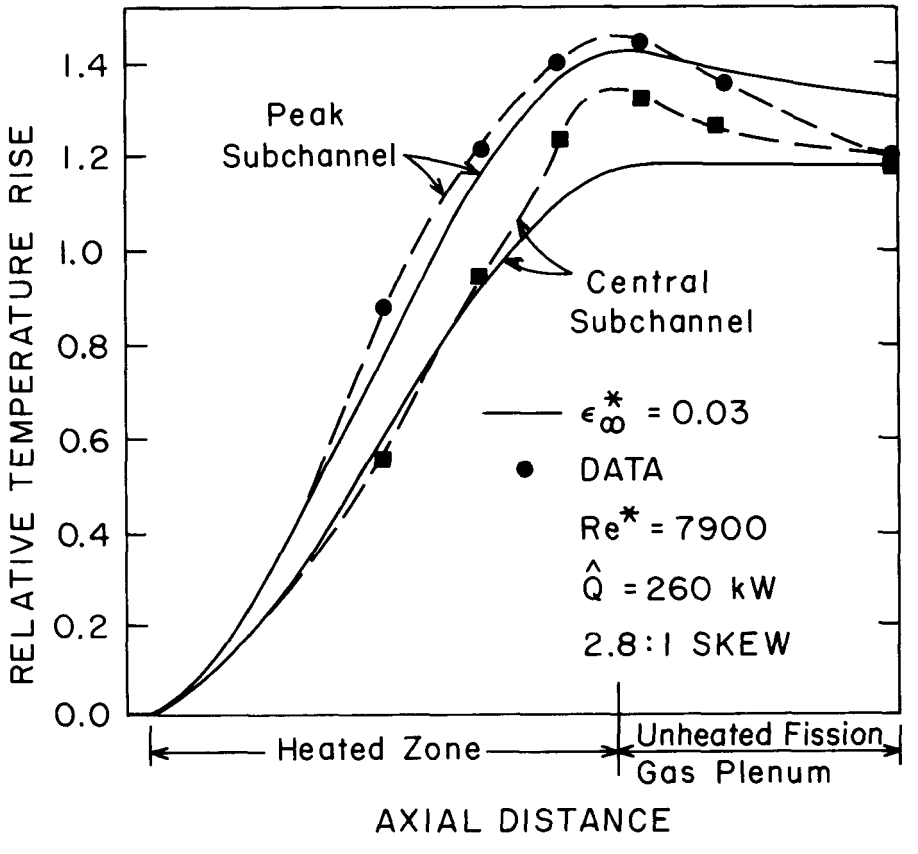

Fig. 32 Comparison of Calculated and Measured Axial Temperature Distribution for Peak and Central Subchannels (2.8:1 Skew)

Figures 30 and 31 illustrate the transverse temperature profiles at the exit of the subassembly (top of the unheated fission gas plenum region). At high Reynolds number (Fig. 30), there seems to be considerably more mixing between the side and interior channels as predicted by the present model, also in agreement with COTEC calculations [14]. At low Reynolds number (Fig. 31), the predicted profile is in excellent agreement to the measured data.

Figure 32 shows a longitudinal temperature distribution at Reynolds number of 7900 corresponding to 2.8:1 power skew. The agreement between predictions and measured data is good in the heated section with prediction of peak temperature becoming more conservative near the subassembly outlet. In the upper unheated region as mentioned earlier, in high Reynolds number range, mixing appears to be much stronger than predicted, leading to flatter measured transverse profile.

4.3.2 Comparison With Water Test Data

The Toshiba Water simulation test assembly shown schematically in Fig. 33, consists of 91 helically-wound wire spacer rods arranged in a triangular pitch configuration. Each simulator rod contains an electrically heated element to simulate nuclear heating with a chopped cosine axial power distribution [25, 26]. Table IV summarizes the geometric characteristics of the test assembly. Figure 33 also shows a cross sectional view of the rod bundle and the thermocouple locations placed at vertical planes L2 and L3.

Experimentally, bundle operating parameters were adjusted to achieve the desired flow rate and inlet temperature, then the power was gradually increased to the selected level. Measurements were taken following attainment of the steady-state operating conditions.

An interesting feature of these water simulation experiments is that due to the small thermal conductivity of the coolant, the impact of intra-assembly heat transfer is quite insignificant as compared to the buoyancy-induced flow redistribution. Thus, the data provide an excellent data base for confirmation of buoyancy-induced flow redistribution in rod bundle geometries.

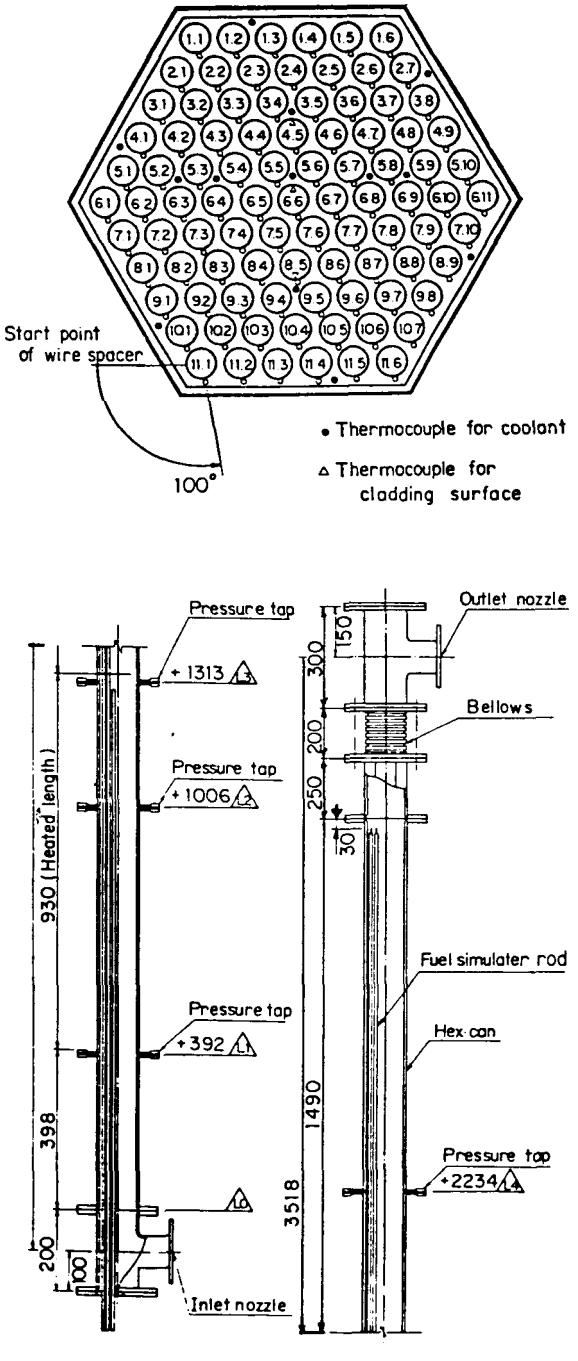

Fig. 33 Schematic of the Toshiba 91-Pin Test Model

Table IV Geometric Characteristics of the TOSHIBA 91 Pin Test Model

D_r	(m)	6.5×10^{-3}
D_w	(m)	1.3×10^{-3}
p/D_r	(-)	1.21
ℓ	(m)	0.07730
ℓ_1	(m)	0.06815
ℓ_2	(m)	0.00457
L_h	(m)	0.930
A_r	(m^2)	3.32×10^{-5}
A_w	(m^2)	1.33×10^{-6}
A_p	(m^2)	5.17×10^{-3}
D_{e1}	(m)	3.12×10^{-3}
D_{e2}	(m)	6.12×10^{-3}
D_{e3}	(m)	4.33×10^{-3}
D_{ea}	(m)	4.01×10^{-3}
α_1		0.7774
α_2		0.2086
α_3		0.0140
λ_1		0.3566
λ_2		0.5204
λ_3		0.5234
λ_a		0.3931

Recall in Eq. (3), κ, the molecular conduction correction factor was introduced to account for the reduction in effective conductivity of sodium due to the presence of the fuel rods. However, in the present experiment, the thermal conductivity of fuel rod simulators is much greater than the coolant (water). Thus, at low flow rates, heat tends to conduct much easier through the steel cladding and the wire-wrap than water (coolant), thus κ may be greater than unity.

The mixing parameter ε_∞^* is not very important for the Reynolds number regimes of these experiments and thus, the existing model is assumed to be valid.

In order to simulate the hydro-dynamic characteristics of the Toshiba assembly, the following friction factor correlations are used:

$$f = 37.4\ Re^{-0.872} \qquad Re \leq 1200 \qquad (101a)$$

$$f = 41.7/Re + 0.12\ Re^{-0.159} \qquad Re > 1200 \qquad (101b)$$

These relations compare favorably with the unheated test data as recommended by Mawatari, et al. [25].

A. Uniform Power Distribution

Figure 34 shows the comparison between measured [25,26] and calculated transverse temperature distribution corresponding to uniform transverse power distribution.

It is evident that good agreement exists between the measured and predicted results. At high Reynolds number the calculated relative temperature rise is within 9% of the experimentally measured values (less than 4°K in actual temperature).

At low Reynolds number the maximum discrepancy is seen to occur near the edges where the calculated relative temperature rise is within about 15% of the measured data (< 6°K in actual temperature).

Experiment	●	○
Calculation	——	– – –
Test No.	HT303-1	HT303-2
Re^*	336	3330
$\hat{\Delta T}$ (K)	38.6	36.1
T^* (K)	314	318

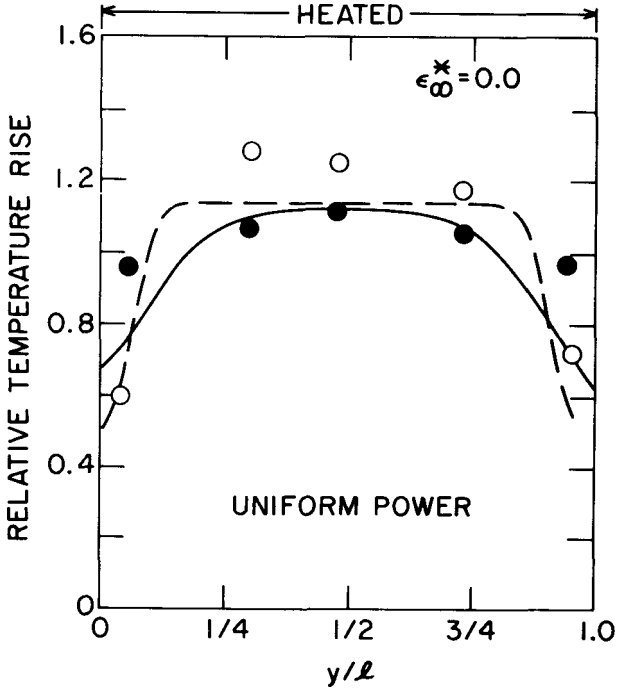

Fig. 34 Comparison of Calculated and Measured Transverse Temperature Distribution for Toshiba Experiments (Uniform)

B. Non-Uniform Power Distribution

Figure 35 shows the comparison between measured and calculated transverse temperature distribution corresponding to a non-uniform transverse power distribution.

In this case, one half of the bundle is heated uniformly (51 rods) while the other half (remaining 40 rods) are unheated. This gives rise to a large temperature gradient between the heated and unheated halves of the test section.

It is clearly evident that at high Reynolds number the agreement between the calculated and measured data is excellent. However, at low Reynolds number natural convection conditions, experimental measurements indicate significant energy redistribution to the unheated side of the bundle, while the present calculations show a much smaller flattening effect.

This may be attributed to three effects, namely; (1) continued swirl flow mixing at low flows, (2) enhanced molecular conduction through the cladding and the wire-wraps, and (3) bowing and bundle distortion caused by large transverse power gradient across the assembly.

Experiment	●	○
Calculation	———	- - - -
Test No.	HT401-1	HT401-10
Re^*	334	2920
$\hat{\Delta T}$ (K)	40.2	38.3
T^* (K)	314	319

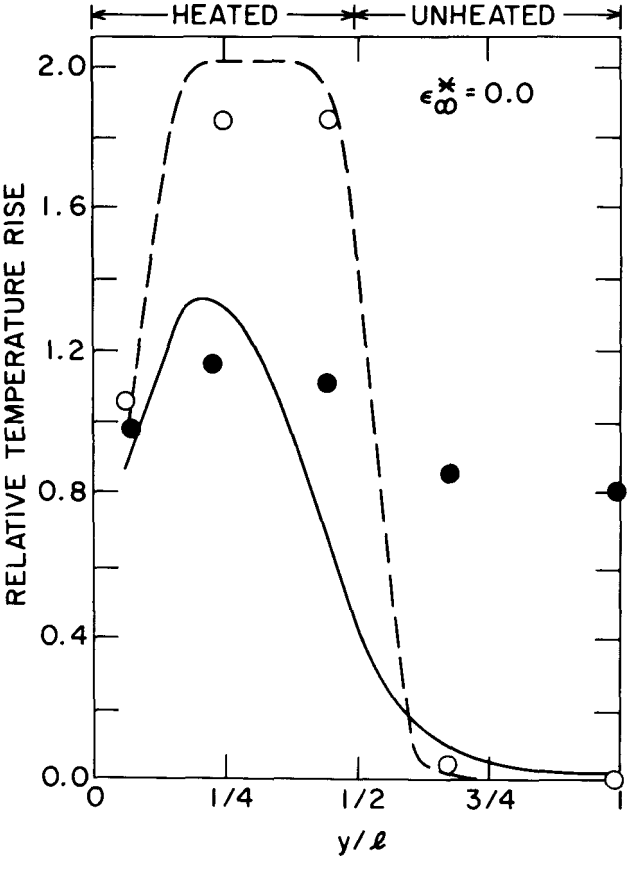

Fig. 35 Comparison of Calculated and Measured Transverse Temperature Distribution for Toshiba Experiments (Partially Uniform)

5. TRANSIENT POROUS-BODY MODEL

The model described in the previous chapter is applicable to steady-steady or quasi-steady processes. However, for the study of protected loss-of-flow events in LMFBR subassemblies, where the flow regime changes quickly from forced to mixed and eventually free convection, a time dependent model is desirable.

In this chapter, the previously developed (see 4.1) parabolic flow model is extended to include transient processes. The model and the resulting computer code is then used to post-predict the 61-pin rod bundle transient experiments conducted at Westinghouse [27].

5.1 Governing Equations

The basic conservation equations of section 2.1 can be easily extended to include the time-dependent terms assuming that the Boussinesq approximation for incompressible fluids holds (density is a constant of motion, i.e., $\frac{\partial \rho}{\partial t} = 0$), thus:

a) Conservation of Mass:

$$\frac{\partial(\rho u)}{\partial x} + \frac{\partial(\rho v)}{\partial y} = 0 \tag{102}$$

b) Conservation of Energy:

$$\frac{\partial T}{\partial t} + u\frac{\partial T}{\partial x} + v\frac{\partial T}{\partial y} = \alpha_e \frac{\partial^2 T}{\partial y^2} + \frac{Q'''(x,y)}{\rho c_p} \tag{103}$$

c) Conservation of Axial Momentum:

$$\frac{\partial u}{\partial t} + u\frac{\partial u}{\partial x} + v\frac{\partial u}{\partial y} = -\frac{1}{\rho}\frac{\partial P}{\partial x} - g\frac{\rho^*}{\rho}[1 - \beta(T-T^*)] + \nu\frac{\partial^2 u}{\partial y^2} + \frac{f}{2D_e\lambda^2}u^2 \tag{104}$$

Subject to the following initial and boundary conditions:

Initial Conditions

$$\left.\begin{aligned} u(x,y,o) &= \text{known} \\ v(x,y,o) &= \text{known} \\ T(x,y,o) &= \text{known} \end{aligned}\right\} \text{ Through Steady-State Solution,} \qquad (105)$$

Boundary Conditions

$$\begin{aligned} u(o,y,t) &= \text{specified} \\ T(o,y,t) &= \text{specified} \\ Q'''(x,y,t) &= \text{specified} \end{aligned} \qquad (106)$$

Furthermore, the heat flux at the duct walls is assumed to be continuous.

The energy equations for the stagnant sodium region adjacent to the duct wall and the duct wall structure can be written as:

Stagnant Sodium

$$M_s C_s \frac{dT_s}{dt} = \frac{k_d}{\delta_d} A_d (T_d - T_s) \qquad \begin{matrix} s=1,N \\ d=2,N-1 \end{matrix} \qquad (107)$$

Duct Wall

$$M_d C_d \frac{dT_d}{dt} = \frac{k_d}{\delta_d} A_d (T_s - T_d) + \frac{k_s}{\Delta y} A_d (T_{d'} - T_d) \qquad (108)$$

$$d' = 3 \quad \text{for} \quad d = 2$$

$$d' = N-2 \quad \text{for} \quad d = N-1$$

where M is the mass, C is the specific heat, k is the thermal conductivity, δ is the wall thickness, A is the heat transfer area, and the subscripts d and s refer to the duct wall and the sodium, respectively.

The forms of equations (107) and (108) indicate that the duct wall outer surface is at equilibrium with the stagnant sodium layer (usually present between subassemblies).

Initially (t = o) the adiabatic boundary condition is identically satisfied, that is:

$$\begin{cases} T_1 = T_2 = T_3 \\ T_N = T_{N-1} = T_{N-2} \end{cases} \tag{109}$$

5.2 Method of Solution

5.2.1 Finite Difference Equations

In finite difference form, Equations (102) through (108) can be expressed as follows:

Mass Continuity

$$\left[\frac{(\rho u)_{i+1,j} + (\rho u)_{i+1,j+1} - (\rho u)_{i,j} - (\rho u)_{i,j+1}}{2\Delta x}\right]^{k+1} + \left[\frac{(\rho v)_{i+1,j+1} - (\rho v)_{i+1,j}}{\Delta y}\right]^{k+1} = 0 \tag{110}$$

Energy

$$\left[\frac{T^{k+1}_{i+1,j} - T^{k}_{i+1,j}}{\Delta t}\right] + u^{k+1}_{i,j}\left[\frac{T^{k+1}_{i+1,j} - T^{k+1}_{i,j}}{\Delta x}\right] + v^{k+1}_{i,j}\left[\frac{T^{k+1}_{i+1,j+1} - T^{k+1}_{i+1,j-1}}{2\Delta y}\right] = \tag{111}$$

$$\alpha_e \left[\frac{T^{k+1}_{i+1,j+1} - 2\,T^{k+1}_{i+1,j} + T^{k+1}_{i+1,j-1}}{(\Delta y)^2}\right] + \frac{Q'''^{k+1}_{i,j}}{\rho c_p}$$

Axial Momentum

$$\left[\frac{u_{i+1,j}^{k+1} - u_{i+1,j}^{k}}{\Delta t}\right] + u_{i,j}^{k+1}\left[\frac{u_{i+1,j}^{k+1} - u_{i,j}^{k+1}}{\Delta x}\right] + v_{i,j}^{k+1}\left[\frac{u_{i+1,j+1}^{k+1} - u_{i+1,j-1}^{k+1}}{2\Delta y}\right]$$

$$= -\left[\frac{\Delta\tilde{P}}{\Delta x}\right]_{i+1}^{k+1} - \frac{f_{i,j}^{k+1}}{2D\lambda_{i,j}^{2}} u_{i,j}^{k+1} u_{i+1,j}^{k+1} + g\beta\,(T_{i+1,}^{k+1} - T^{*k+1}) +$$

$$\nu_{i,j}\left[\frac{u_{i+1,j+1}^{k+1} - 2\,u_{i+1,j}^{k+1} + u_{i+1,j-1}^{k+1}}{(\Delta y)^2}\right] \qquad (112)$$

Stagnant Sodium

$$\left[\frac{M_s\,C_s}{\Delta t} + \frac{k_d}{\delta_d} A_d\right] T_{i+1,s}^{k+1} - \frac{k_d}{\delta_d} A_d\, T_{i+1,d}^{k+1} = \frac{M_s\,C_s}{\Delta t}\, T_{i+1,s}^{k} \qquad (113)$$

Duct Wall

$$\left[\frac{M_d\,C_d}{\Delta t} + \frac{k_d}{\delta_d} A_d + \frac{k_s}{\Delta y} A_d\right] T_{i+1,d}^{k+1} - \frac{k_d}{\delta_d} A_d\; T_{i+1,s}^{k+1} - \frac{k_s}{\Delta y}\; A_d\, T_{i+1,d'}^{k+1}$$

$$= \frac{M_d\,C_d}{\Delta t}\, T_{i+1,d}^{k} \qquad (114)$$

where Δt is the time-step, and the superscripts k and k+1 denote the previous and current time values, respectively.

The time-differencing forms of Eqs. (110) through (114) are based on the fully implicit formulation, which are unconditionally stable [28] for any value of Δt. However, the time-step size is governed by the desired degree of accuracy which is discussed in the following subsection.

Equations (110) through (114) can be recasted into the familiar matrix forms described in section 4.2.1 to obtain:

$$\begin{bmatrix} \phi_{i,1} & \sigma_{i,2} & 0 & 0 & 0 & \cdots & 0 \\ \zeta_{i,1} & \phi_{i,2} & \sigma_{i,3} & 0 & 0 & \cdots & 0 \\ 0 & \zeta_{i,2} & \phi_{i,3} & \sigma_{i,4} & 0 & \cdots & 0 \\ \vdots & \ddots & \ddots & \ddots & \ddots & & \vdots \\ & & & & & & 0 \\ & & & & & & \sigma_{i,N} \\ 0 & \cdots & \cdots & \cdots & \cdots & \zeta_{i,N-1} & \phi_{i,N} \end{bmatrix} \begin{bmatrix} T^{k+1}_{i+1,1} \\ T^{k+1}_{i+1,2} \\ T^{k+1}_{i+1,3} \\ \vdots \\ T^{k+1}_{i+1,N-1} \\ T^{k+1}_{i+1,N} \end{bmatrix} = \begin{bmatrix} C_{i,1} \\ C_{i,2} \\ C_{i,3} \\ \vdots \\ C_{i,N-1} \\ C_{i,N} \end{bmatrix} \tag{115}$$

where:

$$\phi_{i,1} = \phi_{i,N} = \left[\frac{M_s C_s}{\Delta t} + \frac{k_d}{\delta_d} A_d\right] \tag{116a}$$

$$\phi_{i,2} = \phi_{i,N-1} = \left[\frac{M_d C_d}{\Delta t} + \frac{k_d}{\delta_d} A_d + \frac{k_s}{\Delta y} A_d\right] \tag{116b}$$

$$\phi_{i,j} = \left[\frac{1}{\Delta t} + \frac{u_{i,j}^{k+1}}{\Delta x} + \frac{2\alpha_e}{(\Delta y)^2}\right] \tag{116c}$$

$$\sigma_{i,2} = \sigma_{i,N} = -\left[\frac{k_d}{\delta_d} A_d\right] \tag{116d}$$

$$\sigma_{i,3} = -\left[\frac{k_s}{\Delta y} A_d\right] \tag{116e}$$

$$\sigma_{i,j} = \left[\frac{v_{i,j-1}^{k+1}}{2\Delta y} - \frac{\alpha_e}{(\Delta y)^2}\right] \tag{116f}$$

$$\zeta_{i,1} = \zeta_{i,N-1} = -\left[\frac{k_d}{\delta_d} A_d\right] \tag{116g}$$

$$\zeta_{i,N-2} = -\left[\frac{k_s}{\Delta y} A_d\right] \tag{116h}$$

$$\zeta_{i,j} = \left[\frac{v_{i,j+1}^{k+1}}{2\Delta y} + \frac{\alpha_e}{(\Delta y)^2}\right] \tag{116i}$$

$$C_{i,1} = \left[\frac{M_s\ C_s}{\Delta t}\right] T^k_{i,1} \tag{116j}$$

$$C_{i,2} = \left[\frac{M_d\ C_d}{\Delta t}\right] T^k_{i,2} \tag{116k}$$

$$C_{i,j} = \left[\frac{Q'''^{k+1}_{ij}}{\rho c_p} + \frac{T^k_{i,j}\ u^{k+1}_{i,j}}{\Delta x} + \frac{T^k_{i,j}}{\Delta t}\right] \quad j = 3,4,\ldots,N-2 \tag{116ℓ}$$

$$C_{i,N-1} = \left[\frac{M_d\ C_d}{\Delta t}\right] T^k_{i,N-1} \tag{116m}$$

$$C_{i,N} = \left[\frac{M_s\ C_s}{\Delta t}\right] T^k_{i,N} \tag{116n}$$

Similarly, Eqs. (89) and (112) can be written as:

$$\begin{bmatrix}
\rho_{i+1,3} & \rho_{i+1,4} & \rho_{i+1,5} & \rho_{i+1,6} & \rho_{i+1,7} & \cdots & \rho_{i+1,N-2} & 0 \\
\gamma_{i+1,3} & \Omega_{i+1,4} & 0 & 0 & 0 & \cdots & 0 & \frac{1}{\Delta x} \\
\Gamma_{i+1,3} & \gamma_{i+1,4} & \Omega_{i+1,5} & 0 & 0 & & & \\
0 & \Gamma_{i+1,4} & \gamma_{i+1,5} & \Omega_{i+1,6} & 0 & & & \\
0 & 0 & \ddots & \ddots & \ddots & & 0 & \frac{1}{\Delta x} \\
0 & 0 & \cdots & 0 & \Gamma_{i+1,N-4} & \gamma_{i+1,N-3} & \Omega_{i+1,N-2} & \frac{1}{\Delta x}
\end{bmatrix}
\begin{bmatrix}
u^{k+1}_{i+1,3} \\ u^{k+1}_{i+1,4} \\ \\ \\ u^{k+1}_{i+1,N-2} \\ \Delta\tilde{P}^{k+1}_{i+1}
\end{bmatrix}$$

$$= \begin{bmatrix} S_{i+1} \\ C_{i+1,3} \\ C_{i+1,4} \\ \vdots \\ C_{i+1,N-2} \end{bmatrix} \tag{117a}$$

and

$$u^{k+1}_{i+1,1} = u^{k+1}_{i+1,2} = u^{k+1}_{i+1,N-1} = u^{k+1}_{i+1,N} = 0 \tag{117b}$$

where,

$$\gamma_{i+1,j} = \left[\frac{1}{\Delta t} + \frac{u^{k+1}_{i,j}}{\Delta x} + \frac{f^{k+1}_{i,j}}{2D_{i,j}} \frac{u^{k+1}_{i,j}}{\lambda^2_{i,j}} + \frac{2\nu_{i,j}}{(\Delta y)^2} \right] \tag{118a}$$

$$\Omega_{i+1,j} = \left[\frac{v^{k+1}_{i,j}}{2\Delta y} - \frac{\nu_{i,j}}{(\Delta y)^2} \right] \tag{118b}$$

$$\Gamma_{i+1,j} = -\left[\frac{v^{k+1}_{i,j}}{2\Delta y} + \frac{\nu_{i,j}}{(\Delta y)^2} \right] \tag{118c}$$

$$S_{i+1} = \sum_{j=3}^{N-2} \left[\rho_{i,j}\, u_{i,j}\right]^{k+1} \qquad (118d)$$

$$C_{i+1,j} = \frac{1}{\Delta t}\, u^{k}_{i+1,j} + \frac{u^{k+1}_{i,j}}{\Delta x} + g\beta \left[T^{k+1}_{i+1,j} - T^{*k+1}\right] \qquad (118e)$$

5.2.2 Numerical Solution Procedure

The numerical solution procedure is somewhat similar to the steady-state calculations described in Section 4.2.2. The steps are to:

1) Carry out the steady-state initialization (t = 0) and set the time step.

2) Calculate the forcing functions (i.e., time-dependent Q''', u_{in}, T^*).

3) Start at i=1 row and solve Eq. (115) for $T^{k+1}_{2,1}$, $T^{k+1}_{2,2}$,....., $T^{k+1}_{2,N}$ using the Gaussian elimination technique [22].

4) Calculate the physical properties as a function of $T_{i+1,j}$'s.

5) Solve Eq. (117) for $u^{k+1}_{2,1}$, $u^{k+1}_{2,2}$,....., $u^{k+1}_{2,N}$ and $\Delta\tilde{P}^{k+1}_{2}$ using the Gauss-Jordan reduction method [22].

6) Back substitute into Eq. (110) to obtain $v^{k+1}_{2,1}$, $v^{k+1}_{2,2}$,....., $v^{k+1}_{2,N}$.

7) March in the stream-wise direction up to i=M row; repeating steps (3) through (6).

8) Adjust the time step using:

$$\text{if} \quad \begin{cases} \left| \dfrac{T_{i,j}^{k+1} - T_{i,j}^{k}}{T_{i,j}^{k}} \right| \leq \varepsilon \; ; \; \Delta t^{k+1} = = 2\Delta t^{k} \\ \text{otherwise} \; ; \; \Delta t^{k+1} = \Delta t^{k}/2 \end{cases} \tag{119}$$

However the time step must be limited to

$$\Delta t_{min} \leq \Delta t \leq \Delta t_{max} \tag{120}$$

9) Advance the time and repeat steps (2) through (8) above.

The present steady-state and transient model has been assembled into a computer code, named TWIST.

The user's manual for the TWIST code along with the source listing is given in Appendix B. It must be noted, that code modifications to include other boundary conditions can be readily made; therefore the program structure is sufficiently generalized to perform a variety of steady-state and transient calculations.

5.3 Results and Comparison with Experimental Data

The transient porous-body model described in the previous sections is used to simulate the heat transfer tests performed at the Westinghouse blanket test model described earlier in sections 3.1.2.2 and 4.3.1.

The experiments were performed by first establishing steady state conditions (power input, flow, temperature) and then decreasing the power input and sodium flow at pre-programmed rates [27]. The test series included tests with heat input to all rods, and also to four rows (26 rods) only. The transients simulated both undercooling and overcooling events.

A. Undercooling Event

Engel, et al., [27] report results for four transient undercooling events corresponding to various heat-input gradients.

For the purpose of the current simulation, Test Run 613 is chosen. This test corresponds to 1:0 maximum-to-minimum heat input, where only 26 of the 61 rods were uniformly heated giving rise to large temperature gradients between the heated and unheated halves of the test section.

Initially, the bundle was operating at 188 kw power, 56 gpm flow and 588K sodium inlet temperature condition. The bundle power and sodium flow rates were changed in a pre-programmed manner to achieve the rates displayed in Figs. 36 and 37.

In steady-state operations, the power-to-flow ratio is a measure of the mean sodium temperature rise through the test section (see Fig. 38). During the transient, the temperature rise is also affected by the stored heat released from the heater rods and/or the duct walls. It must be noted that the present model assumes that the heat input is directly deposited into the coolant, and thus neglects the heat storage effects which can influence the early stages of the transient. However, modification of the model to include fuel pin to coolant heat transfer is straightforward.

Figures 39 through 41 illustrate the effect of transient operation on cross-assembly temperature profiles. Also shown are the corresponding measured values.

It is seen that a significant profile flattening takes place, similar to the steady state cases studied earlier in Chapter 4. Furthermore, maximum discrepancies between the calculated and measured temperatures occur in the unheated side of the bundle, similar to the earlier steady-state observations. However, the peak sodium temperatures are in excellent agreement with the test data.

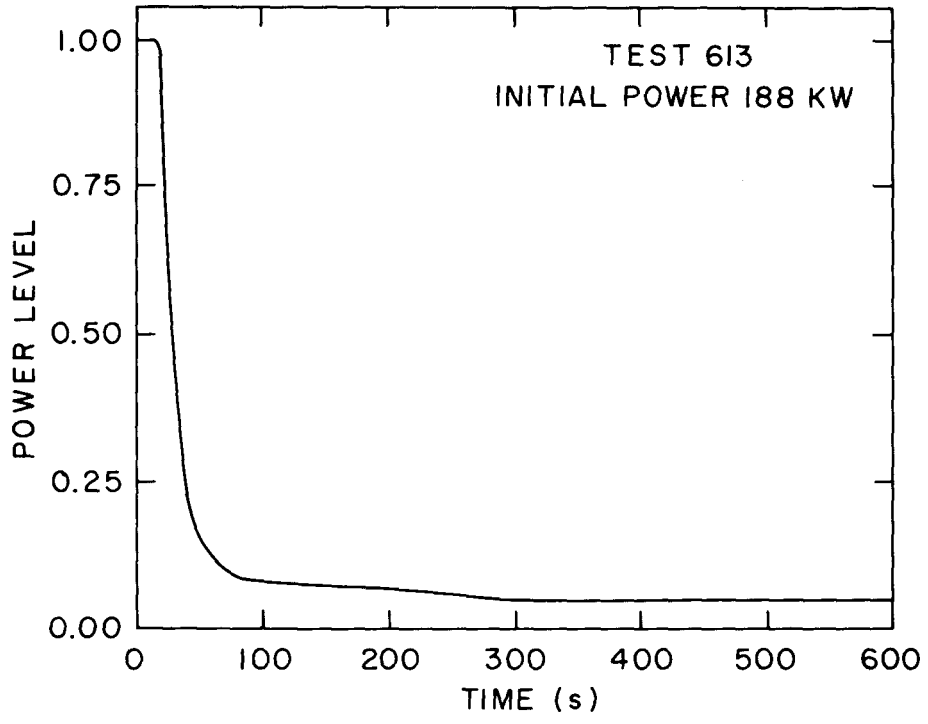

Fig. 36 Input Power Level (Test 613)

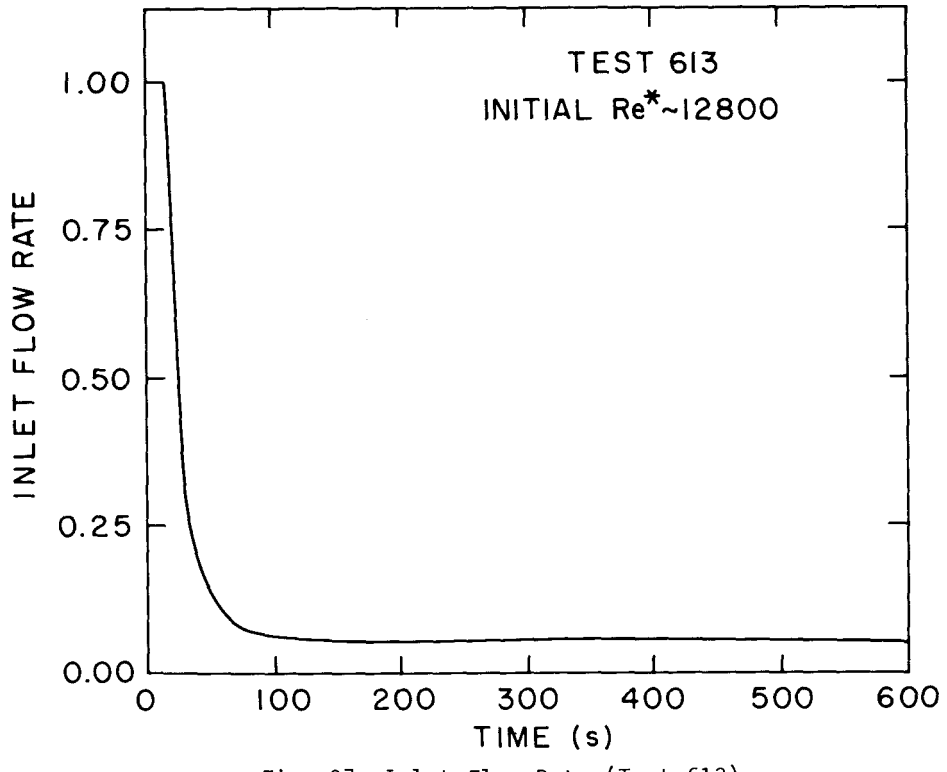

Fig. 37 Inlet Flow Rate (Test 613)

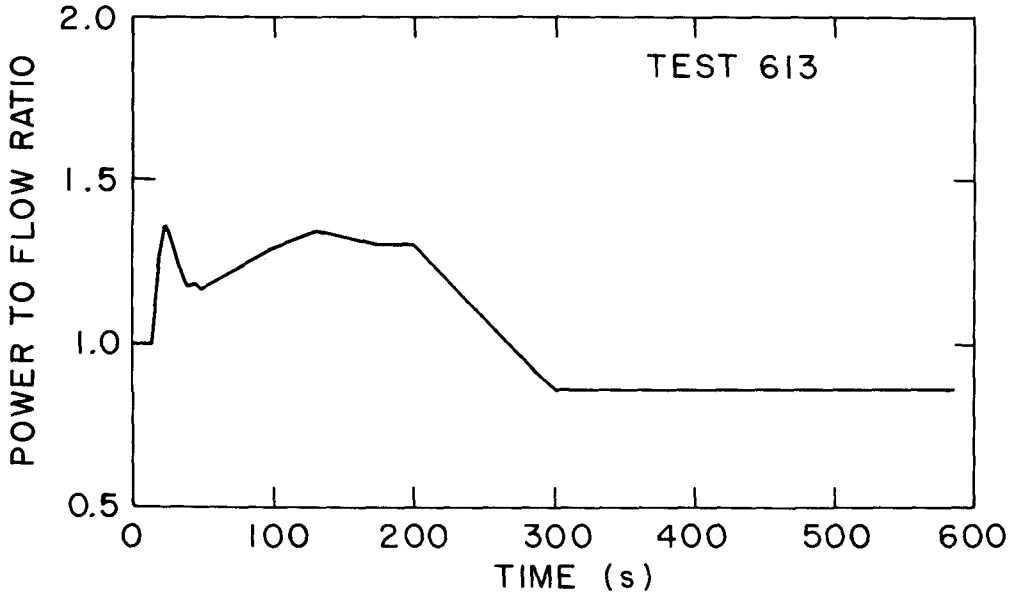

Fig. 38 Power to Flow Ratio (Test 613)

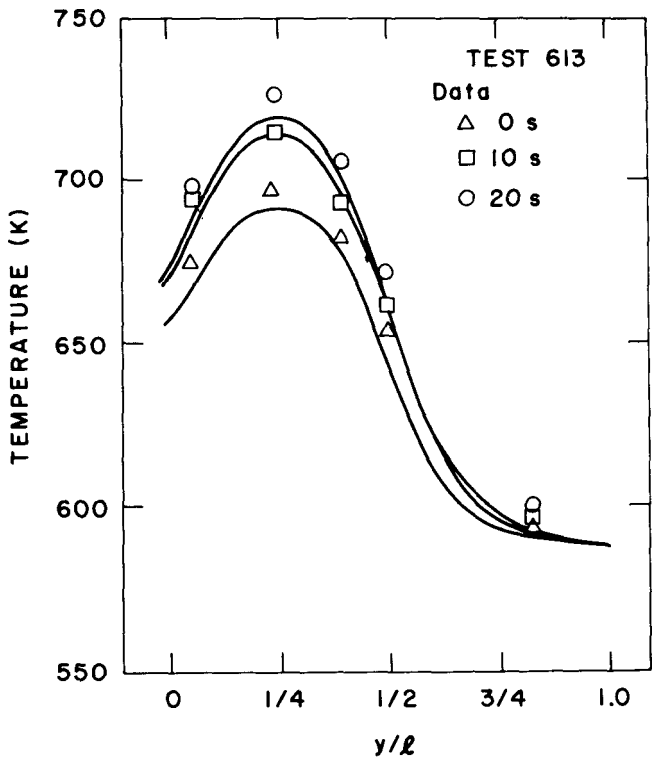

Fig. 39 Comparison of Calculated and Measured Transient Temperature Distributions for Test 613 (Early)

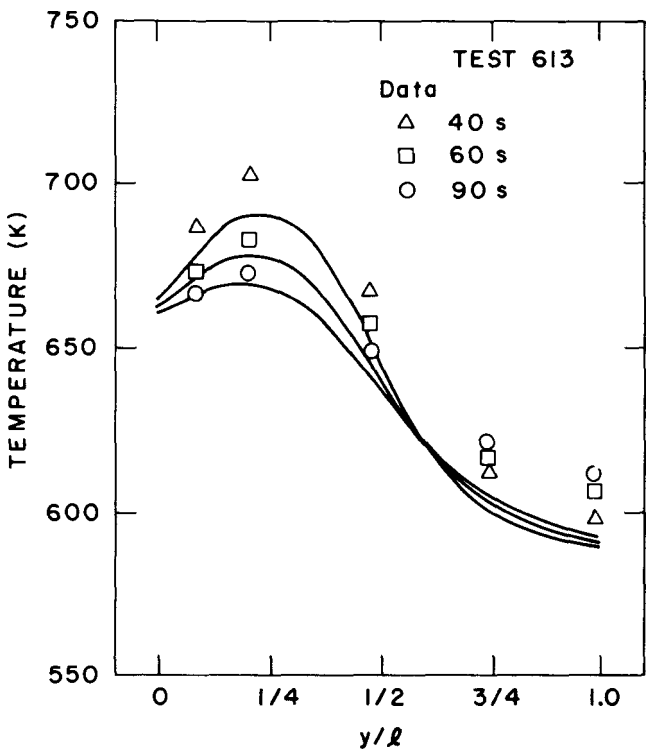

Fig. 40 Comparison of Calculated and Measured Transient Temperature Distribution for Test 613 (Intermediate)

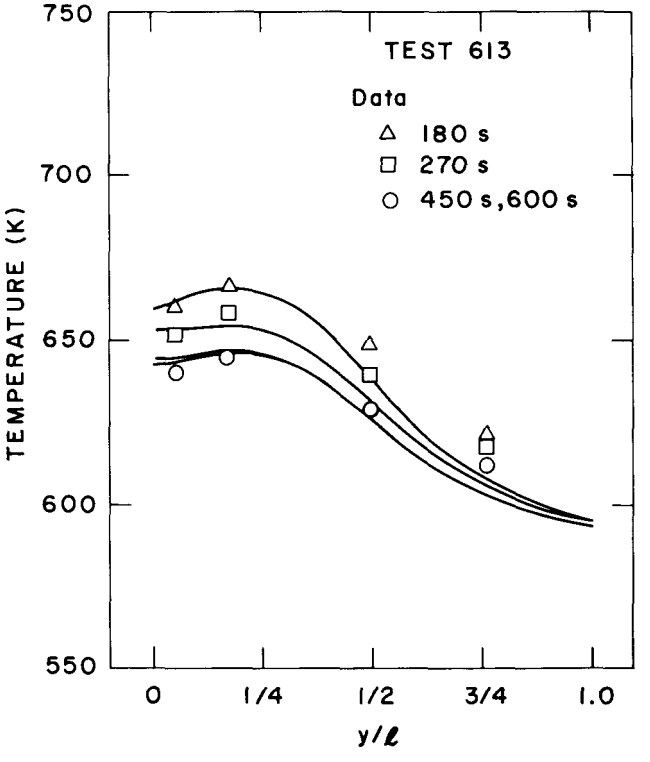

Fig. 41 Comparison of Calculated and Measured Transient Temperature Distributions for Test 613 (Late)

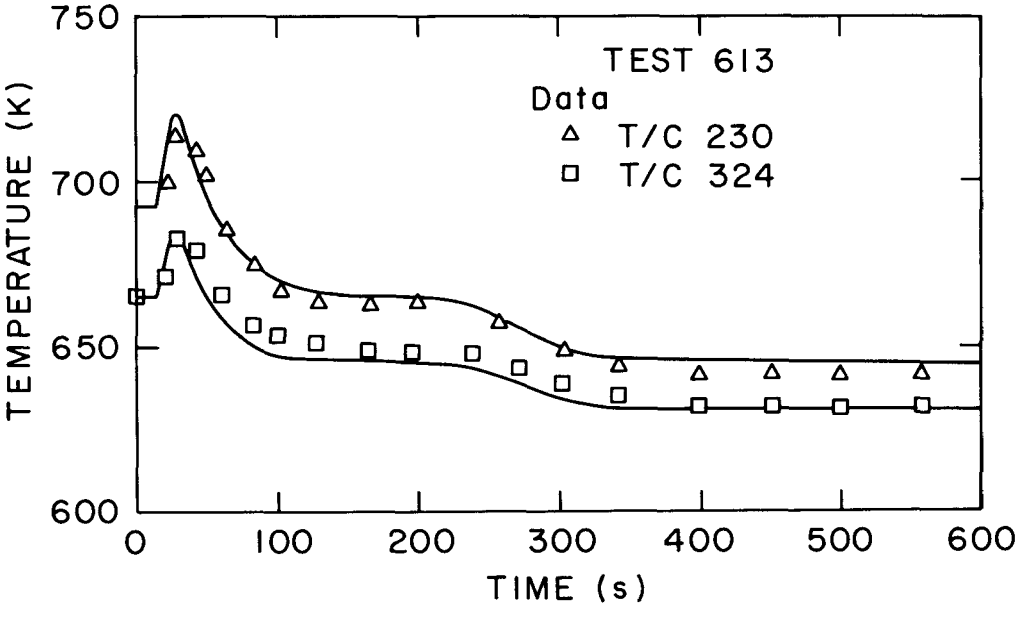

Fig. 42 Comparison of Calculated and Measured Temporal Variations of Sodium Temperature at T/C #230 and #324 for Test 613

Figure 42 shows that peak sodium temperatures are in excellent agreement with the measured data where the temperatures follow the behavior of the power to flow ratio (Fig. 38). However, the peak temperatures are higher during the initial high flow part of the transient even when the power-to-flow ratio peaked back to near initial high values later in the transient. This reflects contribution of buoyancy-induced flow redistribution and transverse thermal conduction effects which had been observed in low flow steady state tests. Heat transfer to the surrounding sodium and structures is also a significant contributing effect.

B. Overcooling Event

Engel, et al. [27] also performed two transient overcooling events; namely, run numbers 609 and 611, corresponding to heat input gradients of 2.8 to 1, and uniform distribution across the bundle.

Figure 43 shows the transient power-to-flow ratio forcing function approximating the measured values of the run number 611. Initially, the bundle was operating at 440 kw power, 56 gpm flow and 588 K sodium inlet temperature condition.

Following the transient initiation the power and flow rates are changed in order to achieve a rapid undercooling of the subassembly as shown by the power-to-flow ratio in Fig. 43.

Figures 44 and 46 illustrate the cross-assembly temperature profiles as calculated by the present model. Clearly, the overcooling effect is quite evident early in the transient, where the impact of heat storage in the duct and surrounding sodium region is also illuscrated (it must be noted that cross-assembly temperature data were not reported for Test 611 in Ref. [27]).

Following the increase in power-to-flow ratio, caused by reduction in sodium flow rate, the sodium temperatures across the assembly increase as shown in Fig. 46. Here again, the effect of temperature flattening at low Reynolds number is clearly evident.

Figures 47 and 48 show the comparisons at selected thermocouple locations with the experimental measurements of Engel, et al. [27].

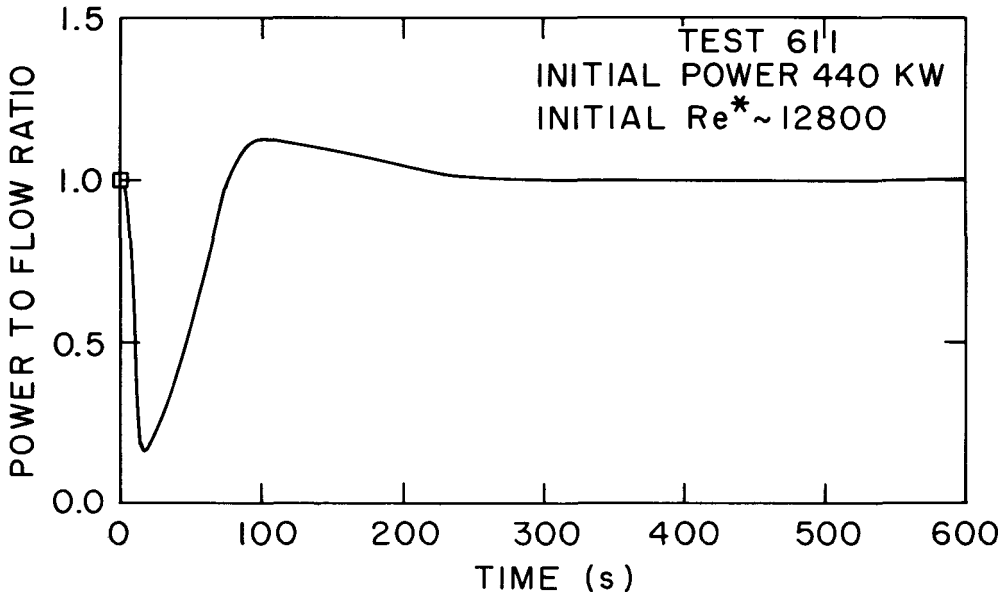

Fig. 43 Power to Flow Ratio (Test 611)

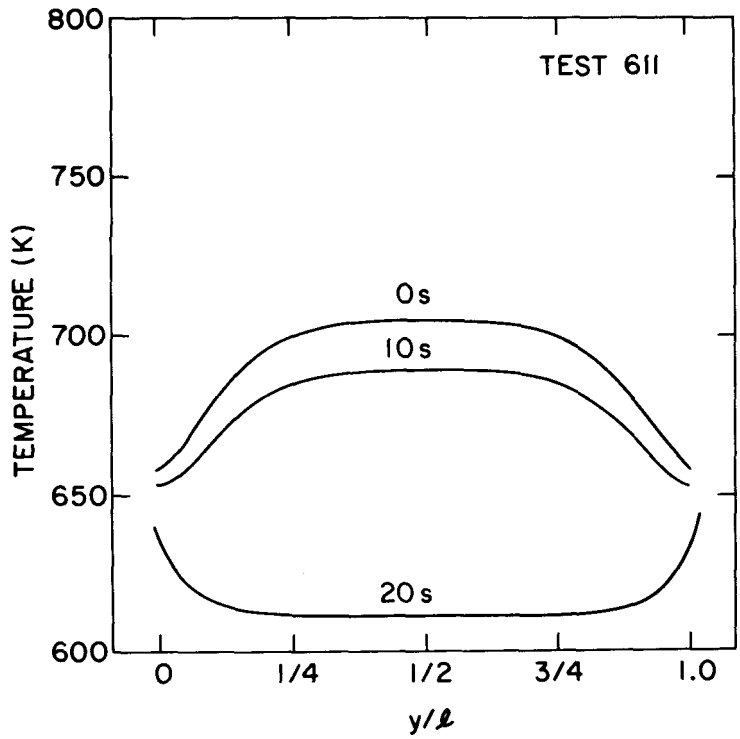

Fig. 44 Calculated Transient Temperature Distributions for Test 611 (Early)

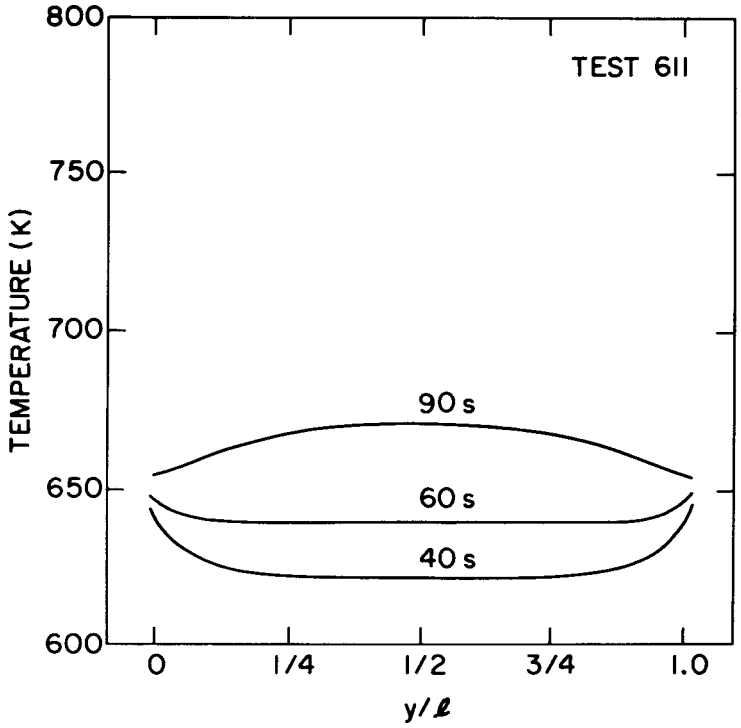

Fig. 45 Calculated Transient Temperature Distributions for Test 611 (Intermediate)

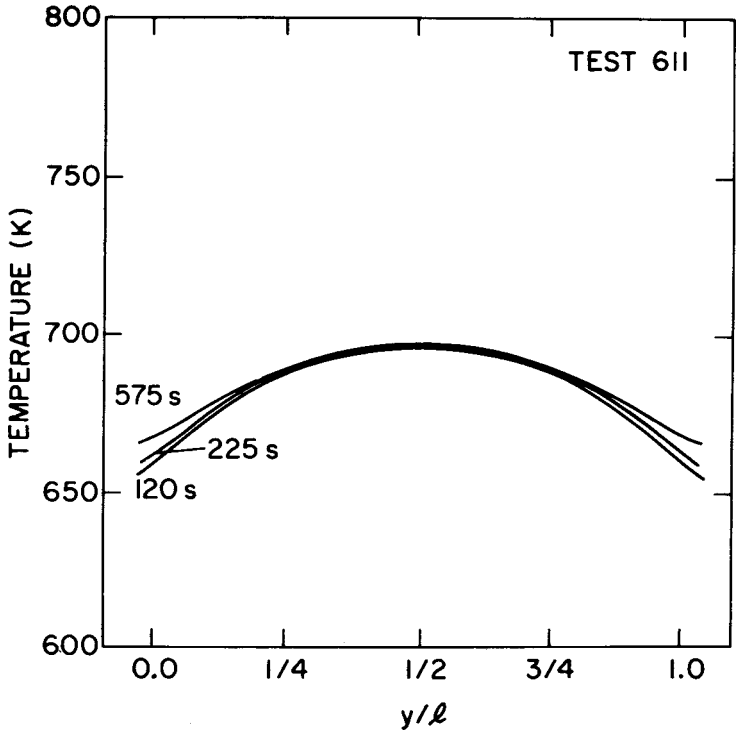

Fig. 46 Calculated Transient Temperature Distributions for Test 611 (Late)

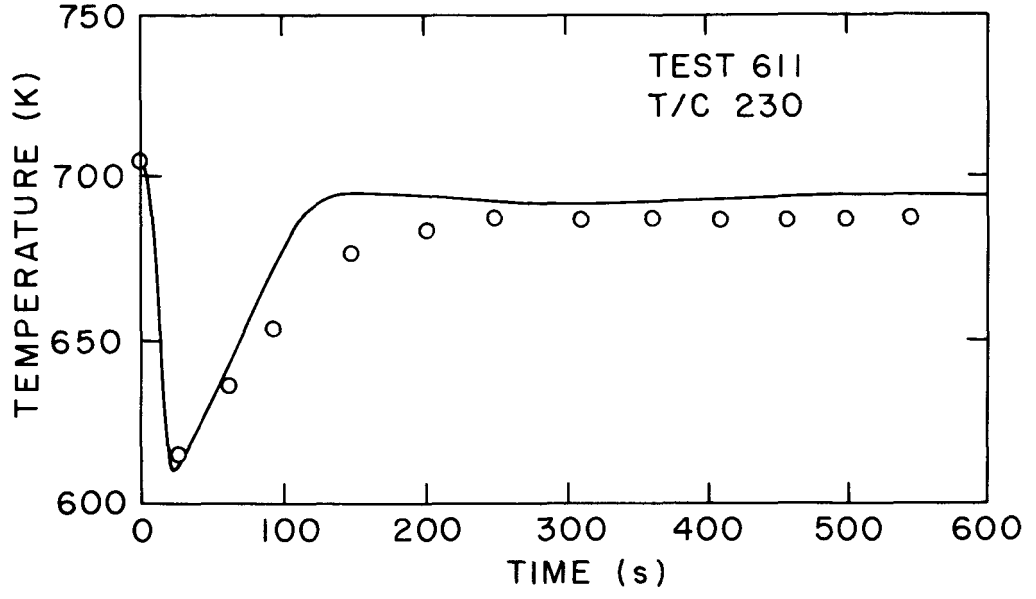

Fig. 47 Comparison of Calculated and Measured Temporal Variations of Sodium Temperature at T/C #230 for Test 611

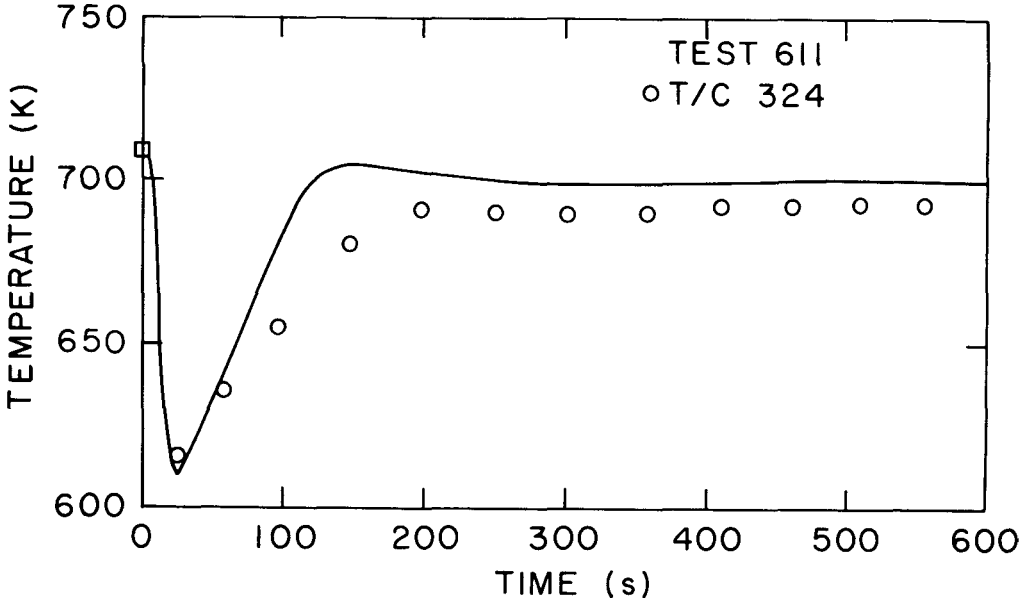

Fig. 48 Comparison of Calculated and Measured Temporal Variations of Sodium Temperature at T/C #324 for Test 611

It is seen that good agreement is obtained except between 100 to 200 seconds where the present model tends to overpredict the temperature as a result of the absence of fuel pin modeling, and perhaps inaccurate power and flow forcing functions as they were taken from a rather illegible figure of the original publication [27].

It is important to note, that the machine time requirements, for the aforementioned transients ranged from 5 to 10 times faster than real time depending on the accuracy criterion and the maximum allowable time step.

6. SUMMARY, CONCLUSIONS AND FUTURE WORKS

6.1 Summary

Two-dimensional porous-body models for study of the temperature flattening effect caused by buoyancy-induced intra-subassembly flow redistribution and transverse thermal conduction were proposed.

In Chapter 2, governing equations and porous-body parameters were set forth. In Chapter 3, approximate integral solutions for two limiting cases of flow redistribution and transverse conduction were developed. The approximate solutions provide excellent insight into the problem, while at the same time, the flow redistribution model can be used to determine maximum sodium temperatures within representative LMFBR assemblies under forced, mixed and natural convection conditions.

Detailed finite difference solutions based upon a parabolic flow model were developed in Chapter 4. The steady state model was then used to post-predict a number of sodium and water experiments.

Finally, a transient two-dimensional porous-body model applicable to forced, mixed and free convection regimes was developed in Chapter 5. This model was also applied to recent experimental measurements.

6.2 Conclusions

The importance of heat transfer and flow regime changes on LMFBR subassembly sodium flow behavior was demonstrated through approximate and detailed steady state and transient solutions to two-dimensional porous-body equations, and comparisons with experimental data.

Numerical results supported by experimental data indicate that,

1) Thermal buoyancy-induced flow redistribution is the dominant mode of the intra-assembly temperature flattening.

2) Flow regime change is significant.

3) Transverse thermal conduction can become quite significant at low flow natural convection conditions.

4) The proposed integral solution for calculation of the maximum sodium temperature within an LMFBR subassembly may be adequate under most of the natural circulation conditions.

5) The detailed two-dimensional model is quite accurate and highly efficient, and can therefore be used either directly or in conjunction with a system code for detailed calculation of intra-subassembly dynamics.

6.3 Future Works

The two-dimensional model described in this report is sufficient for representation of intra-subassembly behavior. However, in order to include inter-subassembly heat transfer processes as well, one needs to obtain a more complete representation of temperature and velocity fields within the entire assembly.

Therefore, for a complete three-dimensional analysis of the assembly; the Z-component of the velocity can be incorporated into the conservation equations as:

a) Conservation of Mass

$$\frac{\partial(\rho u)}{\partial x} + \frac{\partial(\rho v)}{\partial y} + \frac{\partial(\rho w)}{\partial z} = 0 \qquad (121)$$

b) Conservation of Energy

$$\frac{\partial T}{\partial t} + u\frac{\partial T}{\partial x} + v\frac{\partial T}{\partial y} + w\frac{\partial T}{\partial z} = \alpha_e \left(\frac{\partial^2 T}{\partial y^2} + \frac{\partial^2 T}{\partial z^2}\right) + \frac{Q'''(x,y,z)}{\rho c_p} \qquad (122)$$

c) Conservation of Axial Momentum

$$\frac{\partial u}{\partial t} + u\frac{\partial u}{\partial x} + v\frac{\partial u}{\partial y} + w\frac{\partial u}{\partial z} = -\frac{1}{\rho}\frac{\partial P}{\partial x} - g\frac{\rho^*}{\rho}\left[1 - \beta\,(T-T^*)\right] + \nu\left[\frac{\partial^2 u}{\partial y^2} + \frac{\partial^2 u}{\partial z^2}\right]$$

$$+ \frac{f}{2D\lambda^2}\,u^2 \qquad (123)$$

This model corresponds to the usual assumptions that transverse momentum flux is small, that gradients in the x-direction are smaller than those in the other directions, and $P = P(x)$ only. This model is as yet incomplete, because, Equations (121) through (123) represent three equations in four unknowns, u, v, w, and T. (As in the previous 2-D case considered earlier, P is not a true unknown in the same sense as u, v, w, and T since $P = P(x)$ only.) An additional relation between v and w must be specified in order to have a complete set.

One such additional relation between v and w is suggested by Carlson [21, 29] as:

$$\frac{w}{z} = \frac{v}{y} \qquad (124)$$

This relation, originally proposed for square ducts, assumes that at each point in the duct cross section the transverse velocity vector is directed towards the direct center line. Such an approximation should of course be verified and/or modified for application to large aspect ratio channels (subassemblies). Modifications include formulation of transverse momentum equations, while retaining the parabolic nature of the equations ($\partial^2/\partial x^2 = 0$).

The present two-dimensional model should also be incorporated into the Super System Code (SSC) [30] for best-estimate prediction of protected loss-of-flow transients in LMFBRs.

REFERENCES

1. M. Khatib-Rahbar and K.B. Cady, "Dynamical Models and Numerical Simulation of System-Wide Transients in Loop-Type LMFBRs," Nucl. Eng. & Design, 64, 259-281, (1981)

2. E.U. Khan, "LMFBR In-Core Thermal-Hydraulics: The State of the Art and U.S. Research and Development Needs," Pacific Northwest Laboratory, PNL-3337/UC-32 (April 1980).

3. E.U. Khan, W.M. Rohsenow, A.A. Sonin and N.E. Todreas, "Manual for ENERGY I, II, III Computer Programs," Massachusetts Institute of Technology, Report COO-2245-18TR, (May 1975).

4. C.L. Wheeler, et al., "COBRA-IV-I: An Interim Version of COBRA for Thermal-Hydraulic Analysis of Rod Bundle Nuclear Fuel Element and Cores", Pacific Northwest Laboratory, BNWL-1962, (March 1976).

5. T.L. George, et al., COBRA-WC: A Version of COBRA for Single-Phase Multiassembly Thermal-Hydraulic Transient Analysis," Pacific Northwest Laboratory, PNL-3259 (1980). Also see AICHE Symposium Series, No. 199, Vol. 76, 205-214.

6. W.L. Chen, M.A. Grolmes and M. Ishii, "A Simple Forced Diversion Model for Study of Thermal-Hydraulic Transients in LMFBR Subassembly," Nucl. Eng. & Design, 45, 53-66 (1978).

7. H.G. Johnson, "CORA - A Computer Code for Thermal and Hydraulic Coupling of Reactor Core Assemblies," Hanford Engineering Development Laboratory, TC-1505, (September 1979).

8. W.T. Sha, et al., "COMMIX-1: A Three-Dimensional Transient Single-Phase Component Computer Program for Thermal-Hydraulic Analysis," NUREG/CR-0785, ANL-77-96, (September 1978).

9. Informal information obtained from J.E. Meyer on "Transverse Heat Transfer in an LMFBR Core," (January 1979).

10. Informal information obtained from J.E. Meyer on "Intra-Assembly Buoyancy Effects in an LMFBR Core," (June 1979).

11. Informal information obtained from J.E. Meyer on "Heat Transfer Within the Coolant of an LMFBR Core," (April 1979).

12. F.C. Engel, R.A. Markley and B. Minushkin, "Buoyancy Effects on Sodium Coolant Temperature Profiles Measured in an Electrically Heeated Mock-up of a 61-Rod Breeder Reactor Blanket Assembly," ASME paper 78-WA/HT-25, (1978).

13. F.E. Engel, and R.A. Markley, "ARD 61-Rod Electrically Heated Blanket Mock-up Heat Transfer Test Results for Turbulent Flow Operation and Comparison with COTEC Predictions," Paper presented at the Core T & H Technical Group Meeting, Argonne National Laboratory, April 24-25, (1979).

14. F.C. Engel, B. Minushkin, R.J. Atkins and R.A. Markley, "Characterization of Heat Transfer and Temperature Distributions in an Electrically Heated Model of an LMFBR Blanket Assembly," Nucl. Eng. & Design, 62, 335-347, (1980).

15. F.C. Engel, R.A. Markley and B. Minushkin, "Temperature Profiles in Natural and Forced Circulation of Sodium Through a Vertical LMFBR Blanket Test Assembly," American Institute of Chemical Engineers Symposium Series, 208, Milwaukee, (1981).

16. F.C. Engel, R.A. Markley and A.A. Bishop, "The Effects of Radial Heat Flux Gradients and Flow Regimes on the Peak Sodium Temperature Rise in Wire Wrapped Rod Bundles," Proceedings of the Topical Meeting on Advances in Reactor Physics and Core Thermal Hydraulics, NUREG/CP-0034, Vol. 2, (1982).

17. D.R. Spencer and R.A. Markley, "Friction Factor Correlation for 217-Pin Wire-Wrap-Spaced LMFBR Fuel Assemblies," Trans. Am. Nucl. Soc. 39, 1014, (1981).

18. E.H. Novendstern, "Pressure Drop Model for Wire-Wrapped Fuel Assemblies," Trans. Am. Nucl. Soc. 14, 660 (1971).

19. F.C. Engel, R.A. Markley and A.A. Bishop, "Laminar, Transition and Turbulent Parallel Flow Pressure Drop Across Wire Wrap Spaced Rod Bundles, Nucl. Sci. & Eng. 69, 290-296 and 74, 226, (1977).

20. C. Chiu, "Investigation of Coolant Mixing and Flow Split for LMFBR Wire-Wrapped Assemblies," PhD Thesis, Massachusetts Institute of Technology, (1977).

21. R.W. Hornbeck, "Numerical Marching Techniques for Fluid Flows With Heat Transfer," National Aeronautics and Space Administration, NASA-SP-297, Washington, D.C. (1973).

22. B. Carnahan, H.A. Luther, and J.O. Wilkes, Applied Numerical Methods, John Wiley & Sons, Inc. (1969).

23. J. Juneau and E.U. Khan, "Analysis of Steady-State Comnbined Forced and Free Convection Data in Rod Bundles," Argonne National Laboratory, FRA-TM-116, (January 1979).

24. A.K. Agrawal and M. Khatib-Rahbar, "Dynamic Simulation of LMFBR Systems," Atomic Energy Review 18, No. 2, 329, IAEA, Vienna (1980).

25. K. Mawatari, F. Namekawa, N. Handa, F. Kasahara, and Y. Ishida, "Natural Circulation Decay Heat Removal Experiments and Analysis in An LMFBR Fuel Assembly," Proceedings of International Topical Meeting on Fast Reactor Safety, Lyon, France, July 18-21 (1982).

26. F. Namekawa to M. Khatib-Rahbar, Personal Communication, Toshiba Nuclear Engineering Laboratory (April 1983)

27. F.C. Engel, R.A. Markley and B. Minushkin, "Loss of Flow Transient Heat Transfer Tests of a Full Size LMFBR Blanket Model," ASME Paper No. 82-WA/HT-35 (1982).

28. D. Potter, Computational Physics, John Wiley & Sons, London (1973).

29. G.A. Carlson, "Laminar Entrance Flow in a Square Duct," Ph.D. Thesis, Carnegie Institute of Technology (1966).

30. J.G. Guppy, et al., "An Advanced Thermohydraulic Simulation Code for Transients in LMFBRs, SSC, Rev. 0," Brookhaven National Laboratory Report, BNL-NUREG-51650 (April 1983).

APPENDIX A

USER'S MANUAL FOR FREDIS

The approximate integral method described in Section 3.1 is implemented in the FREDIS (Flow REDIStribution Model) code.

FREDIS integrates Equations (40) and (41) using the user supplied geometry and bundle inlet conditions.

The integration procedure is based upon the Gear method. However, other numerical integration techniques may be readily substituted.

In this Appendix, the code flow chart, together with the description of various subroutines, code input, code output and limitations are discussed. The FORTRAN source listing is also included.

A.1 PROGRAM FLOWCHART AND CODE STRUCTURE

a) MAIN DRIVER

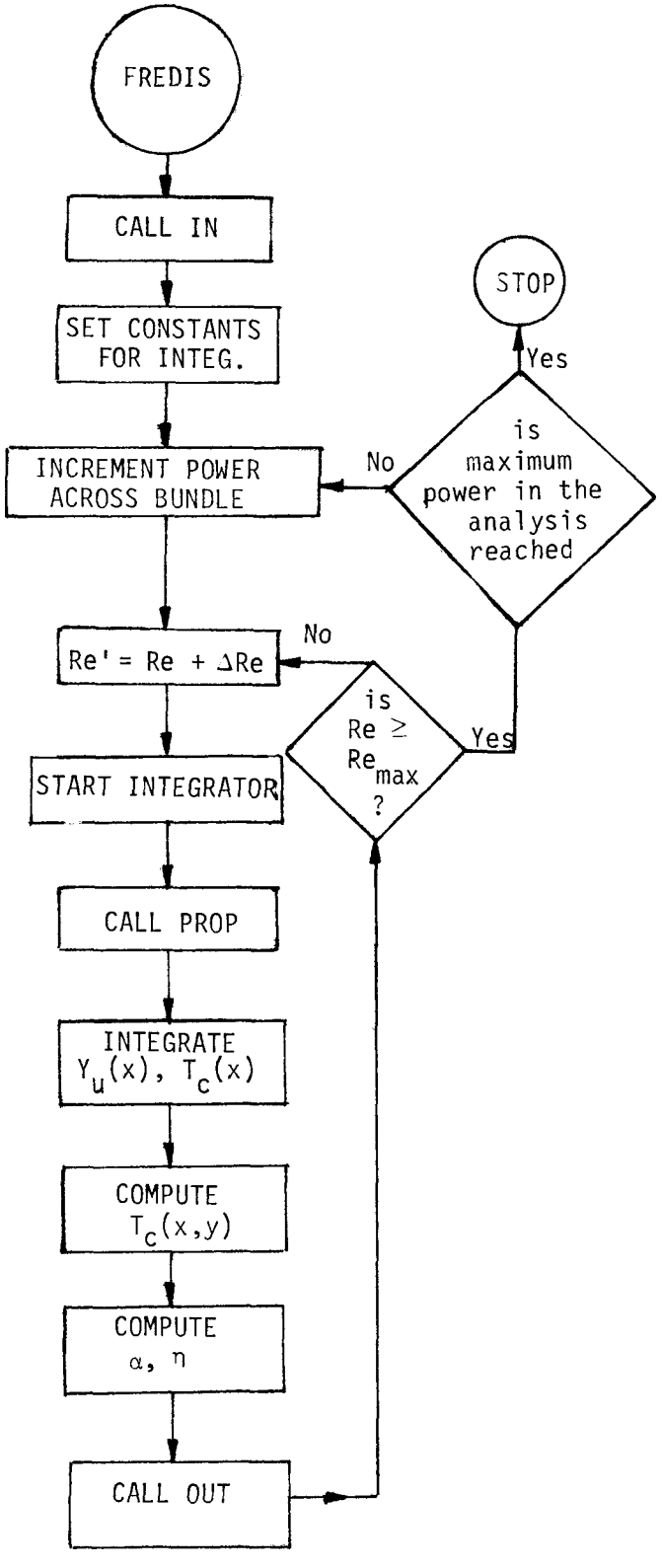

b) INTEGRATOR DRIVER

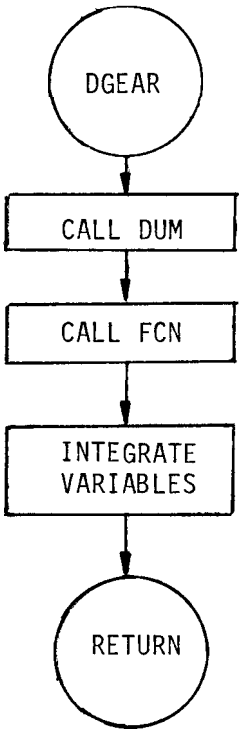

c) DIFFERENTIAL EQUATIONS

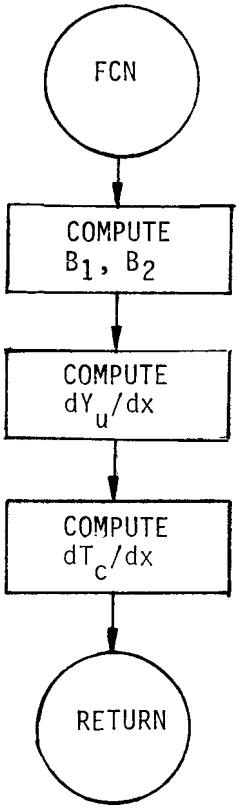

```
      PROGRAM FREDIS(INPUT,OUTPUT,TAPE1,TAPE2=OUTPUT,TAPE98)
C
C PROGRAM TO COMPUTE FLOW REDISTRIBUTION PARAMETERS INSIDE
C       A ROD BUNDLE DUE TO THERMAL BUOYANCY
C
C
      COMMON /NEW/   DH
      COMMON /DATA/ TIN,YDE, ALAM,ALH,AL2,F,QPPP,WBAR,RE,AMU
      COMMON /UNIT/    INP,IOUP,ISAVE
      COMMON /WHICH/ II,YYY(3),TTT(3)
      COMMON /SAVE/  NXRE,XRE(50),XQ(50),TEMP(11,3,50),DIST(11)
C
      COMMON /INTEG/ NEQ, Z, H, ZEND, Y(2),INDEX
      COMMON /NEW2/    Q
      COMMON /NEW4/   DELTAT
C
      DIMENSION IWK(2), WK(30)
C
      EXTERNAL FCN
      EXTERNAL DUM
C
C
C     READ INPUT DATA
C
      CALL IN
C
C    SET CONSTANT DATA FOR INTEGRATOR
C      METH = 1 ADAMS METHOD
C           = 2 GEAR METHOD
C      MITER = 2 CHORD METH,JACOBIAN COMP. INTERNALLY
C            = 3   "     "   , DIAGONAL JACOBIAN COMP.
C
C       TOL(ERANCE) SHOULD BE LESS THAN OR EQUAL TO 1.E-3
C
      DO 1 L=1,3
      TTT(L) = 0.0
      YYY(L) = 0.0
1      CONTINUE
      NEQ = 2
      METH = 2
      MITER = 2
      IEND= 0
      TOL = 5.E-04
C
C       REYNOLDS NUMBER STEPS
C
      DELTR1 = 50.
      DELTR2 = 100.
      DELTR3 = 500.
      DELTR4 = 2000.
C
C       STEPS FOR DELTAT
C
      DT1 = 25.
      DT2 = 75.
      DO 7777 M1=1,8
      IF(M1.LE.3)    DELTAT = DELTAT + DT1
      IF(M1.GT.3)    DELTAT = DELTAT + DT2
C
C           PERFORM CALCULATIONS FOR INCREASING REYNOLDS NUMBERS
C
      DO 1000 I=1,NXRE
      Q = 0.0
      IF(XRE(1).EQ.0.0)   GOTO 1003
C
C       REYNOLDS NUMBERS WERE PRESCRIBED IN INPUT
C
      RE = XRE(I)
      GOTO 1004
1003     IF(RE.LT.600.)  RE = RE + DELTR1
      IF(RE.GE.1000.0.AND.RE.LE.7000.) RE=RE+DELTR3
      IF(RE.GE.600.0.AND.RE.LT.1000.)
     +    RE = RE + DELTR2
      IF(RE.GT.7000.)    RE = RE + DELTR4
1004       II = I
C
C     START UP INTEGRATOR
C
      CALL START
C
C      COMPUTE PROPERTIES,FRICTION FACTOR,AVERAGE INLET
C       VELOCITY AND POWER ACROSS THE BUNDLE
C
      CALL PROP
C
C     INTEGRATE Y(Z) AND TCOOL(Z)
C
      CALL DGEAR(NEQ,FCN,DUM,Z,H,Y,ZEND,TOL,METH,MITER,
     +       INDEX,IWK,WK,IER)
C
C     COMPUTE T(X,Z)
C
      CALL TXZ
C
C     COMPUTE THE TEMPERATURE RISE HOT CHANNEL FACTOR
C
      CALL FF
C
C     OUTPUT RESULTS
C
      CALL OUT
```

```
C
C
C
1000    CONTINUE
7777    CONTINUE
C
      STOP
      END
      SUBROUTINE DUM(N,X,Y,PD)
C
C     DUMMY ROUTINE NEEDED BY INTEGRATOR
C
      INTEGER N
      REAL Y(N),PD(N,N),X
      RETURN
C
      END
      SUBROUTINE FCN(NEQ,Z,Y,YPRIME)
C
C     THIS SUBROUTINE COMPUTES DY/DZ AND DTCOOL/DZ
C
C
      COMMON /NEW1/    AKE
      COMMON /DATA/  TIN,YDE,ALAM,ALH,AL2,F,QPPP,WBAR,RE,AMU
      COMMON /WHICH/   II,YYY(3),TTT(3)
      COMMON /OTHER/ BZERO,EXPON,T,DELTAH,DHBAR,FDELTA,FSUBF,
     C   CP, RHO,BTWO,BONE
      REAL Y(NEQ),YPRIME(NEQ)
C
C
C        COMPUTE COEFFICIENTS B1 AND B2 AS FUNCTIONS OF
C     Y(Z) AND EXPON
C
      GEX = 1. - EXPON
      AMULT = 2./AL2**2*AKE/(RHO*CP)/WBAR**EXPON
      Y1 = Y(1)*((1.+Y(1))**GEX-(1.-Y(1))**GEX)
      Y2 = 2.*(2.-(1.+Y(1))**GEX-(1.-Y(1))**GEX)
      R1 = AMULT * (Y1+Y2)
      R2 = AMULT * Y1
      IF(RE.LE.400.)   R1 = R2 = 0.0
      CALL COMPB(Y,NEQ,EXPON,BONE,BTWO)
C
C        COMPUTE DERIVATIVES
C
      FACT = QPPP / ( RHO*CP*WBAR )
      DYDZ = FACT * (1.-(F-1.)/Y(1)) / ( BZERO * BONE *
     +     WBAR**(1.-EXPON))
      DYDZ = DYDZ + R1/(BZERO*BONE*WBAR**GEX)
C
      DTCDZ = FACT - BZERO*BTWO*(WBAR**(1.-EXPON)) *
     +   DYDZ
      DTCDZ = DTCDZ + R2
C
C          TRANSFER DERIVATIVES TO INTEGRATOR ARRAYS
C
      YPRIME(1) = DYDZ
      YPRIME(2) = DTCDZ
C
C       SAVE DATA FOR Z=1/4 AND Z=1/2 OF HEATED LENGTH
C
      ZTEST1 = ALH/4.
      ZTEST2 = ALH/2.
      IF(ABS(Z-ZTEST1).GT.10.0E-02)   GOTO 1
      YYY(1) = Y(1)
      TTT(1) = Y(2)
      GOTO 2
1      IF(ABS(Z-ZTEST2).GT.10.0E-02)   GOTO 2
      YYY(2) = Y(1)
      TTT(2) = Y(2)
2      CONTINUE
C
C
      RETURN
      END
      SUBROUTINE COMPB(Y,N,EX,BONE,BTWO)
C
C       THIS SUBROUTINE COMPUTES COEFFICIENTS B1 AND B2
C         FUNCTIONS OF Y(Z) AND EXPON NEEDED BY DIFF. EQ.S
C
      DIMENSION Y(N)
C
C
C
      YY = Y(1)
      YYP2 = ( YY + 1.) ** (2. - EX)
      YYP4 = ( YY + 1.) ** (4. - EX)
      YYM2 = ( 1. - YY) ** (2. - EX)
      YYM4 = ( 1. - YY) ** (4. - EX)
C
      B11 = (YYP2-YYM2)/(8.-4.*EX)
      B12 = ((YYP4-YYM4)/(4.-EX)-(YYP2-YYM2)/(2.-EX))/
     +   (4.*YY*YY)
      B13 = -((YYP2+YYM2-2.)/(4.-2.*EX))*(1./YY**3 -
     +     1./YY)
      B14 = (YYP4+YYM4-2.)/(8.*YY**3-2.*EX*YY**3)
C
      BONE = B11 + B12 - B13 - B14
C
      B21 = (YYP2-YYM2)/(2.-EX)
      B22 = (YYP4-YYM4)/(4.-EX)
C
```

```
      BTWO = (B21 + (B22-B21)/(YY**2))/4.0
C
C
      RETURN
      END
      SUBROUTINE IN
C
C      INPUT SUBROUTINE
C
C
      COMMON /NEW/    DH
      COMMON /NEW4/    DELTAT
      COMMON /DATA/  TIN,YDE,ALAM,ALH,AL2,F,QPPP,WBAR,RE,AMU
      COMMON /SAVE/    NXRE,XRE(50),XQ(50)
      COMMON /UNIT/    INP,IOUP,ISAVE
C
C
      NAMELIST /CONTR/    NXRE
      NAMELIST /GEOM1/    YDE,ALAM
      NAMELIST /GEOM2/    ALH,AL2
      NAMELIST /DATIN/    TIN,F,RE
      NAMELIST /REYNOL/    XRE
C
C
      INP = 1
      IOUP = 2
      ISAVE = 98
      READ(INP,CONTR)
      READ(INP,GEOM1)
      READ(INP,GEOM2)
      READ(INP,DATIN)
      READ(INP,REYNOL)
C
C
1     FORMAT(I3)
      IF(XRE(1).EQ.0.0)    DELTAT = 0.
C
      WRITE(ISAVE,1)    NXRE
C
C
      RETURN
      END
      SUBROUTINE START
C
C     THIS SUBROUTINE FIRES UP DGEAR
C
C
      COMMON /INTEG/ NEQ, Z, H, ZEND, Y(2),INDEX
      COMMON /DATA/TIN,YDE,ALAM,ALH,AL2,F,QPPP,WBAR,RE,AMU
C
C
      NEQ = 2
      Z = 0.0
      H = 1.E-04
C
C      SET Y(1) TO A VERY SMALL NUMBER (NEARLY ZERO)
C
      Y(1) = 1.E-06
      Y(2) = TIN
      ZEND = ALH
      INDEX = 1
C
      RETURN
      END
      SUBROUTINE PROP
C
C      THIS SUBROUTINE COMPUTES PROPERTIES AND FRICTION FACTOR:
C           CF(RE), EXPON(RE)
C
      COMMON /NEW/    DH
      COMMON /NEW1/    AKE
      COMMON /NEW2/    Q
      COMMON /NEW10/    C9GRAS,RI,BUOY,FRIC
      COMMON /NEW4/    DELTAT
      COMMON /DATA/  TIN,YDE,ALAM,ALH,AL2,F,QPPP,WBAR,RE,AMU
      COMMON/OTHER/  BZERO,EXPON,T,DELTAH,DHBAR,FDELTA,FSUBF,
     C    CP,RHO,BTWO,BONE
C
C
      DATA C1,C2,C3/-2.4892,220.65,-.21389/
      DATA R0,R1,R2,R3/1011.597,-.22051,-1.922243E-05,
     D     5.63769E-09/
C
C      FRICTION FACTOR IS FOR BLANKET ASSEMBLIES
C
      TT = TIN
      EXPON = 1.
      CF = 110.
      IF(RE.GT.550.)    EXPON = .25
      IF(RE.GT.550.)    CF = .48
      FRIC = CF/RE**EXPON
C
      RHO = R0+R1*TT+R2*TT*TT+R3*TT*TT*TT
C
C       POROUS BODY AREA
C
      AP = SQRT(3.) * AL2 * AL2 / 2.0
C
C      SET THE THERMAL EXPANSION COEFFICIENT
C
      BETA = 2.91E-04
```

```
C
C          OTHER SODIUM PROPERTIES
C
      CP = 1630.22 - .83354*TT + 4.62838E-04*TT*TT
      RHS = C1 + C2/TT + C3*ALOG(TT)
      AMU = 10.**(RHS)
      AKE = 109.7 - 6.4499E-02*TT + 1.1728E-05*TT*TT
C
C         COMPUTE INLET VELOCITY AND POWER
C
      IF(Q.EQ.0.0)   GOTO 10
      DH = Q/(RE*AMU*AP*ALAM/YDE)
      GOTO 20
10       TFIN = TIN + DELTAT
      DH = SUM(TIN,TFIN)
20          CONTINUE
      WBAR = RE*ALAM*AMU/(RHO*YDE)
      QPPP = RHO*WBAR*DH/ALH
C
C         COMPUTE COEFFICIENT BZERO
C
      BZERO = CF*ALAM**(EXPON-2.)*AMU**EXPON*RHO**(1.-EXPON)/
     +    (9.81*BETA*YDE**(1.+EXPON)*RHO) *
     +    (1. - EXPON/2.)*WBAR
      IF(EXPON.GE.1.0)   BZERO = CF*AMU*WBAR/(19.62*ALAM*
     +    BETA*YDE*YDE*RHO)
C
C         GRASHOFF NUMBER
C
      C9GRAS = 9.81*BETA*RHO**2*YDE**3*DELTAT/
     +    (AMU**2 )
C
C         RICHARDSON NUMBER
C
      RI = C9GRAS/RE/RE
C
C         BUOYANCY PARAMETER
C
      BUOY = 2.*RI / FRIC
C
C
      RETURN
      END
      SUBROUTINE TXZ
C
C     THIS SUBROUTINE COMPUTES T(X,Z), NAMELY FOR:
C          X=AL2    AND
C          Z=ALH
C
C    EQUATION IN GENERAL IS :
C  T = TCOOL(Z) + G(WBAR,EXPON)*((1.+X/AL2*Y(Z))**(2.-EXPON)
C         -1.)
C          .
C
C
      COMMON /DATA/ TIN,YDE,ALAM,ALH,AL2,F,QPPP,WBAR,RE,AMU
      COMMON /INTEG/  NEQ,Z,H,ZEND,Y(2),INDEX
      COMMON /OTHER/ BZERO,EXPON,T,DELTAH,DHBAR,FDELTA,FSUBF,
     C    CP,RHO,BTWO,BONE
      COMMON /SAVE/  NXRE,XRE(50),XQ(50),TEMP(11,3,50),
     +    DIST(11)
      COMMON /WHICH/  II,YYY(3),TTT(3)
C
      AL = AL2
      AL2P = AL / 2.
      DX = AL/10.
      YYY(3) = Y(1)
      TTT(3) = Y(2)
C
      T = Y(2) + BZERO*(WBAR)**(1.-EXPON)/(2.-EXPON)*
     +       ((1. + Y(1))**(2.-EXPON) -1.)
C
C          SAVE RESULTS FOR SLICE
C
      DO   2  JJ=1,3
      X = -AL2P - DX
      DO 1 KK=1,11
      X = X + DX
      TX=TTT(JJ)+BZERO*WBAR**(1.-EXPON)/(2.-EXPON)*
     +    ((1.+X/AL2P*YYY(JJ))**(2.-EXPON)-1.)
      TEST = (TX-TIN)/(Y(2)-TIN)
      DIST(KK) = X
      TEMP(KK,JJ,II) = TEST
1     CONTINUE
2     CONTINUE
C
      RETURN
      END
      SUBROUTINE FF
C
C       THIS SUBROUTINE COMPUTES THE TEMPERATURE RISE HOT
C        CHANNEL FACTOR AND TEMPERATURE PEAKING FACTOR
C
      COMMON /NEW/   DH
      COMMON /DATA/ TIN,YDE,ALAM,ALH,AL2,F,QPPP,WBAR,RE,AMU
      COMMON /INTEG/ NEQ,Z,H,ZEND,Y(2),INDEX
      COMMON /OTHER/ BZERO,EXPON,T,DELTAH,DHBAR,FDELTA,FSUBF,
     C    CP,RHO,BTWO,BONE
C
C       TEMPERATURE PEAKING FACTOR
C
```

```
      FDELTA = (T-TIN)/(Y(2)-TIN)
C
C          HOT CHANNEL FACTOR
C
      FSUBF = (FDELTA - 1.) / (F - 1.)
C
C
      RETURN
      END
      FUNCTION SUM(T1,T2)
C
C       THIS FUNCTION COMPUTES DELTAH(T1,T2)
C
      C0 = 1630.22
      C1 = -0.83354
      C2 = 4.62838E-04
      SUM = C0*(T2-T1) + C1/2.*(T2**2-T1**2) +'
     + C2/3.*(T2**3-T1**3)
C
C
      RETURN
      END
      SUBROUTINE OUT
C
C     THIS SUBROUTINE IS THE OUTPUT ROUTINE
C
      COMMON /NEW2/    Q
      COMMON /NEW10/   C9GRAS,RI,BUOY,FRIC
      COMMON /DATA/ TIN,YDE,ALAM,ALH,AL2,F,QPPP,WBAR,RE,AMU
      COMMON /UNIT/ INP,IOUP,ISAVE
      COMMON /WHICH/    II
      COMMON /SAVE/    NXRE,XRE(50),XQ(50),TEMP(11,3,50),DIST(11)
      COMMON /OTHER/ BZERO,EXPON,T,DELTAH,DHBAR,FDELTA,FSUBF,
     C     CP,RHO,BTWO,BONE
C
      WRITE(2,2)
      WRITE(2,100)
100   FORMAT(6H    TIN ,15X,2H Q,15X,2HRE,15X,5HFSUBF,12X,4HWBAR)
      WRITE(2,1)  TIN,Q,RE,FSUBF,WBAR
1       FORMAT(5E15.7)
2           FORMAT(2X,50(1H*),//)
      WRITE(2,102)  C9GRAS,RI,BUOY,FRIC
102    FORMAT(3X,6HGRASHO,2X,E15.7,4X,4HRICH,2X,E15.7,
     +    4X,4HBUOY,2X,E15.7,4X,4HFRIC,2X,E15.7)
      WRITE(ISAVE,1000) II,RE
1000    FORMAT(I3,E16.6)
C
C       SAVE DATA FOR PLOTTING
C
      DO 10 J=1,3
      WRITE(ISAVE,1001) ((DIST(K),TEMP(K,J,II)),K=1,11)
10      CONTINUE
1001    FORMAT(11E10.3)
      WRITE(ISAVE,1002)    FSUBF,BUOY
1002    FORMAT(2E16.6)
C
C
      RETURN
      END
```

A.2 ALPHABETICAL DESCRIPTION OF ASSOCIATED SUBROUTINES

COMPB: This subroutine computes coefficients B_1 and B_2 as functions of $Y_u(x)$.

Parameters:

Y	dependent variables
N	number of dependent variables
EX	friction factor exponent
BONE	coefficient B_1, Eq. 42
BTWO	coefficient B_2, Eq. 43

DUM: Dummy Routine needed by integrator package.

Parameters:

N	number of dependent variables
X	unused
Y	dependent variables
PD	unused

FCN: This subroutine computes $\frac{dY_u}{dx}$ and $\frac{dT_c}{dx}$

Parameters:

NEQ	number of differential equations
Z	independent variable x
Y	dependent variables; $Y_u(x)$ and $T_c(x)$
YPRIME	value of dY_u/dx and dT_c/dx)

FF: This subroutine computes $\alpha^* = (T - T^*)/(T - T^*)$ and $\eta^* = (\alpha^*-1)/(F-1)$

IN: Input subroutine

OUT: Output subroutine

PROP: This subroutine computes physical properties and friction factor based on average conditions.

START: This subroutine sets initial values and constants needed by integrator.

TXZ: This subroutine computes T(x,y)

WREDIS: Main program driver

Auxiliary Routines:

DGEAR: Integrator package from IMSLX Program Library (version 1981); can use Adam's method or Gear's method to integrate system of differential equations;

Parameters:

NEQ	number of differential equations
FCN	external routine which computes R.H.S. of differential equations
DUM	dummy external routine
Z	independent variable
H	initial step on independent variable
Y	array of dependent variables
ZEND	final value of independent variable
TOL	tolerance
METH	method used to integrate
MITER	defines which chord method used in integration
INDEX	unused
IWK	internal dimensions of working area for dependent variables
WK	working area for integration

A.3 DESCRIPTION OF INPUT

TAPE 1 is defined as the input file; input consists of 5 NAMELIST groups as follows:

NAMELIST/CONTR/	NXRE	number of Reynolds numbers for which steady-state calculations are desired.
NAMELIST/GEOM1/	YDE	subassembly hydraulic diameter, m
	ALAM	subassembly channel porosity
NAMELIST/GEOM2/	ALH	subassembly heated length, m
	AL2	subassembly flat-to-flat, m
NAMELIST/DATIN/	TIN	inlet temperature, K
	F	peak to average power
	RE	initial Reynolds number
NAMELIST/REYNOL/	XRE	specific Reynolds numbers for which steady-state calculations is desired; if the first is = 0.0, the program will automatically step in Re and power (up to 30 Re values can be specified).

The following is a sample input file

```
$CONTR   NXRE=40    $END
$GEOM1   YDE=3.7713E-03, ALAM=.2546   $END
$GEOM2   ALH=1.143,  AL2=.11312   $END
$DATIN   TIN=590.23, F=1.4723, RE=50.   $END
$REYNOL  XRE=0.,0.,0.,0.   $END
```

This run will perform calculations for a power skew case of 2:1, inlet T of 590.23 K, starting at Re = 50, stepping automatically in Re and power for 40 progressively increasing Reynolds numbers.

A.4 DESCRIPTION OF OUTPUT

TAPE 2 is defined as the output file, while TAPE 99 is defined as the result storage file for eventual plotting and/or display.

On output the following data is displayed:

TIN	-	inlet temperature, K
Q	-	average power, watts/m^2
RE	-	Reynolds number
FSUBF	-	hot channel factor, η^*
WBAR	-	average velocity, m/s
C9GRAS	-	Grashof number
RI	-	Richardson number
BUOY	-	buoyancy parameter (2RI/FRIC)
FRIC	-	friction factor

The following data is stored:

NXRE	-	number of Reynolds numbers for which steady-state calculations are to be performed
II	-	Reynolds number index, $1 \leq II \leq NXRE$
RE	-	current Reynolds number
DIST(k)	-	node position, (k = 1,11), m
TEMP(k,J,II)	-	Temperature at position k for Reynolds number index II at J = 1 (one fourth of heated length); J = 2 (one half of heated length); J = 3 (exit of heated section), K
FSUBF	-	temperature peaking factor α^*
BUOY	-	buoyancy parameter

Following is a sample output as generated by FREDIS:

```
*** WARNING WITH FIX ERROR  (IER =  67) FROM IMSL ROUTINE DGEAR
 ************************************************

  TIN                 Q                 RE                FSUBF               WBAR
  .5902300E+03  0.                .1000000E+03   .2081656E+00   .2551634E-02
  GRASHO      .2679620E+05    RICH      .2679620E+01    BUOY      .4872036E+01    FRIC      .1100000E+01
*** WARNING WITH FIX ERROR  (IER =  67) FROM IMSL ROUTINE DGEAR
 ************************************************

  TIN                 Q                 RE                FSUBF               WBAR
  .5902300E+03  0.                .1500000E+03   .3066541E+00   .3827451E-02
  GRASHO      .2679620E+05    RICH      .1190942E+01    BUOY      .3248024E+01    FRIC      .7333333E+00
*** WARNING WITH FIX ERROR  (IER =  67) FROM IMSL ROUTINE DGEAR
 ************************************************

  TIN                 Q                 RE                FSUBF               WBAR
  .5902300E+03  0.                .2000000E+03   .3917585E+00   .5103268E-02
  GRASHO      .2679620E+05    RICH      .6699050E+00    BUOY      .2436018E+01    FRIC      .5500000E+00
*** WARNING WITH FIX ERROR  (IER =  67) FROM IMSL ROUTINE DGEAR
 ************************************************

  TIN                 Q                 RE                FSUBF               WBAR
  .5902300E+03  0.                .2500000E+03   .4625741E+00   .6379084E-02
  GRASHO      .2679620E+05    RICH      .4287392E+00    BUOY      .1948815E+01    FRIC      .4400000E+00
*** WARNING WITH FIX ERROR  (IER =  67) FROM IMSL ROUTINE DGEAR
 ************************************************

  TIN                 Q                 RE                FSUBF               WBAR
  .5902300E+03  0.                .3000000E+03   .5206782E+00   .7654901E-02
  GRASHO      .2679620E+05    RICH      .2977355E+00    BUOY      .1624012E+01    FRIC      .3666667E+00
*** WARNING WITH FIX ERROR  (IER =  67) FROM IMSL ROUTINE DGEAR
 ************************************************

  TIN                 Q                 RE                FSUBF               WBAR
  .5902300E+03  0.                .3500000E+03   .5683969E+00   .8930718E-02
  GRASHO      .2679620E+05    RICH      .2187445E+00    BUOY      .1392010E+01    FRIC      .3142857E+00
*** WARNING WITH FIX ERROR  (IER =  67) FROM IMSL ROUTINE DGEAR
 ************************************************

  TIN                 Q                 RE                FSUBF               WBAR
  .5902300E+03  0.                .4000000E+03   .6080088E+00   .1020654E-01
  GRASHO      .2679620E+05    RICH      .1674762E+00    BUOY      .1218009E+01    FRIC      .2750000E+00
*** WARNING WITH FIX ERROR  (IER =  67) FROM IMSL ROUTINE DGEAR
 ************************************************

  TIN                 Q                 RE                FSUBF               WBAR
  .5902300E+03  0.                .4500000E+03   .6412715E+00   .1148235E-01
  GRASHO      .2679620E+05    RICH      .1323269E+00    BUOY      .1082675E+01    FRIC      .2444444E+00
*** WARNING WITH FIX ERROR  (IER =  67) FROM IMSL ROUTINE DGEAR
 ************************************************

  TIN                 Q                 RE                FSUBF               WBAR
  .5902300E+03  0.                .5000000E+03   .6694783E+00   .1275817E-01
  GRASHO      .2679620E+05    RICH      .1071848E+00    BUOY      .9744073E+00    FRIC      .2200000E+00
*** WARNING WITH FIX ERROR  (IER =  67) FROM IMSL ROUTINE DGEAR
 ************************************************

  TIN                 Q                 RE                FSUBF               WBAR
  .5902300E+03  0.                .5500000E+03   .6936627E+00   .1403399E-01
  GRASHO      .2679620E+05    RICH      .8858248E-01    BUOY      .8858248E+00    FRIC      .2000000E+00
*** WARNING WITH FIX ERROR  (IER =  67) FROM IMSL ROUTINE DGEAR
 ************************************************

  TIN                 Q                 RE                FSUBF               WBAR
  .5902300E+03  0.                .7000000E+03   .8265928E+00   .1786144E-01
  GRASHO      .2679620E+05    RICH      .5468612E-01    BUOY      .1172034E+01    FRIC      .9331828E-01
*** WARNING WITH FIX ERROR  (IER =  67) FROM IMSL ROUTINE DGEAR
 ************************************************

  TIN                 Q                 RE                FSUBF               WBAR
  .5902300E+03  0.                .8000000E+03   .8645263E+00   .2041307E-01
  GRASHO      .2679620E+05    RICH      .4186906E-01    BUOY      .9278002E+00    FRIC      .9025447E-01
*** WARNING WITH FIX ERROR  (IER =  67) FROM IMSL ROUTINE DGEAR
 ************************************************

  TIN                 Q                 RE                FSUBF               WBAR
  .5902300E+03  0.                .9000000E+03   .8913175E+00   .2296470E-01
  GRASHO      .2679620E+05    RICH      .3308173E-01    BUOY      .7549837E+00    FRIC      .8763561E-01
*** WARNING WITH FIX ERROR  (IER =  67) FROM IMSL ROUTINE DGEAR
 ************************************************

  TIN                 Q                 RE                FSUBF               WBAR
  .5902300E+03  0.                .1000000E+04   .9108358E+00   .2551634E-01
  GRASHO      .2679620E+05    RICH      .2679620E-01    BUOY      .6278588E+00    FRIC      .8535741E-01
*** WARNING WITH FIX ERROR  (IER =  67) FROM IMSL ROUTINE DGEAR
 ************************************************
```

```
  TIN                Q                RE                FSUBF             WBAR
  .5902300E+03  0.                .1500000E+04    .9582280E+00    .3827451E-01
  GRASHO      .2679620E+05    RICH      .1190942E-01    BUOY      .3088178E+00    FRIC      .7712913E-01
*** WARNING WITH FIX ERROR  (IER =  67) FROM IMSL ROUTINE DGEAR
 ************************************************

  TIN                Q                RE                FSUBF             WBAR
  .5902300E+03  0.                .2000000E+04    .9753961E+00    .5103268E-01
  GRASHO      .2679620E+05    RICH      .6699050E-02    BUOY      .1866635E+00    FRIC      .7177674E-01
*** WARNING WITH FIX ERROR  (IER =  67) FROM IMSL ROUTINE DGEAR
 ************************************************

  TIN                Q                RE                FSUBF             WBAR
  .5902300E+03  0.                .2500000E+04    .9836270E+00    .6379084E-01
  GRASHO      .2679620E+05    RICH      .4287392E-02    BUOY      .1263185E+00    FRIC      .6788225E-01
*** WARNING WITH FIX ERROR  (IER =  67) FROM IMSL ROUTINE DGEAR
 ************************************************

  TIN                Q                RE                FSUBF             WBAR
  .5902300E+03  0.                .3000000E+04    .9882004E+00    .7654901E-01
  GRASHO      .2679620E+05    RICH      .2977355E-02    BUOY      .9181207E-01    FRIC      .6485761E-01
*** WARNING WITH FIX ERROR  (IER =  67) FROM IMSL ROUTINE DGEAR
 ************************************************

  TIN                Q                RE                FSUBF             WBAR
  .5902300E+03  0.                .3500000E+04    .9910750E+00    .8930718E-01
  GRASHO      .2679620E+05    RICH      .2187445E-02    BUOY      .7010401E-01    FRIC      .6240570E-01
*** WARNING WITH FIX ERROR  (IER =  67) FROM IMSL ROUTINE DGEAR
 ************************************************

  TIN                Q                RE                FSUBF             WBAR
  .5902300E+03  0.                .4000000E+04    .9929867E+00    .1020654E+00
  GRASHO      .2679620E+05    RICH      .1674762E-02    BUOY      .5548540E-01    FRIC      .6035680E-01
*** WARNING WITH FIX ERROR  (IER =  67) FROM IMSL ROUTINE DGEAR
 ************************************************

  TIN                Q                RE                FSUBF             WBAR
  .5902300E+03  0.                .4500000E+04    .9943355E+00    .1148235E+00
  GRASHO      .2679620E+05    RICH      .1323269E-02    BUOY      .4515856E-01    FRIC      .5860546E-01
*** WARNING WITH FIX ERROR  (IER =  67) FROM IMSL ROUTINE DGEAR
 ************************************************

  TIN                Q                RE                FSUBF             WBAR
  .5902300E+03  0.                .5000000E+04    .9953490E+00    .1275817E+00
  GRASHO      .2679620E+05    RICH      .1071848E-02    BUOY      .3755471E-01    FRIC      .5708194E-01
*** WARNING WITH FIX ERROR  (IER =  67) FROM IMSL ROUTINE DGEAR
 ************************************************

  TIN                Q                RE                FSUBF             WBAR
  .5902300E+03  0.                .5500000E+04    .9960936E+00    .1403399E+00
  GRASHO      .2679620E+05    RICH      .8858248E-03    BUOY      .3178537E-01    FRIC      .5573790E-01
*** WARNING WITH FIX ERROR  (IER =  67) FROM IMSL ROUTINE DGEAR
 ************************************************

  TIN                Q                RE                FSUBF             WBAR
  .5902300E+03  0.                .6000000E+04    .9966682E+00    .1530980E+00
  GRASHO      .2679620E+05    RICH      .7443389E-03    BUOY      .2729589E-01    FRIC      .5453853E-01
*** WARNING WITH FIX ERROR  (IER =  67) FROM IMSL ROUTINE DGEAR
 ************************************************

  TIN                Q                RE                FSUBF             WBAR
  .5902300E+03  0.                .6500000E+04    .9970937E+00    .1658562E+00
  GRASHO      .2679620E+05    RICH      .6342296E-03    BUOY      .2372813E-01    FRIC      .5345802E-01
*** WARNING WITH FIX ERROR  (IER =  67) FROM IMSL ROUTINE DGEAR
 ************************************************

  TIN                Q                RE                FSUBF             WBAR
  .5902300E+03  0.                .7000000E+04    .9975538E+00    .1786144E+00
  GRASHO      .2679620E+05    RICH      .5468612E-03    BUOY      .2084205E-01    FRIC      .5247673E-01
 ************************************************

  TIN                Q                RE                FSUBF             WBAR
  .5902300E+03  0.                .9500000E+04    .9987790E+00    .2424052E+00
  GRASHO      .2679620E+05    RICH      .2969108E-03    BUOY      .1221366E-01    FRIC      .4861948E-01
 ************************************************

  TIN                Q                RE                FSUBF             WBAR
  .5902300E+03  0.                .1150000E+05    .9993048E+00    .2934379E+00
  GRASHO      .2679620E+05    RICH      .2026178E-03    BUOY      .8742603E-02    FRIC      .4635182E-01
 ************************************************

  TIN                Q                RE                FSUBF             WBAR
  .5902300E+03  0.                .1350000E+05    .9996547E+00    .3444706E+00
  GRASHO      .2679620E+05    RICH      .1470299E-03    BUOY      .6603556E-02    FRIC      .4453052E-01
 ************************************************
```

A.6 LIMITATIONS

The following limitations must be kept in mind:

1. For F=1 (Uniform Distribution) η^* is set to unity.

2. Appropriate flow-dependent friction factor parameters must be inputed. The present version uses the blanket assembly correlations given in Table I as default values.

3. The integrator subroutine DGEAR should be substituted with an equivalent integration routine, if not available.

APPENDIX B

USER'S MANUAL FOR TWIST

The steady-state and transient parabolic flow model developed in Chapters 4 and 5 have been implemented into the TWo-dimensional Intra-Subassembly Thermal-hydraulics (TWIST) code.

TWIST is a highly modular computer program capable of calculating a number of steady-states sequentially, or as initial conditions to the transient calculations, using user supplied boundary conditions and transient forcing functions.

B.1 PROGRAM FLOW CHART AND CODE STRUCTURE

1) MASTER DRIVER

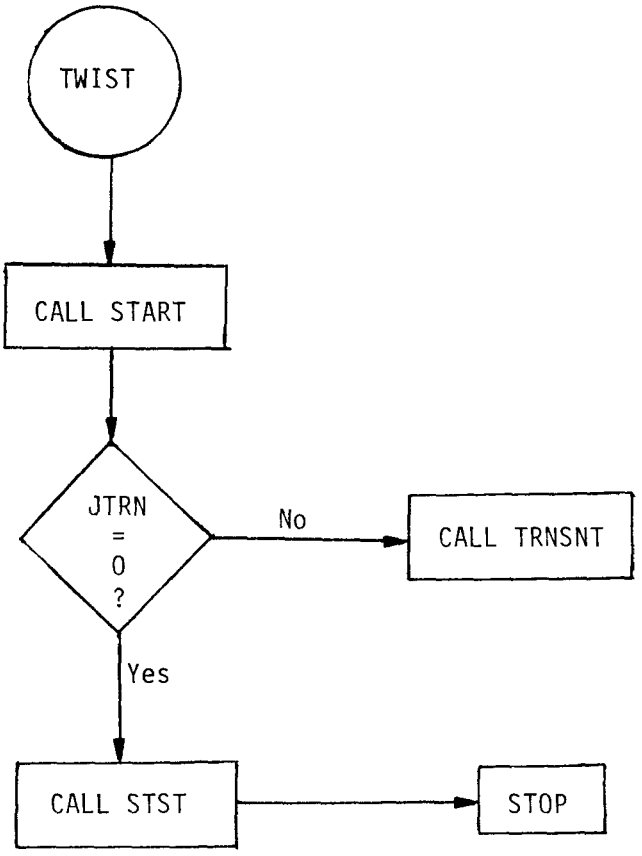

2) START MODULE

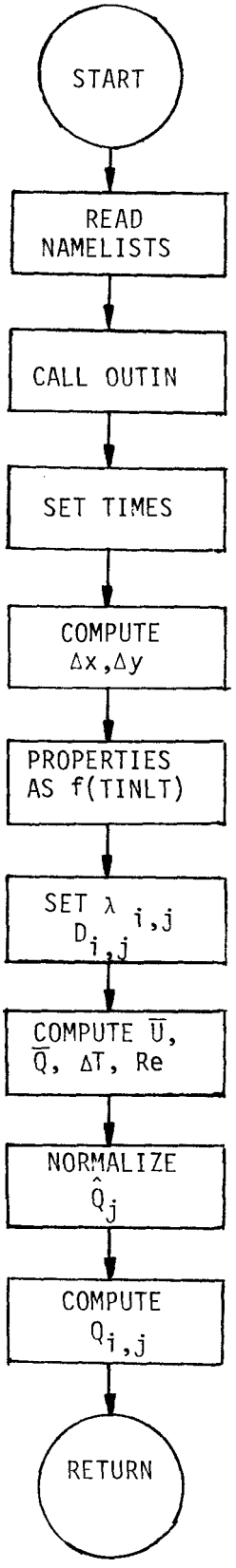

3) STEADY-STATE DRIVER

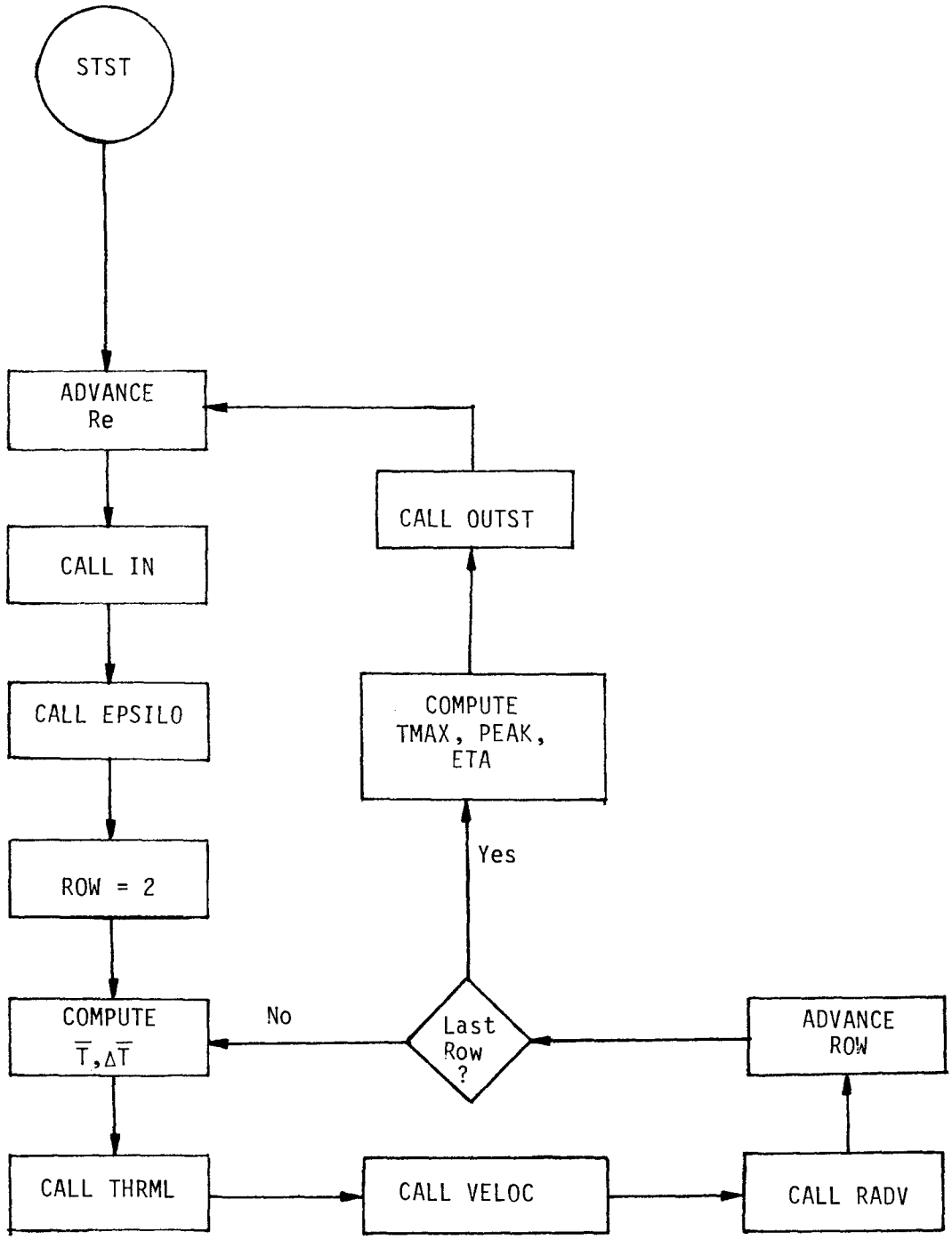

5) DRIVER FOR ENERGY EQUATION

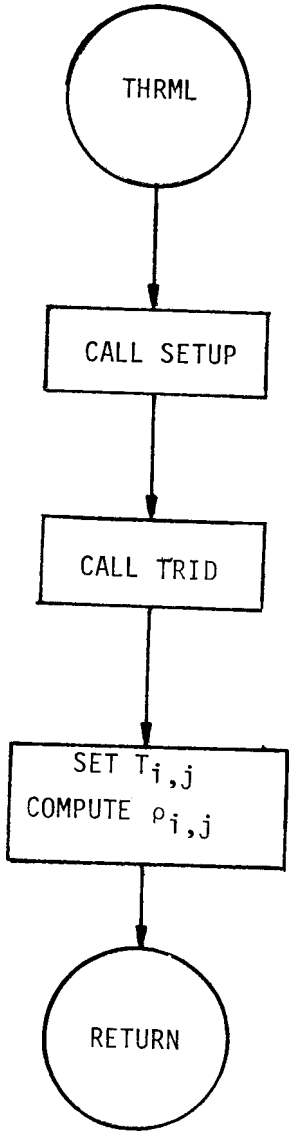

6) DRIVER FOR AXIAL MOMENTUM EQUATION

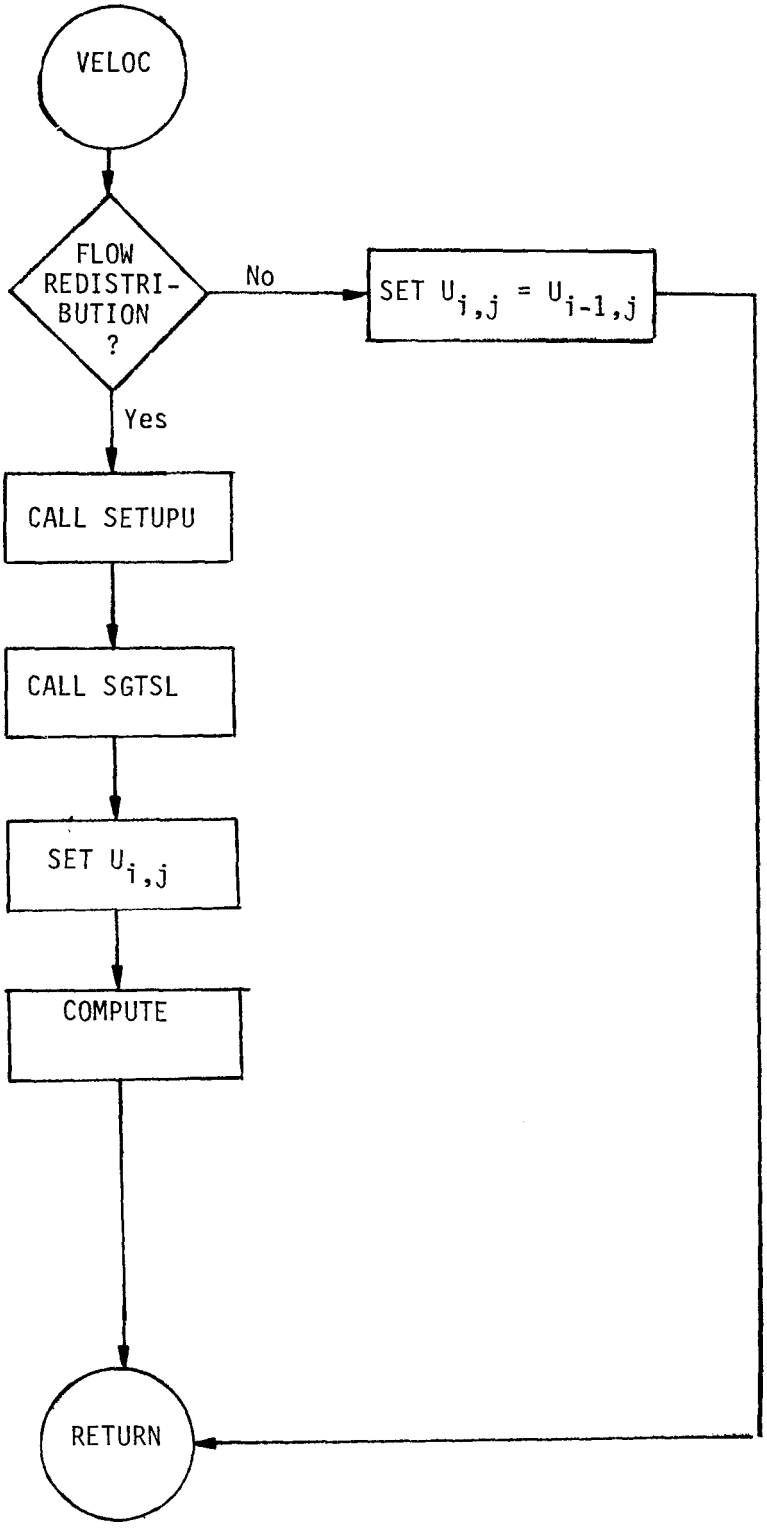

4) TRANSIENT DRIVER

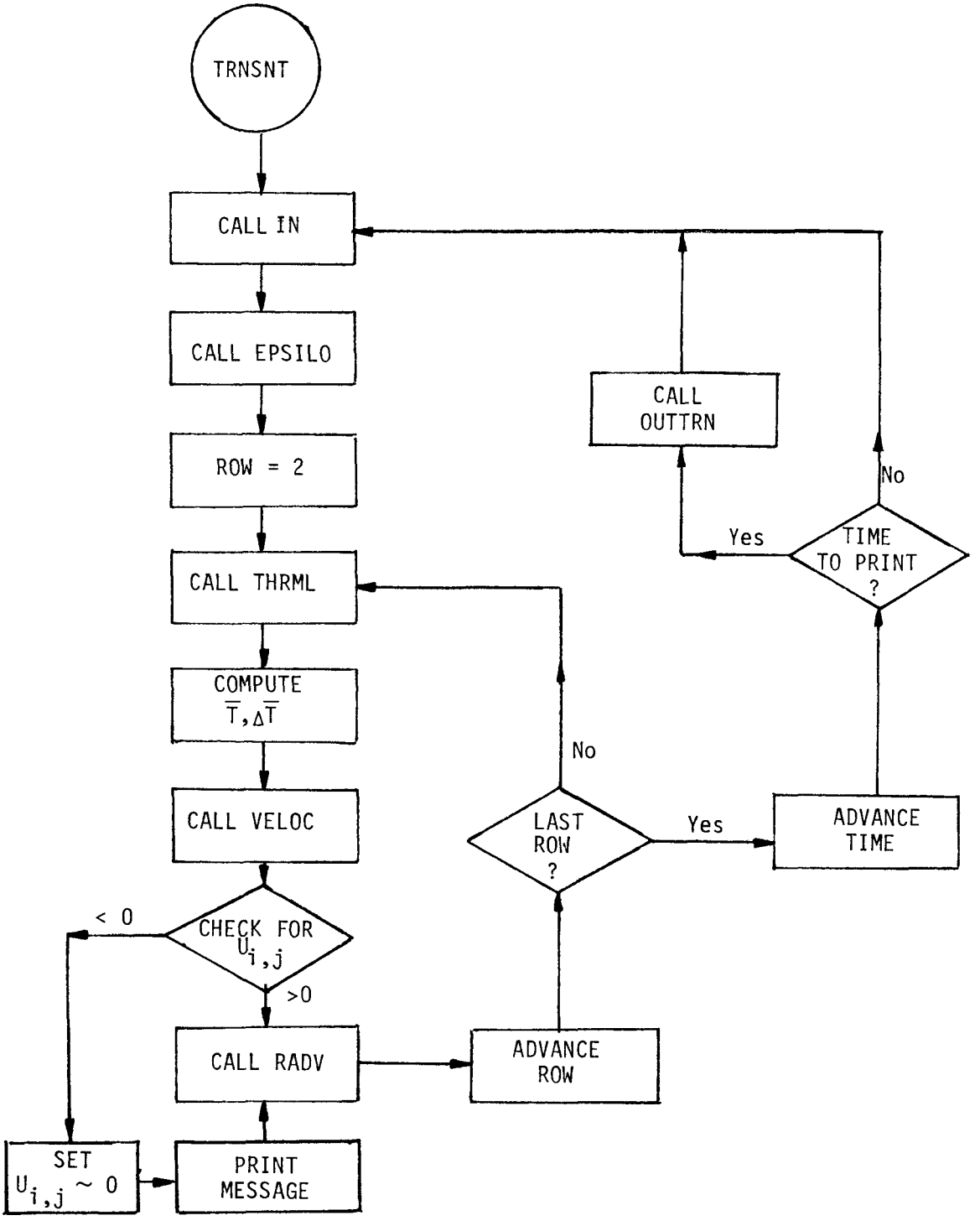

```
      PROGRAM TWIST(INPUT,OUTPUT,TAPE1,TAPE2=OUTPUT,TAPE98)
C
C       PROGRAM TO COMPUTE TWO DIMENSIONAL TEMP. AND VELOCITY
C         DISTRIBUTION IN A ROD BUNDLE.
C       X IS AXIAL DIRECTION  ( U )
C       Y IS TRANSVERSE DIRECTION ( V )
C         U IS AXIAL VELOCITY
C         V IS TRANSVERSE VELOCITY
C
C       NEEDS AS BOUNDARY CONDITIONS
C
C        T(1,J)    T DISTRIB. ≤ INLET
C        U(1,J)    U DISTRIB. ≤ INLET
C        V(1,J)    V DISTRIB. ≤ INLET
C
C           OTHER DEFINITIONS  :
C        XL    AXIAL LENGTH OF ASSEMBLY
C        YL    ASSEMBLY FLAT-TO-FLAT
C        N     NUMBER OF RADIAL NODES
C        M     NUMBER OF AXIAL NODES
C
      COMMON /TRNOP/    JTRN
C
C          READ INPUT DATA
C
      CALL START
C
C          IF JTRN = 0 COMPUTE STEADY STATE ONLY
C
      IF(JTRN.EQ.0)   CALL STST
C
C          IF JTRN = 1 COMPUTE TRANSIENT
C
      IF(JTRN.EQ.1)   CALL TRNSNT
C
C
      STOP
      END
      SUBROUTINE START
C
C       THIS SUBROUTINE READS INPUT DATA
C         THROUGH 12 NAMELIST GROUPS
C
      COMMON /TRNOP/   JTRN
C
      COMMON /DATIN/ IDETAI,NRE,MODE,ALINT,ALEXT,YDINT,YDEXT,REEND,
     +     QNORM(40)
C
      COMMON /MORE/ AMU,F,FRIC,DTAV,YDE,BETA,TINLT,ALAM,RE,
     +     DELTAT,PEAK,ETA,QBAR,TBAR,XKF,ICOND,IREDS
C
      COMMON /KNOW/ XL,YL,N,M,RHO,CP,ALPHA,ALK,DX,DY,UBAR,
     +     CF,EPSII, Q(40,40)
C
      COMMON /AXIA/ XLLFGP,XLH,XLUFGP,MLFGP,MH,MUFGP,
     +     DXLFGP,DXH,DXUFGP
C
      COMMON /LAMBDA/  ALAJ(40),YD(40),USTAR,UBOLD,TBOLD
C
      COMMON /TIMER/ STIME,SDELT,CTIME,CTIMS,DTTRN,SEND,SDMAX,SDMIN
C
      COMMON /PRINTR/ SPRNT,SNEXT,DTPRNT
C
      COMMON /STRC/ XMS,CS,DELTAW,XMC1,XMCN
C
      COMMON /SS/   UZERO,QZERO
C
      COMMON /U/ TIME(40),URAT(40),NTIME
C
      COMMON /P/ TIM(40) ,PW(40),NTIM
C
C        NAMELIST GROUPS
C
      NAMELIST /OPTION/   JTRN
C
      NAMELIST /CONTR/ IDETAI,NRE,IREDS,ICOND,N,
     +     MLFGP,MH,MUFGP
C
      NAMELIST /GEOM1/ XLLFGP,XLH,XLUFGP,YL
C
      NAMELIST /GEOM2/ ALAM,ALINT,ALEXT
C
      NAMELIST /GEOM3/ YDE,YDINT,YDEXT
C
      NAMELIST /INITC/ RE,REEND,TINLT,EPSII,QBAR,
     +     DELTAT,UBAR
C
      NAMELIST /PROP/   BETA
C
      NAMELIST /RADQ/  QNORM
C
      NAMELIST /TIMES/  SDMIN,SDMAX,DTPRNT,SEND
C
      NAMELIST /WALL/ XMS,CS,DELTAW,XMC1,XMCN
C
      NAMELIST /UTIME/ TIME,URAT
C
      NAMELIST /PTIME/ TIM , PW
C
C
C          READ INPUT DATA FROM NAMELISTS
```

```
C
      READ(1,OPTION)
      READ(1,CONTR)
      READ(1,GEOM1)
      READ(1,GEOM2)
      READ(1,GEOM3)
      READ(1,INITC)
      READ(1,PROP)
      READ(1,RADQ)
      READ(1,TIMES)
      READ(1,WALL)
      READ(1,UTIME)
      READ(1,PTIME)
C
C       SET TRANSIENT TIME AND INTERVALS
C
C        INITIAL TIME
C
      STIME = 0.0
C         PRINTOUT TIME
      SPRNT = STIME
C         NEXT PRINTOUT TIME
      SNEXT = SPRNT
      IF(SDMAX.EQ.0.0)   SDMAX = 1.E-05
C        THE LATTER IS NECESSARY TO AVOID DIVISION BY 0
C
C         INITIAL TIME STEP
      SDELT = SDMAX / 32.0
C
C        MODE=0 MEANS THAT UBAR IS NOT SPECIFIED,HENCE WILL BE COMPUTED
C        FROM REYNOLDS NUMBER
C
      MODE = 0
      IF(UBAR.GT.0.0)   MODE = 1
C
C         DEFINE ASSEMBLY GEOMETRY
C
      XL = XLH + XLUFGP + XLLFGP
      DXH = XLH / FLOAT(MH-1)
      DXLFGP = 0.0
      DXUFGP = 0.0
      IF(MLFGP.EQ.0)   GOTO 1
      DXLFGP = XLLFGP /FLOAT(MLFGP-1)
      DXH = XLH / FLOAT(MH)
1       IF(MUFGP.EQ.0)   GOTO 2
      DXUFGP = XLUFGP / FLOAT(MUFGP)
2      M = MLFGP + MH + MUFGP
      DY = YL / FLOAT(N-3)
C
C        COMPUTE PROPERTIES AS FUNCTION OF INLET CONDITIONS
C
      RHO = DENS(TINLT)
      CP = CAP(TINLT)
      AMU = VISC(TINLT)
C
C        SET CONDUCTION AND DISTRIBUTION PARAMETERS
C
C          NO CONDUCTION
      IF(ICOND.EQ.0)   EPSII = 0.0
C          CALCULATE TORTUOSITY
      XKF = ALAM / (1. + .5*(1.-ALAM))
C          NO FLOW REDISTRIBUTION
      IF(IREDS.EQ.0)   BETA = 0.0
C
C           SET ASSEMBLY POROSITIES AND HYDR. DIAMETERS
C
      YD(1) = YD(N) = YDEXT
      YD(2) = YD(N-1) = YDEXT
      YD(3) = YD(N-2) = YDEXT
      ALAJ(1) = ALAJ(N) = ALEXT
      ALAJ(2) = ALAJ(N-1) = ALEXT
      ALAJ(3) = ALAJ(N-2) = ALEXT
      DELY = (YDEXT - YDINT) /3.
      YD(4) = YD(N-3) = YDEXT - DELY
      YD(5) = YD(N-4) = YDEXT - 2.*DELY
      DELA = (ALEXT - ALINT) / 3.
      ALAJ(4) = ALAJ(N-3) = ALEXT - DELA
      ALAJ(5) = ALAJ(N-4) = ALEXT - 2.*DELA
      NEND = N - 5
      DO 90 JJ=6,NEND
      ALAJ(JJ) = ALINT
      YD(JJ) = YDINT
90        CONTINUE
C
C       DEFINE INLET AVER. VELOCITY,TOTAL POWER AND AVERAGE TEMP. RISE
C
      IF(MODE.EQ.1)   GOTO 91
      UBAR = RE *ALAM * AMU / RHO / YDE
      GOTO 92
91        RE = UBAR * RHO * YDE / ALAM / AMU
92        CONTINUE
      IF(QBAR.EQ.0.0)   GOTO 100
      AP = SQRT(3.) / 2. * YL*YL
      QBAR = QBAR / XLH / AP
      DELTAT = QBAR * XLH / RHO / CP / UBAR
      GOTO 101
100       QBAR = DELTAT * RHO * CP * UBAR / XLH
101       CONTINUE
      UZERO = UBAR
      QZERO = QBAR
C
```

```
C          MASS OF STRUCTURE PER AXIAL NODE
C
      XMS = XMS / FLOAT(M-1)
C
C          NUMBER OF DATA POINTS IN FORCING FUNCTIONS TABLES
C
      DO 200 KT = 2,40
      IF(TIME(KT).LE.0.0)   GOTO 200
      NTIME = KT
200      CONTINUE
C
      DO 201 KT=2,40
      IF(TIM(KT).LE.0.0)   GOTO 201
      NTIM = KT
201       CONTINUE
C
C          NORMALIZE RADIAL POWER DISTRIBUTION, USING SIMPSON'S RULE
C
      NMM = N - 3
      QTOT = QNORM(3) + QNORM(N-2)
      DO 400 J=4,NMM
      COEF = 4.
      JL = J - (J/2) * 2
      IF(JL.NE.0)  COEF = 2.
      QTOT = QTOT + QNORM(J) * COEF
400           CONTINUE
      QTOT = QTOT / 3. / FLOAT(N-5)
      DO 410 J=1,N
410       QNORM(J) = QNORM(J) / QTOT
C
C           COMPUTE POWER SKEW (PEAK-TO-AVERAGE)
C
      F = QNORM(3)/((QNORM(3)+QNORM(N-2))/2.)
C
C           AXIAL POWER DISTRIBUTION IS IN THE SHAPE OF A CHOPPED
C           COSINE CURVE, WITH PEAK-TO-AVERAGE OF 1.4
C
      X = 0.0
      DO 500 I=1,M
      QX = 1.4*COS(.8738*3.14156*((X-XLLFGP)/XLH - .5))
      IF(I.LE.MLFGP.OR.I.GT.(MLFGP+MH)) QX = 0.0
      DXX= DXLFGP
      IF(I.GE.MLFGP) DXX= DXH
      X = X + DXX
      DO 600 J=1,N
      Q(I,J) = QBAR * QNORM(J) * QX
      IF(J.EQ.1.OR.J.EQ.N)   Q(I,J) = 0.0
      IF(J.EQ.2.OR.J.EQ.(N-1))   Q(I,J) = 0.0
600      CONTINUE
500      CONTINUE
C
C
      CALL OUTIN
C
C
      RETURN
      END
      SUBROUTINE   STST
C
C       THIS SUBROUTINE IS THE STEADY-STATE DRIVER
C
C
      COMMON /KNOW/  XL, YL, N, M, RHO, CP, ALPHA, ALK, DX, DY, UBAR,
     +     CF,      EPSII,
     +      Q(40,40)
C
      COMMON/AXIA/ XLLFGP,XLH,XLUFGP,MLFGP,MH,MUFGP,
     +   DXLFGP,DXH,DXUFGP
C
      COMMON /DATIN/   IDETAI,NRE,MODE,ALINT,ALEXT,YDINT,YDEXT,REEND,
     +   QNORM(40)
C
C
      COMMON /UNKN/    T(40,40), U(40,40), V(40,40),DEN(40,40)
C
C
      COMMON /MORE/ AMU,F,FRIC,DTAV,YDE,BETA,TINLT,ALAM,RE
     +   ,DELTAT,PEAK,ETA,QBAR,TBAR,XKF,ICOND,IREDS
C
      COMMON /LAMBDA/ ALAJ(40),YD(40),USTAR,UBOLD,TBOLD
C
C
C       SET REYNOLDS NUMBER STEPS
C
      DELRE1 = 100.
      DELRE2 = 500.
      DELRE3 = 5000.
C
C       BEGIN  COMPUTATIONS
C
      DO 700 IRE = 1,NRE
C
C          GET INLET CONDITIONS
      UBOLD = UBAR
C
      CALL IN
C
C       COMPUTE EDDY DIFFUSIVITY OF HEAT
C
      CALL EPSILO
C
```

```
      TBAR = TINLT
C
C        NOW MARCH FROM ROW TWO TO TOP OF ASSEMBLY
C
      X = 0.0
      DO 100 I=2,M
C
C          FIND WHETHER IT IS A PLENA SLICE OR HEATED
C         COMPUTE TBAR FOR SLICE FROM DELTAT
C
      DX = DXLFGP
      IF(I.GT.MLFGP) DX = DXH
      IF(I.GT.(MLFGP+MH))  DX = DXUFGP
      X = X + DX
      TBOLD = TBAR
      TBAR = TINLT + 1.4*QBAR/RHO/CP/UBAR*XLH/
     +   (3.14156*.8738)*(SIN(.8738*3.14156*
     +   ((X-XLLFGP)/XLH-.5)) + .98)
      IF(I.LE.MLFGP.OR.I.GT.(MLFGP+MH)) TBAR = TBOLD
      DTAV = TBAR - TBOLD
C
C        THERMAL CALCULATIONS FOR ROW I
C
      CALL THRML(I)
C
C       NOW SOLVE   FOR U(I,J)
C
      CALL VELOC(I)
C
C       FINALLY COMPUTE V(I,J)
C
      CALL RADV(I)
C
C       DETAILED PRINTOUT ACTIVATED
C
      IF(IDETAI.EQ.0)   GOTO 600
C
      II = I - 1
      CALL OUTROW(II)
600     CONTINUE
C
C          CALCULATIONS DONE FOR ROW I
C
100     CONTINUE
C
C       DISPLAY RESULTS FOR EXIT ROW
C
      CALL OUTROW(M)
C
C       FIND TMAX IN LAST ROW
C          COMPUTE HOT CHANNEL FACTOR AND TEMP. PEAKING FACTOR
C
      TMAX = T(M,1)
      DO 400 J=2,N
      IF(T(M,J).GT.TMAX)  TMAX = T(M,J)
400    CONTINUE
      PEAK = (TMAX - TINLT) / (TBAR - TINLT)
      ETA = 1.
      IF(F.EQ.1.)   GOTO 477
      ETA = (PEAK - 1.) / (F - 1.)
477          CONTINUE
      CALL OUTST
C
C          ADVANCE REYNOLDS NUMBER
C
      DELRE = DELRE1
      IF(RE.GE.1500.)   DELRE = DELRE2
      IF(RE.GE.6000.)   DELRE = DELRE3
      RE = RE + DELRE
      IF(RE.GT.REEND)    STOP
700     CONTINUE
C
C
      RETURN
      END
      SUBROUTINE TRNSNT
C
C
C       THIS SUBROUTINE IS THE TRANSIENT DRIVER
C
      COMMON /KNOW/  XL, YL, N, M, RHO, CP, ALPHA, ALK, DX, DY, UBAR,
     +    CF,       EPSII, Q(40,40)
C
      COMMON /DATIN/ IDETAI,NRE,MODE,ALINT,ALEXT,YDINT,YDEXT,REEND,
     +   QNORM(40)
C
      COMMON/AXIA/ XLLFGP,XLH,XLUFGP,MLFGP,MH,MUFGP,
     +   DXLFGP,DXH,DXUFGP
C
      COMMON /UNKN/   T(40,40), U(40,40), V(40,40),DEN(40,40)
C
      COMMON /MORE/ AMU,F,FRIC,DTAV,YDE,BETA,TINLT,ALAM,RE
     +   ,DELTAT,PEAK,ETA,QBAR,TBAR,XKF,ICOND,IREDS
C
      COMMON /LAMBDA/ ALAJ(40),YD(40),USTAR,UBOLD,TBOLD
C
      COMMON /TIMER/ STIME,SDELT,CTIME,CTIMS,DTTRN,SEND,SDMAX,SDMIN
C
      COMMON /PRINTR/ SPRNT,SNEXT,DTPRNT
C
      DIMENSION TOLD(40,40)
```

```
C
C
C       SAVE DATA FROM PREVIOUS TIME STEP;
C         GET INLET CONDITIONS AND COMPUTE EDDY DIFFUSIVITY
C
      JNEG = 0
      JPRNT = 0
700      CONTINUE
C
      UBOLD = UBAR
      CALL IN
      CALL EPSILO
      DO 500 J=1,N
      DO 500 I=1,M
      TOLD(I,J) = T(I,J)
500         CONTINUE
C
      TBAR = TINLT
C
C         MARCH UP THE ASSEMBLY
C
      DO 100 I=2,M
C
      TBOLD = TBAR
      DX = DXLFGP
      IF(I.GT.MLFGP)    DX = DXH
      IF(I.GT.(MLFGP+MH))    DX = DXUFGP
C
C      THERMAL CALCULATIONS FOR ROW I
C
      CALL THRML(I)
C
C     COMPUTE TBAR FOR ROW I, USING SIMPSON'S RULE
C
      NLAST = N - 2
      TBAR = 0.0
      DO 121 J=3,NLAST
      COEF = 2.0
      JJ = J - 2*(J/2)
      IF(JJ.NE.0)  COEF = 4.0
      TBAR = TBAR + COEF*T(I,J)*U(I,J)
121      CONTINUE
      TBAR = TBAR / 3. / FLOAT(N-3)
      TBAR = TBAR / UBAR
      DTTRN = TBAR - TBOLD
C
C       NOW SOLVE   FOR U(I,J)
C
      CALL VELOC(I)
C
C       CHECK FOR NEGATIVE VELOCITY
C        IF ANY U IS <0 , SET IT TO 1.E-5 UNTIL IT RECOVERS
C          ALSO, PRINT A MESSAGE^
C
      JNEG = 0
      DO 261 JJ=3,NLAST
      IF(U(I,JJ).LT.0.0)    JNEG = JJ
      IF(U(I,JJ).LT.0.0)    U(I,JJ) = UBAR * 1.0E-05
261      CONTINUE
      IF(JNEG.EQ.0)    GOTO 262
      IF(JPRNT.EQ.1)     GOTO 262
      JPRNT = 1
      PRINT*,"   AT TIME = ",STIME," IN ROW ",I," AT NODE ",
     +    JNEG,"  U WAS NEGATIVE "
262      CONTINUE
      IF(JNEG.GT.0)    GOTO 263
      IF(JPRNT.EQ.0)    GOTO 263
      PRINT *,"  U RECOVERED AT TIME =",STIME
      JPRNT = 0
263       CONTINUE
C
C       FINALLY COMPUTE V(I,J)
C
      CALL RADV(I)
C
      IF(IDETAI.EQ.0)    GOTO 600
C
C       DETAILED PRINTOUT ACTIVATED
C
      II = I - 1
      CALL OUTROW(II)
600     CONTINUE
C
C
C         END CALCULATIONS FOR SLICE I
C
100      CONTINUE
C
C
      DTTRN = TBAR - TINLT
      IF(STIME.NE.SPRNT)    GOTO 333
C
C       IT IS TIME TO PRODUCE GENERAL PRINTOUT
C
      SPRNT = SPRNT + DTPRNT
      SNEXT = SNEXT + DTPRNT
C
      CALL OUTTRN
      CALL OUTROW(M)
333      CONTINUE
C
```

```
C      ADVANCE TIME AND RESET INTERVALS
C
       DTMAX = 0.0
       DO 555 I=1,M
       DO 555 J=1,N
       DT = ABS((TOLD(I,J)-T(I,J))/T(I,J))
       IF(DT.GT.DTMAX) DTMAX = DT
555        CONTINUE
       IF(DTMAX.LE.0.005)  SDELT = 2.0*SDELT
       IF(DTMAX.GT.0.01)   SDELT = SDELT/2.0
       IF(SDELT.GT.SDMAX)   SDELT = SDMAX
       IF(SDELT.LT.SDMIN)  SDELT = SDMIN
       IF((STIME+SDELT).GT.SNEXT)
      +   SDELT = SNEXT - STIME
       STIME = STIME + SDELT
       IF(STIME.GT.SEND)   STOP
       GOTO 700
C
C
       END
       SUBROUTINE THRML(I)
C
C         THIS SUBROUTINE SOLVES THE ENERGY EQUATION
C
       COMMON /UNKN/ T(40,40),U(40,40),V(40,40),DEN(40,40)
C
       COMMON /WORK/ C(40), D(40), E(40), B(40)
C
       COMMON /KNOW/ XL,YL,N,M,RHO,CP,ALPHA,ALK,DX,DY,UBAR,CF,EPSII,
      +     Q(40,40)
C
C
C          COMPUTE MATRIX TERMS FOR ROW I AND R.H.S.
C
       CALL SETUP(I)
C
C          SOLVE A(C,D,E) * T = B
C
         CALL TRID(C,D,E,B,N)
C
C          B NOW CONTAINS T(I,J)
C
       DO 100  J=1,N
       T(I,J) = B(J)
       DEN(I,J) = DENS(T(I,J))
100         CONTINUE
C
C
       RETURN
       END
       SUBROUTINE RADV(I)
C
C          THIS SUBROUTINE COMPUTES THE TRANSVERSE VELOCITY
C            DISTRIBUTION USING THE CONTINUITY EQUATION
C
       COMMON /UNKN/    T(40,40),U(40,40),V(40,40),DEN(40,40)
C
       COMMON /KNOW/   XL,YL,N,M,RHO,CP,ALPHA,ALK,DX,DY,UBAR,CF,EPSII
      +     Q(40,40)
C
C
C
       NLP = N - 2
C
       DO 100 J=2,NLP
       V(I,J) = (DEN(I,J-1)*V(I,J-1) - DY/2./DX*
      +    (DEN(I,J-1)*U(I,J-1) + DEN(I,J)*U(I,J) -
      +     DEN(I-1,J-1)*U(I-1,J-1) -
      +     DEN(I-1,J)*U(I-1,J)   )   ) /DEN(I,J)
100         CONTINUE
C
C
       RETURN
       END
       SUBROUTINE TRID(A,B,C,R,N)
C
C          SUBROUTINE TO SOLVE A SET OF LINEAR EQUATIONS WITH
C            TRIDIAGONAL MATRIX OF COEFFICIENTS BY GAUSSIAN
C            ELIMINATION OF THE FORM :
C                    MAT(A,B,C) * X = R
C          ORDER OF MAT IS N*N
C            RESULT IS RETURNED IN R
C
       DIMENSION A(40),B(40),C(40),R(40)
C
       DIMENSION X(40)
C
       IF(B(N).EQ.0.0)   GOTO 400
       A(N) = A(N)/B(N)
       R(N) = R(N)/B(N)
C
       DO 100 I=2,N
       II = -I + N + 2
       BN = 1./(B(II-1) - A(II)*C(II-1))
       IF(II.GT.2) A(II-1) = A(II-1) * BN
       R(II-1) = (R(II-1)-C(II-1)*R(II)) * BN
100          CONTINUE
C
       X(1) = R(1)
       DO 200 I=2,N
       X(I) = R(I) - A(I)*X(I-1)
```

```
200             CONTINUE
C
      DO 300 I=1,N
      R(I) = X(I)
300             CONTINUE
C
      RETURN
C
C
400       CONTINUE
      PRINT *," STOP CALCULATIONS BECAUSE ELEMENT IN DIAGONAL = 0."
C
      STOP
C
      END
      SUBROUTINE EPSILO
C
C         THIS SUBROUTINE COMPUTES THE THERMAL CONDUCTIVITY
C          OF THE COOLANT AND SUBSEQUENTLY EDDY
C     DIFFUSIVITY OF HEAT AND EFFECTIVE THERMAL DIFFUSIVITY
C
      COMMON /KNOW/ XL,YL,N,M,RHO,CP,ALPHA,ALK,DX,DY,UBAR,
     +      CF,EPSII, Q(40,40)
C
      COMMON /MORE/ AMU,F,FRIC,DTAV,YDE,BETA,TINLT,ALAM,RE,
     +      DELTAT,PEAK,ETA,QBAR,TBAR,XKF,ICOND,IREDS
C
C
C
      ALK = CON( TINLT )
C
      IF(ICOND.EQ.0)    ALK = 1.0E-05
C
      EPSI = EPSII*( 1. - (1.-RE/7000.)**2 )
      IF(RE.GE.7000.)    EPSI = EPSII
      EPSIH = UBAR * YDE * EPSI
C
      ALPHA = EPSIH + XKF*ALK/RHO/CP
C
C
      RETURN
      END
      SUBROUTINE SETUPU(I)
C
C       THIS SUBROUTINE COMPUTES TERMS OF EQUATIONS
C               A(C,D,E) * U = B
C           FOR AXIAL VELOCITY COMPONENT U
C
C
      COMMON /KNOW/ XL,YL,N,M,RHO,CP,ALPHA,ALK,DX,DY,UBAR,CF,
     +  EPSII, Q(40,40)
C
      COMMON /UNKN/ T(40,40),U(40,40),V(40,40),DEN(40,40)
C
      COMMON /WORK/ C(40),D(40),E(40),B(40)
C
      COMMON /NEWWK/  A(40,40),WK(40),IWK(40)
C
      COMMON /MORE/ AMU,F,FRIC,DTAV,YDE,BETA,TINLT,ALAM,RE,
     +  DELTAT,PEAK,ETA,QBAR,TBAR,XKF,ICOND,IREDS
C
      COMMON /LAMBDA/ ALAJ(40),YD(40),USTAR,UBOLD,TBOLD
C
      COMMON /TIMER/ STIME,SDELT,CTIME,CTIMS,DTTRN,SEND,SDMAX,SDMIN
C
C         COMPUTATIONS ARE PERFORMED FOR COOLANT ONLY;
C           AT WALLS AND FOR STAGNANT COOLANT U IS = 0
C
      II = I
      DELTIM = CTIME / SDELT
      NLAST = N - 2
      NFIRST = 3
      NU = N - 3
      RHOBAR = DENS( TBAR )
      ANU = AMU/RHOBAR/DY/DY
      DO 77 III=1,40
      DO 77 JJJ=1,40
      A(III,JJJ) = 0.0
77        CONTINUE
C
C          FIRST ROW OF A(I,J)
C
      DO 1 J=NFIRST,NLAST
      A(1,J-2) = DEN(II,J)
1         CONTINUE
C
C         LAST COLUMN OF A(I,J)
C
      DO 2 JI=NFIRST,NLAST
      A(JI-1,NU) = 1. / DX
2         CONTINUE
C
C       COEFFICIENTS OF U(I,J)
C
      DO 100 JJ=NFIRST,NLAST
      JD = JJ - 1
      AL = ALAJ(JJ)
      IF(II.LE.2)  AL = ALAM
      YDIAM = YD(JJ)
      IF(II.LE.2)  YDIAM = YDE
      A(JD,JD-1) = U(II-1,JJ)/DX + 2.*ANU
      REIJ=DEN(II-1,JJ)*YDIAM*U(II-1,JJ)/AL/AMU
```

```
      FIJ = FRC(REIJ)
      A(JD,JD-1) = A(JD,JD-1) + U(II-1,JJ)*FIJ/2./YDIAM/AL**2
     +       +  DELTIM
100      CONTINUE
C
C       COEFFICIENTS OF U(I,J-1)
C
      NSUB = NFIRST + 1
      DO 200 JJ=NSUB,NLAST
      JC = JJ - 1
      A(JC,JC-2) = -V(II-1,JJ-1)/2./DY - ANU
200     CONTINUE
C
C     COEFFICIENTS OF U(I,J+1)
C
      NSUP = NLAST - 1
      DO 300 JJ=NFIRST,NSUP
      JE = JJ - 1
      A(JE,JE) = V(II-1,JJ+1)/2./DY - ANU
300       CONTINUE
C
C
C     R. H. S.
C
      B(1) = 0.0
      DO 400 J=NFIRST,NLAST
      B(1) = B(1) + DEN(II-1,J)*U(II-1,J)
400        CONTINUE
C
      DO 500 KB = 2,NU
      B(KB) = U(II-1,KB+1)*U(II-1,KB+1)/DX +
     +     9.81*BETA*(T(II,KB+1) - TINLT) +
     +     DELTIM * U(II,KB+1)
500         CONTINUE
C
C       AUGMENT MATRIX A WITH R.H.S. COLUMN
C
      DO 600 KK=1,NU
      A(KK,NU+1) = B(KK)
600       CONTINUE
C
C
      RETURN
      END
      SUBROUTINE VELOC(I)
C
C       THIS SUBROUTINE COMPUTES AXIAL VELOCITY IN ROW I
C
      COMMON /LAMBDA/ ALAJ(40),YD(40),USTAR,UBOLD,TBOLD
C
      COMMON /MORE/ AMU,F,FRIC,DTAV,YDE,BETA,TINLT,ALAM,RE,
     +    DELTAT,PEAK,ETA,QBAR,TBAR,XKF,ICOND,IREDS
C
      COMMON /WORK/  C(40),D(40),E(40),B(40)
C
      COMMON /NEWWK/ A(40,40),WK(40),IWK(40)
C
      COMMON /KNOW/  XL,YL,N,M,RHO,CP,ALPHA,ALK,DX,DY,UBAR,
     +    CF,EPSII, Q(40,40)
C
      COMMON /UNKN/ T(40,40),U(40,40),V(40,40),DEN(40,40)
C
C
      USTAR = 0.0
      NLAST = N - 2
C
C     IN THE ABSENCE OF BUOYANCY INDUCED FLOW REDISTRIBUTION,
C       SET THE AXIAL VELOCITY TO THE INLET VELOCITY
C
      IF(IREDS.EQ.0)   GOTO 130
C
C       COMPUTE TERMS OF THE EQUATION
C           A(C,D,E) * U = B
C
      CALL SETUPU(I)
C
C         INVERT EQUATION
C
      NU = N - 3
      NUP1=NU + 1
      CALL SOLVEU(A,B,NU,NUP1)
C
C       NOW B CONTAINS U
C
      DO 125 J=3,NLAST
      U(I,J) = B(J-2)
125         CONTINUE
      GOTO 132
130          CONTINUE
      DO 131 J=1,N
      U(I,J) = U(I-1,J)
131          CONTINUE
132        CONTINUE
C
C       COMPUTE AVERAGE U FOR ROW I,USING SIMPSON'S RULE
C
      USTAR = 0.0
      DO 727 JJ=3,NLAST
      COEF = 4.
      JJL = JJ - 2 * (JJ/2)
      IF(JJL.NE.0)   COEF = 2.
```

```
      USTAR = USTAR + COEF * U(I,JJ)
727      CONTINUE
      USTAR = USTAR * DY / 3. / YL
C
C
      RETURN
      END
      SUBROUTINE SOLVEU(A,X,M,N)
C
C       SUBROUTINE TO INVERT EQUATION A(M,M)*X = A(N)
C         USING THE GAUSS-JORDAN REDUCTION METHOD
C
      DIMENSION A(40,40),X(40)
C
C         A IS NON-SINGULAR
C
      DO 100 K=1,M
      KP1 = K + 1
C
C        NORMALIZE BY PIVOT A(K,K)
C
      PIVOT = A(K,K)
      DO 200  J=KP1,N
      A(K,J) = A(K,J) / PIVOT
200         CONTINUE
      A(K,K) = 1.0
C
C          REDUCE OFF-DIAGONAL TERMS
C
      DO 100 II=1,M
      IF(II.EQ.K)   GOTO 100
      IF(A(II,K).EQ.0.0)   GOTO 100
      DO 310 JJ=KP1,N
      A(II,JJ) = A(II,JJ) - A(II,K)*A(K,JJ)
310         CONTINUE
      A(II,K) = 0.0
100         CONTINUE
C
C       SOLUTION IS IN A(I,N)
C
      DO 400 K=1,M
      X(K) = A(K,N)
400         CONTINUE
C
C
      RETURN
      END
      SUBROUTINE IN
C
C     THIS SUBROUTINE INITIALIZES ARRAYS AND SETS INLET
C         BOUNDARY CONDITIONS
C
      COMMON  /KNOW/ XL,YL,N,M,RHO,CP,ALPHA,ALK,DX,DY,UBAR,CF
     +     ,  EPSII,  Q(40,40)
C
      COMMON  /UNKN/ T(40,40),U(40,40),V(40,40),DEN(40,40)
C
      COMMON /MORE/ AMU,F,FRIC,DTAV,YDE,BETA,TINLT,ALAM
     +  ,RE,DELTAT,PEAK,ETA,QBAR,TBAR,XKF,ICOND,IREDS
C
      COMMON /LAMBDA/ ALAJ(40),YD(40),USTAR,UBOLD,TBOLD
C
      COMMON /TIMER/  STIME,SDELT,CTIME,CTIMS,DTTRN,SEND,SDMAX,SDMIN
C
      COMMON /SS/ UZERO,QZERO
C
      COMMON /STRC/ XMS,CS,DELTAW,XMC1,XMCN
C
      COMMON/AXIA/ XLLFGP,XLH,XLUFGP,MLFGP,MH,MUFGP,
     +   DXLFGP,DXH,DXUFGP
C
      COMMON /DATIN/ IDETAI,NRE,MODE,ALINT,ALEXT,YDINT,YDEXT,REEND,
     +     QNORM(40)
C
      COMMON /TRNOP/ JTRN
C
C
C
      DO 80 J=1,N
      DEN(1,J) = RHO
80         CONTINUE
C
      IF(MODE.EQ.1)   GOTO 91
      UBAR = RE * ALAM * AMU / RHO / YDE
      GOTO 92
91        RE = UBAR * RHO * YDE / ALAM / AMU
92        CONTINUE
      FRIC = FRC( RE )
C
C       FOR TRANSIENT CALCULATIONS COMPUTE ADVANCED UBAR AND POWER
C
      URT = UR(STIME)
      UBAR = UZERO * URT
      RE = UBAR*RHO*YDE/ALAM/AMU
C
      CTIME = 0.0
      IF(STIME.GT.0.0)   CTIME = 1.0
      CTIMS = 0.0
      IF(STIME.GT.0.0)   CTIMS = 1.0
      P = POVERW(STIME)
C
```

```
      QBAR = P * QZERO* UBAR / UZERO
C
C       U(1,J) AT INLET IS = 0 AT WALLS AND FOR STAGNANT COOLANT,
C       CALCULATE U(1,J) SO THAT THE AVERAGE VALUE BECOMES UBAR
C        USING THE SIMPSON'S RULE
C       IN OTHER NODES
C
      DO 100 I=1,M
      DO 100 J = 1,N
      V(I,J) = 0.0
      U(I,J) = UBAR*3.*FLOAT(N-3)/(6.*FLOAT((N-3)/2)-2.)
      IF(J.EQ.1.OR.J.EQ.N)  U(I,J) = 0.0
      IF(J.EQ.2.OR.J.EQ.(N-1))  U(I,J) = 0.0
100     CONTINUE
      DO 200 I=1,M
      DO 200 J=1,N
      IF(STIME.GT.0.0)   GOTO 201
      T(I,J)   =   TINLT
201      CONTINUE
200         CONTINUE
      X = 0.0
      DO 500 I=1,M
      QX = 1.4*COS(.8738*3.14156*((X-XLLFGP)/XLH-.5))
      IF(I.LE.MLFGP.OR.I.GT.(MLFGP+MH))   QX = 0.0
      DX = DXLFGP
      IF(I.GE.MLFGP)  DX = DXH
      X = X + DX
      DO 600 J=1,N
      Q(I,J) = QBAR * QNORM(J) * QX
      IF(J.EQ.1.OR.J.EQ.N)   Q(I,J) = 0.0
      IF(J.EQ.2.OR.J.EQ.(N-1))   Q(I,J) = 0.0
600       CONTINUE
500       CONTINUE
C
      RETURN
      END
      SUBROUTINE SETUP(I)
C
C     THIS SUBROUTINE DEFINES, FOR I=2 TO M, THE TRIDIAGONAL
C     TERMS OF   A*T = B
C
C       B = R.H.S.
C       C = SUBDIAGONAL TERMS OF A
C       D =   DIAGONAL     "      "
C       E = SUPERDIAGONAL "      "
C
C
      COMMON /KNOW/ XL,YL,N,M,RHO,CP,ALPHA,ALK,DX,DY,UBAR,CF,
     +       EPSII,  Q(40,40)
C
      COMMON /MORE/ AMU,F,FRIC,DTAV,YDE,BETA,TINLT,ALAM,RE,
     +   DELTAT,PEAK,ETA,QBAR,TBAR,XKF,ICOND,IREDS
C
      COMMON /UNKN/ T(40,40),U(40,40),V(40,40),DEN(40,40)
C
      COMMON /WORK/ C(40),D(40),E(40),B(40)
C
      COMMON /TIMER/ STIME,SDELT,CTIME,CTIMS,DTTRN,SEND,SDMAX,SDMIN
C
      COMMON /STRC/  XMS,CS,DELTAW,XMC1,XMCN
C
      COMMON /LAMBDA/ ALAJ(40),YD(40),USTAR,UBOLD,TBOLD
C
C
      II = I
      CALPHA = ALPHA / DY / DY
      DTIME = CTIME / SDELT
      AREA = SQRT(3.)*YL*DX
      AC2 = ACN1 = AREA
      LSUB = N - 2
C
C     DEFINE DIAGONAL TERMS
C
      DO 100 L=3,LSUB
100    D(L) = U(II-1,L)/DX + 2.*CALPHA + DTIME
C
C       THESE CALCULATIONS ARE FOR THE WALL AND THE
C        EXTERNAL  COOLANT
C
      AKW1 = AKW( T(II,2) )
      AKWN = AKW( T(II,N-1) )
      C1 = CAP(T(II,1))
      CN = CAP(T(II,N))
      D(1) = XMC1*DTIME*C1 + AKW1*AREA/DELTAW
      D(N) = XMCN*DTIME*CN + AKWN*AREA/DELTAW
C
      AK2 = CON(T(II,2))
      AKN1 = CON(T(II,N-1))
C
      D(2) = XMS*CS*DTIME + AKW1*AREA/DELTAW +
     +      AK2 * AC2 / DY
      D(N-1) = XMS*CS*DTIME + AKWN*AREA/DELTAW +
     +      AKN1 * ACN1 / DY
C
C     SUBDIAGONAL TERMS
C
      DO 200 L=3,LSUB
200    C(L) = -(V(II-1,L)/2./DY + CALPHA )
      C(N) = -AKWN * AREA / DELTAW
      E(2) = - AK2 * AC2 / DY
      C(N-1) = - AKN1 * ACN1 / DY
```

```
C
C      SUPERDIAGONAL TERMS
C
       E(1) = -AKW1 * AREA / DELTAW
       C(2) = -AKW1 * AREA / DELTAW
       DO 300 L=3,LSUB
300     E(L) = V(II-1,L)/2./DY - CALPHA
       E(N-1) = -AKWN * AREA / DELTAW
C
C        R.H.S.
C
       DO 400 L=3,LSUB
       B(L) = T(II-1,L) * U(II-1,L) / DX + Q(II,L) / RHO / CP
     +    + DTIME * T(II,L)
400      CONTINUE
       B(1) = XMC1*C1*DTIME*T(II,1)
       B(2) = XMS*CS*DTIME*T(II,2)
       B(N-1) = XMS*CS*DTIME*T(II,N-1)
       B(N) = XMCN*CN*DTIME*T(II,N)
C
C
       RETURN
       END
       SUBROUTINE OUTTRN
C
C         TRANSIENT OUTPUT ROUTINE
C
       COMMON /KNOW/  XL,YL,N,M,RHO,CP,ALPHA,ALK,DX,DY,UBAR,CF,
     +       EPSII,  Q(40,40)
C
       COMMON /UNKN/ T(40,40),U(40,40),V(40,40),DEN(40,40)
C
       COMMON /MORE/ AMU,F,FRIC,DTAV,YDE,BETA,TINLT,ALAM,RE,
     +    DELTAT,PEAK,ETA,QBAR,TBAR,XKF,ICOND,IREDS
C
       COMMON /TIMER/ STIME,SDELT,CTIME,CTIMS,DTTRN,SEND,SDMAX,SDMIN
C
       COMMON /SS/  UZERO,QZERO
C
C
C
       WRITE(2,99)
99      FORMAT(////)
C
       WRITE(2,666)    STIME,SDELT
666      FORMAT(1H ,10(1H*),"     TIME   = ",2F10.4)
       WRITE(2,4)    RE
4      FORMAT("       RE =  ",E12.5)
       WRITE(2,7)    TINLT
7       FORMAT(//,"    INLET TEMPERATURE  = " ,F10.3)
       WRITE(2,8)    DTTRN
8       FORMAT(    " AVERAGE TEMPERATURE RISE = ",F10.3)
       WRITE(2,10)    TBAR
10       FORMAT("     AVERAGE EXIT TEMPERATURE  =  ",F10.3)
       WRITE(2,9)    QBAR
9       FORMAT(    " AVERAGE POWER DENSITY     = ",E12.5)
C
C         TAPE98 STORES DATA FOR PLOTTING
C
       UU = UBAR / UZERO
       QQ = QBAR / QZERO
       QTOU = QQ / UU
       WRITE(98,1)  STIME,UU,DTTRN,QQ,QTOU
1        FORMAT(5E13.6)
       DO 300 L=1,M
       WRITE(98,1) (T(L,J),J=1,N)
300      CONTINUE
C
       RETURN
       END
       SUBROUTINE OUTROW(I)
C
C      THIS SUBROUTINE DISPLAYS RESULTS FOR ROW I
C
       COMMON /TRNOP/    JTRN
C
       COMMON /KNOW/ XL,YL,N,M,RHO,CP,ALPHA,ALK,DX,DY,UBAR,CF,
     +    EPSII,Q(40,40)
C
       COMMON/UNKN/ T(40,40),U(40,40),V(40,40),DEN(40,40)
C
       COMMON /MORE/AMU,F,FRIC,DTAV,YDE,BETA,TINLT,ALAM,RE,DELTAT,
     +  PEAK,ETA,QBAR,TBAR,XKF,ICOND,IREDS
C
       COMMON /TIMER/ STIME,SDELT,CTIME,CTIMS,DTTRN,SEND,SDMAX,SDMIN
C
C
       DIMENSION J(40)
C
       IF(JTRN.EQ.0)    DTTRN = DTAV
       WRITE(2,90)
90       FORMAT( // )
       DO 100 JJ=1,N
100    J(JJ) = JJ
       TBARP = TBAR - DTTRN
       IF(I.EQ.M)    TBARP = TBAR
       TCOMP = TBAR
       GIN = RHO*UBAR
       GOUT = DENS(TBARP) * UBAR
       WRITE(2,76)  I,TCOMP,GIN,GOUT
76       FORMAT("   IN ROW  ",I5,"  AVER TEMP = ",F12.4,
```

```
     +    "    MASS FLOW IN = ",E13.6,"  MASS FLOW OUT = ",
     +   E13.6)
      DO 220 JJ=1,N
      Q(I,JJ) = Q(I,JJ)/QBAR
220       CONTINUE
      JMANY = N / 6
      JP5 = 6
      J1 = -5
      DO 200 JJ=1,JMANY
      WRITE(2,91)
91      FORMAT( / )
      J1 = J1 + JP5
      J5 = J1 + 5
      WRITE(2,77) (J(JJJ),JJJ=J1,J5)
77     FORMAT("  J  ",6I20)
      WRITE(2,78)  (U(I,JU),JU=J1,J5)
78     FORMAT("  U  ",6E20.4)
      WRITE(2,79)  (V(I,JV),JV=J1,J5)
79     FORMAT("  V  ",6E20.4)
      WRITE(2,80)  (T(I,JT),JT=J1,J5)
80     FORMAT("  T  ",6F19.3)
      WRITE(2,81)  (Q(I,JQ),JQ=J1,J5)
81       FORMAT("  Q  ",6E20.4)
200    CONTINUE
C
      ILEFT = JMANY*6 - N
      IF(ILEFT.EQ.0)   GOTO 300
      JMP1 = JMANY*6 + 1
      WRITE(2,77) (J(JJJ),JJJ=JMP1,N)
      WRITE(2,78) (U(I,JU),JU=JMP1,N)
      WRITE(2,79) (V(I,JV),JV=JMP1,N)
      WRITE(2,80) (T(I,JT),JT=JMP1,N)
      WRITE(2,81) (Q(I,JQ),JQ=JMP1,N)
300     CONTINUE
      DO 400 JJ=1,N
      Q(I,JJ) = Q(I,JJ)*QBAR
400       CONTINUE
C
C
      RETURN
      END
      SUBROUTINE OUTIN
C
C     THIS SUBROUTINE PRINTS INPUT DATA
C
C
      COMMON /TRNOP/ JTRN
C
      COMMON /STRC/ XMS,CS,DELTAW,XMC1,XMCN
C
      COMMON /TIMER/ STIME,SDELT,CTIME,CTIMS,DTTRN,SEND,SDMAX,SDMIN
C
      COMMON /PRINTR/ SPRNT,SNEXT,DTPRNT
C
      COMMON /KNOW/ XL,YL,N,M,RHO,CP,ALPHA,ALK,DX,DY,UBAR,
     +    CF,EPSII,Q(40,40)
C
      COMMON /AXIA/ XLLFGP,XLH,XLUFGP,MLFGP,MH,MUFGP,
     +   DXLFGP,DXH,DXUFGP
C
      COMMON /DATIN/ IDETAI,NRE,MODE,ALINT,ALEXT,YDINT,YDEXT,REEND,
     +    QNORM(40)
C
      COMMON /MORE/ AMU,F,FRIC,DTAV,YDE,BETA,TINLT,ALAM,RE,
     +   DELTAT,PEAK,ETA,QBAR,TBAR,XKF,ICOND,IREDS
      COMMON /U/ TIME(40),URAT(40),NTIME
C
      COMMON /P/ TIM(40),PW(40),NTIM
C
C
C
      WRITE(2,100)
100     FORMAT(1H1,10(2H *),18H OPTIONS SELECTED  ,10(2H *))
      WRITE(2,200)
200       FORMAT(10(1H ),/)
      WRITE(2,101) JTRN,IREDS,ICOND,IDETAI
101     FORMAT(20H TRANSIENT OPTION = ,I5,/,
     +   23H FLOW REDISTRIBUTION = ,I5,/,
     +   13H CONDUCTION =  ,I5,/,
     +   21H DETAILED PRINTOUT =  ,I5,//)
      WRITE(2,102)
102     FORMAT(10(2H *),16H GEOMETRIC DATA  ,10(2H *),//)
      WRITE(2,103)  N,MLFGP,MH,MUFGP
103     FORMAT(26H NUMBER OF RADIAL NODES =  ,I5,/,
     +   24H NUMBER OF LFGP NODES =  ,I5,/,
     +   26H NUMBER OF HEATED NODES =  ,I5,/,
     +   24H NUMBER OF UFGP NODES =  ,I5,// )
      WRITE(2,1)  XLLFGP,XLH,XLUFGP,YL
1        FORMAT(28H LOWER FISSION GAS PLENUM = ,F10.4,4H   M /,
     +  26H ASSEMBLY HEATED LENGTH = ,F10.4,4H   M /,
     +  28H UPPER FISSION GAS PLENUM = ,F10.4,4H   M /,
     +  16H FLAT-TO-FLAT =  ,F10.4,4H   M ,//)
      WRITE(2,2)  ALAM,ALINT,ALEXT
2      FORMAT(36H LAMBDA AVERAGE,INTERIOR,EXTERIOR =  ,
     +   3F10.4)
      WRITE(2,3)   YDE,YDINT,YDEXT
3      FORMAT(48H HYDRAULIC DIAMETER AVERAGE,INTERIOR,EXTERIOR =
     +   3E15.4,4H   M  )
      WRITE(2,4)
      WRITE(2,200)
4       FORMAT(///,10(2H *),20H INITIAL CONDITIONS ,10(2H *))
```

```
      WRITE(2,5) RE,REEND,TINLT,DELTAT,QBAR,UBAR
5       FORMAT(18H REYNOLD NUMBER =  ,E15.6,/,
     +    24H FINAL REYNOLD NUMBER =  ,E15.6,/,
     +    21H INLET TEMPERATURE =  ,F14.3,3H  K,/,
     +    26H OVERALL ASSEMBLY DELTAT =  ,F14.3,3H  K,/,
     +    17H AVERAGE POWER =  ,E15.6,7H  WATTS ,/,
     +    26H AVERAGE INLET VELOCITY =  ,E15.6,5H  M/S ,//)
      WRITE(2,6)
6      FORMAT(10(2H *),12H PROPERTIES  ,10(2H *),//)
      WRITE(2,7)  EPSII,BETA
7      FORMAT(25H EPSILON STAR INFINITY =  ,E15.6,/,
     +     8H BETA =  ,E15.6,//)
      WRITE(2,8)
8      FORMAT(10(2H *),33H NORMALIZED RADIAL POWER DENSITY  ,10(2H *),//
     +   )
      WRITE(2,9)  (QNORM(JJ),JJ=1,N)
9      FORMAT(10E12.4)
      WRITE(2,200)
      WRITE(2,10)
10      FORMAT(10(2H *),17H WALL PROPERTIES  ,10(2H *),//)
      WRITE(2,11)  XMS,XMC1,XMCN,DELTAW,CS
11      FORMAT(21H MASS OF STRUCTURE = ,F14.3,13H  KG PER SIDE ,/,
     +  30H MASS OF SURROUNDING SODIUM = ,2F14.3,
     +       22H  KG AT LEFT AND RIGHT   ,/,
     +  18H WALL THICKNESS = ,E15.4,4H   M ,/,
     +  16H STRUCTURE CP =  ,F14.3,6H  J/KG  ,//)
      IF(JTRN.EQ.0)   WRITE(2,201)
201      FORMAT(1H1)
      IF(JTRN.EQ.0)   RETURN
C
      WRITE(2,20)
20      FORMAT(10(2H *),16H TRANSIENT DATA  ,10(2H *),//)
      WRITE(2,21)  SEND,SDMIN,SDMAX,DTPRNT
21      FORMAT(14H FINAL TIME =  ,F14.2,5H  SEC ,/,
     +   34H MINIMUM AND MAXIMUM TIME STEPS =  ,2E15.4,5H  SEC ,/,
     +   18H PRINTOUT EVERY = ,F14.2,5H  SEC ,///)
      WRITE(2,22)
22      FORMAT(30(1H ),18H FORCING FUNCTIONS  ,//)
      WRITE(2,23)
23      FORMAT(10(1H ),27HNORMALIZED VELOCITY VS TIME  ,/)
      WRITE(2,24) ((URAT(JJ),TIME(JJ)),JJ=1,NTIME)
24      FORMAT((3(1H ),2F12.4))
      WRITE(2,25)
25       FORMAT(//,10(1H ),27HPOWER TO FLOW RATIO VS TIME  ,/)
      WRITE(2,24) ((PW(JJ),TIM(JJ)),JJ=1,NTIM)
      WRITE(2,201)
C
C
      RETURN
      END
      SUBROUTINE OUTST
C
C      STEADY STATE OUTPUT ROUTINE
C
      COMMON /KNOW/  XL,YL,N,M,RHO,CP,ALPHA,ALK,DX,DY,UBAR,CF,
     +      EPSII,  Q(40,40)
C
      COMMON /UNKN/ T(40,40),U(40,40),V(40,40),DEN(40,40)
C
      COMMON /MORE/ AMU,F,FRIC,DTAV,YDE,BETA,TINLT,ALAM,RE,
     +   DELTAT,PEAK,ETA,QBAR,TBAR,XKF,ICOND,IREDS
C
C
C
      WRITE(2,99)
99     FORMAT(////)
C
      WRITE(2,3)   F
3     FORMAT("       F =  ",F13.5)
      WRITE(2,4)   RE
4     FORMAT("      RE =  ",E12.5)
      WRITE(2,5)   PEAK
5     FORMAT("   TEMPERATURE PEAKING FACTOR = ",F10.3)
      WRITE(2,6)   ETA
6      FORMAT("   HOT CHANNEL FACTOR    =   ",F10.3)
      WRITE(2,7)   TINLT
7      FORMAT(// "    INLET TEMPERATURE  = " ,F10.3)
      WRITE(2,8)   DELTAT
8      FORMAT(    " AVERAGE TEMPERATURE RISE = ",F10.3)
      WRITE(2,9)   QBAR
9      FORMAT(    " AVERAGE POWER DENSITY    = ",E12.5)
      GRA = 9.81*BETA*RHO**2*YDE**3*DELTAT
     +   /AMU / AMU
      RI = GRA/RE/RE
      BUOY = 2.*RI/FRIC
      GRRE = GRA / RE
C
      WRITE(2,60)   GRA
60    FORMAT("   GRASHOFF NUMBER = ",E12.5)
      WRITE(2,61)   RI
61      FORMAT("    RICHARDSON  NUMBER =",E12.5)
      WRITE(2,62)   GRRE
62     FORMAT("   GR / RE =    ",E12.5)
      WRITE(2,63)   BUOY
63     FORMAT("   BUOYANCY PARAMETER = ",E12.5)
C
C       TAPE98 STORES PLOTTING DATA
C
      WRITE(98,1)   RE,ETA,BUOY,PEAK,DELTAT
1       FORMAT(5E13.6)
      DO 300 L=1,M
```

```
      WRITE(98,1) (T(L,J),J=1,N)
      WRITE(98,1) (U(L,JU),JU=1,N)
300      CONTINUE
C
      RETURN
      END
      FUNCTION UR(T)
C
C     THIS FUNCTION INTERPOLATES BETWEEN TIMES TO
C     RETURN NORMALIZED VELOCITY AT TIME T
C
      COMMON /U/  TIME(40),URAT(40),NTIME
C
      ITIME = 0
      DO 100 IT = 1,NTIME
      ITIME = ITIME + 1
      IF(T.LT.TIME(IT))   GOTO 101
100       CONTINUE
101       IF(ITIME.EQ.NTIME)   GOTO 200
      UR = URAT(ITIME-1) -  ( T-TIME(ITIME-1))*(URAT(ITIME)-
     +  URAT(ITIME-1))/(TIME(ITIME-1)-TIME(ITIME))
      GOTO 210
200      UR = URAT(ITIME)
210      CONTINUE
      RETURN
C
      END
      FUNCTION POVERW(T)
C
C     THIS FUNCTION INTERPOLATES BETWEEN TIMES TO
C       RETURN POWER/FLOW RATIO AT TIME T
C
      COMMON /P/   TIM(40), PW(40),NTIM
C
      ITIME = 0
      DO 100 IT = 1,NTIM
      ITIME = ITIME + 1
      IF(T.LT.TIM(IT))   GOTO 101
100       CONTINUE
101       IF(ITIME.EQ.NTIM)   GOTO 200
      POVERW = PW(ITIME-1) - ( T-TIM(ITIME-1))*(PW(ITIME) -
     +   PW(ITIME-1))/(TIM(ITIME-1)-TIM(ITIME))
      GOTO 210
200       POVERW = PW(ITIME)
210       CONTINUE
C
      RETURN
      END
      FUNCTION AKW(TT)
C
C       THERMAL CONDUCTIVITY FOR WALL
C
      T = TT
      AKW = 9.01748 + 1.62997E-02 * T -
     +    4.80329E-06 * T * T + 2.18422E-09 * T ** 3
C
C
      RETURN
      END
      FUNCTION CON(T)
C
C       SODIUM THERMAL CONDUCTIVITY
C
      CON = 109.7 + (-6.4499E-02 + 1.1728E-05*T)
     +    * T
C
C
      RETURN
      END
      FUNCTION VISC( T )
C
C       SODIUM VISCOSITY
C
      RHS = -2.4892 + 220.65/T -.21389*ALOG(T)
      VISC = 10. ** RHS
C
C
      RETURN
      END
      FUNCTION DENS(T)
C
C       SODIUM DENSITY
C
      DENS = 1011.597 - .22051*T - 1.922243E-5*T*T +
     +   5.63769E-9*T*T*T
C
C
      RETURN
      END
      FUNCTION CAP(T)
C
C       SODIUM HEAT CAPACITY
C
      CAP = 1630.22 - .83354*T + 4.62838E-4*T*T
C
C
      RETURN
      END
      FUNCTION FRC(RE)
C
C     FRICTION FACTOR COEFFICIENT FOR 61-PIN
```

```
C            BLANKET ASSEMBLY
C
      FRC = 110. / RE
      IF(RE.LT.400.)   RETURN
      IF(RE.GT.5000.0)  GOTO 1
      PSI = (RE - 400.) / 4600.
      FRC = 110./RE*SQRT(1.-PSI) + .48/(RE**.25)*SQRT(PSI)
      RETURN
1        CONTINUE
      FRC = .48 * RE**(-.25)
C
C
      RETURN
      END
```

B.2 ALPHABETICAL DESCRIPTION OF THE ASSOCIATED SUBROUTINES

AKW: This function computes the thermal conductivity of structure.
Parameter: T Temperature, K

CAP: This function computes the Heat Capacity of Sodium.
Parameter: T Temperature, K

CON: This function computes the Thermal Conductivity of Sodium.
Parameter: T Temperature, K

DENS: This function computes Sodium Density.
Parameter: T Temperature, K

EPSILO: This subroutine computes Eddy Diffusivity of Heat.

FRC: This function computes Sodium Frictional Coefficient.
Parameter: Re Reynolds number

IN: This subroutine initializes arrays at channel inlet at each iteration.

OUTIN: This subroutine displays input data.

OUTROW: This subroutine displays results for axial slice I.
Parameter: I axial slice number

OUTST: Output subroutine for steady-state calculations.

OUTTRN: Output routine for transient calculations.

POVERW: This function interpolates between times to compute Power/Flow ratio at time t.

Parameter: T time, s

RADV: This subroutine computes the transverse velocity components from the continuity equation.

Parameter: I axial slice number

SETUP: This subroutine computes tridiagonal terms of the coefficient matrix of the energy equation for temperature calculations.

Parameter: I axial slice number

SETUPU: This subroutine computes terms of the coefficient matrix of the axial momentum equation.

Parameter: I axial slice number

SOLVEU: Matrix inverter subroutine, uses the Gauss-Jordan reduction method

Parameters:

A	augmented matrix of coefficients and R.H.S.
X	vector of results
M	leading dimension of A
N	M+1

START: This subroutine reads input data and computes constants and properties.

STST: Driver for steady-state calculations.

THRML: This subroutine drives the energy calculations for axial slice I.

Parameter: I axial slice number

TRID: Tridiagonal matrix inverter; uses the Gaussian elimination method.

Parameters:

A	vector of subdiagonal terms
B	vector of diagonal terms
C	vector of superdiagonal terms
R	R.H.S., on output, result
N	leading dimension of vectors

TRNSNT: This subroutine drives the transient calculations.

TWIST: Main driver.

Parameters defining files:

TAPE1 (input)

TAPE2 (output)

TAPE98 (storage file)

UR: This function interpolates between times to compute normalized inlet average velocity at time t.

Parameters: t time, s

VELOC: This subroutine computes axial velocities from the momentum equation.

Parameter: I axial slice number

VISC: This function computes viscosity of sodium.

Parameter: T Temperature, K

B.3 DESCRIPTION OF INPUT

Input data resides in file "TAPE1", and is organized in 12 NAMELIST groups as follows:

NAMELIST/OPTION/

JTRN - Integer variable which defines whether steady-state or transient* calculations will be performed;

- 0, steady-state
- 1, transient

NAMELIST/CONTR/

IDETAI - Integer control variable for printout

- 0, Summary printouts will be produced at end of each calculational step.
- 1, Detailed printout will be produced for each axial slice at the end of each calculational step.

NRE - total number of Reynolds numbers upon which to perform calculations (For steady-state calculations only)

IREDS - Integer control variable for flow redistribution option

- 0, flow redistribution ignored
- 1, flow redistribution included

ICOND - Integer control variable for conduction model

- 0, conduction and mixing effects ignored
- 1, conduction and mixing effects included

N - Number of radial nodes; N should be equal to N_{heated} + 2 (walls nodes) + 2 (stagnant coolant nodes) and N_{heated} must be odd number; a maximum of 39 nodes is allowed in the present version of the code.

*A steady state initialization is always performed prior to transient calculations.

NAMELIST/CONTR/	MLFGP	-	Number of axial Lower Fission Gas Plenum nodes
	MH	-	Number of axial heated nodes
	MUFGP	-	Number of axial Upper Fission Gas Plenum nodes

NOTE: The sum MLFGP + MH + MUFGP should not exceed 40 in the present version of the code.

NAMELIST/GEOM1/	XLLFGP	-	Lower Fission Gas Plenum Length, m
	XLH	-	Heated channel length, m
	XLUFGP	-	Upper Fission Gas Plenum Length, m
	YL	-	Subassembly flat-to-flat, m
NAMELIST/GEOM2/	ALAM	-	Average porosity
	ALINT	-	Porosity, interior region of the assembly
	ALEXT	-	Porosity, wall region of the assembly
NAMELIST/GEOM3/	YDE	-	Average hydraulic diameter, m
	YDINT	-	Hydraulic diameter, interior region of the assembly, m
	YDEXT	-	Hydraulic diameter, wall region of the assembly, m
NAMELIST/INITC/	Re	-	Initial Reynolds number
	TINLT	-	Inlet temperature, K
	EPSII	-	Value of ε_{∞}^{*}
	QBAR	-	Total power in the assembly, watts
	DELTAT	-	Total assembly average $\Delta\hat{T}$, K
	UBAR	-	Average inlet velocity, m/s

NOTE: Of the parameters RE and UBAR, one needs to be defined, the other should be set to 0.0, and the program will compute it; similarly for the parameters QBAR and DELTAT, where only one needs to be specified.

NAMELIST/PROP/	BETA	-	Thermal expansion coefficient, K^{-1}
NAMELIST/RADQ/	QNOR	-	Radial power distribution in each axial slice; up to 40 values allowed in the present version of the code.

NOTE: Need not be normalized; its real dimensions are QNORM(N), and the first and last two values should be equal to zero (wall and stagnant coolant nodes)

NAMELIST/TIMES/	SDMIN	-	Minimum time step, s
	SDMAX	-	Maximum time step, s
	DTPRNT	-	Printout time, s
	SEND	-	Duration of transient (t_{max}), s
NAMELIST/WALL/	XMS	-	mass of wall on either side of the subassembly, Kg
	CS	-	heat capacity of duct wall, J/(Kg·K)
	DELTAW	-	wall thickness, m
	XMCI	-	mass of stagnant coolant adjacent to the left wall, Kg
	XMCN	-	mass of stagnant coolant adjacent to the right wall, Kg

LIST/UTIME/ Transient normalized velocity forcing function

TIME, URAT - values of normalized inlet average velocity at time, TIME

NOTE: Up to 40 values are allowed in the present version of the code. First all the values of TIME are inputed, then all values of URAT. An additional input is required, equal to -1, at the end of the TIME table.

NAMELIST/PTIME/ Transient power/flow ratio forcing function

TIM, PW - values of normalized power to flow ratio at time, TIM.

NOTE: See above note.

SAMPLE INPUT FILE

Flat Radial Power Distribution for Run # 611 of the Westinghouse 61-Pin Blanket Assembly

```
$OPTION JTRN=1    $END
$CONTR  IDFTAI=0,NRE=1,ICOND=1,N=37,MLFGP=0,MH=20,MUFGP=0$END
$GEOM1  XLLFGP=0.0,XLH=1.143,XLUFGP=0.,YL=.114$END
$GEOM2  ALAM=.2567,ALINT=.2214,ALEXT=.3674$END
$GEOM3  YDE=3.7282E-03,YDINT=3.5163F-03,YDEXT=7.181E-08$END
$INITC  RE=0.,REEND=0.,TINLT=588.,EPSII=.03,QBAR=443E+03,DELTAT=0.,UBAR+
          .3363$END
$PROP   BETA=2.91E-04 $END
$RADQ   QNORM=0.,0.,1.,1.,1.,1.,1.,1.,1.,1.,1.,1.,1.,1.,1.,1.,1.,
  1.,1.,1.,1.,1.,1.,1.,1.,1.,1.,1.,1.,1.,1.,1.,1.,1.,0.,0.,0.,0.,
  0.,  $END
$TIMES  SDMIN=1.0E-05,SDMAX=1.,DTPRNT=5.,SEND=600.  $END
$WALL   XMS=6.,CS=560.,DELTAW=.381E-03,XMC1=20.,SMCN=20.  $END
$UTIME  TIMF=0.,10.,18.,21.,25.,40.,50.,70.,100.,400.,1000.,
  -1.,-1.,-1.,-1.,-1.,-1.,-1.,-1.,-1.,-1.,-1.,-1.,-1.,-1.,-1.,-1.,-1.,
  -1.,-1.,-1.,-1.,-1.,-1.,-1.,-1.,-1.,-1.,-1.,-1.,*
  URAT=1...97,.7,.54,.4,.21,.13,.065,.062,.07,.07,.07
  0.,0.,0.,0.,0.,0.,0.,0.,0.,0.,0.,0.,0.,0.,0.,0.,0.,0.,0.,0.,0.,
  0.,0.,0.,0.,0.,0.,   $END
$PTIME  TIM=0.,7.,15.,17.,19.,25.,50.,75.,75.,95.,100.,
  250.,1000.,   -1.,-1.,-1.,-1.,-1.,-1.,-1.,-1.,-1.,-1.,-1.,-1.,-1.,-1.,
  -1.,-1.,-1.,-1.,-1.,-1.,-1.,-1.,-1.,-1.,-1.,-1.,-1.,-1.,-1.,
  PW=1.,1...2,.18,.15,.1,.5,.98,1.12,1.12,1.,1.,   0.,0.,0.,0.,0.,0.,
  0.,
  0.,0.,0.,0.,0.,0.,0.,0.,0.,0.,0.,0.,0.,0.,0.,0.,0.,0.,0.,0.,0.,0.,
  $END
```

This input will produce a transient run for 600 seconds of transient time; the assembly is modeled by 37 radial and 20 axial nodes; radial power is uniform; the geometry represented is that of Westinghouse 61-pin bundle; average inlet velocity and total power are provided; both forcing functions are provided up to 1000 seconds of transient time; redistribution and conduction with ε_∞^* = .03, are both included; only summary printout will be produced.

* -1. signifies that the end of the input data trable is reached

B.4 DESCRIPTION OF OUTPUT

a) With IDETAI = 1 (Detailed Printout)

For each axial slice in calculational step the following results will be displayed:

i) Slice number, average temperature in the slice, mass flow rate in, and mass flow rate out of the slice.

ii) For each radial node j in slice i

node number j

axial velocity m/s

radial velocity m/s

temperature K

Heat flux $Q_{i,j}/\hat{Q}$

Summary printout will also be displayed at the end of calculation step.

b) With IDETAI = 0 (Summary Printout)

i) Same as a), only for exit of channel, and in addition:

ii) for steady-state calculations:

F	peak to average power
Re	Reynolds number
PEAK	temperature peaking factor
ETA	hot channel factor
TINLT	inlet temperature
DELTAT	average channel temperature rise
QBAR	average power density per axial slice
GRA	Grashof number, Gr^*
Ri	Richardson number
GRRE	$= Gr^*/Re^*$
BUOY	buoyancy parameter = 2 Ri/f

in addition, the following data is stored on file Tape 98 (for plotting purposes):

RE, ETA, BUOY, PEAK, DELTAT (5E13.6)

$T_{i,j}$, $U_{i,j}$ (i = 1, M; j = 1,N) (5E13.6)

iib) for transient calculations:

STIME, SDELT	current time and time step	s
RE	Reynolds number	
TINLT	inlet temperature	K
DTTRN	average temperature rise from inlet to exit of assembly	K
TBAR	average exit temperature	K
QBAR	average power density	watts/m^2

while on file TAPE 98 (plotting file) the following results are stored:

Time, normalized velocity, average temperature rise, normalized power and power-to-flow ratio (5E13.6)

$T_{i,j}$ (i = M; j = 1,N) (5E13.6)

c) Regardless of the value of IDETAI, all input data is displayed at the beginning of execution.

Sample Output:

```
 * * * * * * * * * * OPTIONS SELECTED  * * * * * * * * * *


TRANSIENT OPTION =      1
FLOW REDISTRIBUTION =      1
CONDUCTION =     1
DETAILED PRINTOUT =      0


* * * * * * * * * * GEOMETRIC DATA  * * * * * * * * * *


NUMBER OF RADIAL NODES =     37
NUMBER OF LFGP NODES =      0
NUMBER OF HEATED NODES =     20
NUMBER OF UFGP NODES =      0


LOWER FISSION GAS PLENUM =      0.0000   M
ASSEMBLY HEATED LENGTH =     1.1430   M
UPPER FISSION GAS PLENUM =      0.0000   M
FLAT-TO-FLAT =       .1140   M


LAMBDA AVERAGE,INTERIOR,EXTERIOR =       .2567      .2214      .3674
HYDRAULIC DIAMETER AVERAGE,INTERIOR,EXTERIOR =        .3728E-02       .3516E-02       .7181E-02   M


* * * * * * * * * * INITIAL CONDITIONS  * * * * * * * * * *


REYNOLD NUMBER =      .128681E+05
FINAL REYNOLD NUMBER =     0.
INLET TEMPERATURE =        588.000  K
OVERALL ASSEMBLY DELTAT =        101.989  K
AVERAGE POWER =      .342032E+08  WATTS
AVERAGE INLET VELOCITY =      .336400E+00  M/S


* * * * * * * * * * PROPERTIES  * * * * * * * * * *


EPSILON STAR INFINITY =      .300000E-01
BETA =      .291000E-03


* * * * * * * * * * NORMALIZED RADIAL POWER DENSITY  * * * * * * * * * *


 0.          0.          .1000E+01   .1000E+01   .1000E+01   .1000E+01   .1000E+01   .1000E+01   .1000E+01   .1000E+01
  .1000E+01   .1000E+01   .1000E+01   .1000E+01   .1000E+01   .1000E+01   .1000E+01   .1000E+01   .1000E+01   .1000E+01
  .1000E+01   .1000E+01   .1000E+01   .1000E+01   .1000E+01   .1000E+01   .1000E+01   .1000E+01   .1000E+01   .1000E+01
  .1000E+01   .1000E+01   .1000E+01   .1000E+01   .1000E+01  0.          0.


* * * * * * * * * * WALL PROPERTIES  * * * * * * * * * *


MASS OF STRUCTURE =           .316  KG PER SIDE
MASS OF SURROUNDING SODIUM =         22.000        22.000  KG AT LEFT AND RIGHT
WALL THICKNESS =       .3810E-03   M
STRUCTURE CP =        560.000  J/KG-K


* * * * * * * * * * TRANSIENT DATA  * * * * * * * * * *


FINAL TIME =         600.00  SEC
MINIMUM AND MAXIMUM TIME STEPS =       .1000E-04      .1000E+01  SEC
PRINTOUT EVERY =           5.00  SEC
```

FORCING FUNCTIONS

NORMALIZED VELOCITY VS TIME

1.0000	0.0000
.9700	10.0000
.7000	18.0000
.5400	21.0000
.4000	25.0000
.2100	40.0000
.1300	50.0000
.0650	70.0000
.0620	100.0000
.0700	400.0000
.0700	1000.0000

POWER TO FLOW RATIO VS TIME

1.0000	0.0000
1.0000	7.0000
.2000	15.0000
.1800	17.0000
.1500	19.0000
.2000	25.0000
.5000	50.0000
.9800	75.0000
1.1200	95.0000
1.1200	100.0000
1.0000	250.0000
1.0000	1000.0000

********** TIME = 0.0000 .0313
RE = .12868E+05

INLET TEMPERATURE = 588.000
AVERAGE TEMPERATURE RISE = 103.721
AVERAGE EXIT TEMPERATURE = 691.721
AVERAGE POWER DENSITY = .34203E+08

IN ROW 20 AVER TEMP = 691.7213 MASS FLOW IN = .294833E+03 MASS FLOW OUT = .286523E+03

J	1	2	3	4	5	6
U	0.	0.	.8054E+00	.6130E+00	.4413E+00	.2927E+00
V	0.	0.	.7102E-06	.1741E-05	.1564E-05	.3164E-06
T	658.000	658.000	658.000	662.857	670.143	677.784
Q	0.	0.	.2757E+00	.2757E+00	.2757E+00	.2757E+00

J	7	8	9	10	11	12
U	.2928E+00	.2929E+00	.2931E+00	.2932E+00	.2933E+00	.2933E+00
V	-.1347E-05	-.3121E-05	-.4661E-05	-.5768E-05	-.6381E-05	-.6522E-05
T	684.484	690.032	694.429	697.791	700.285	702.086
Q	.2757E+00	.2757E+00	.2757E+00	.2757E+00	.2757E+00	.2757E+00

J	13	14	15	16	17	18
U	.2934E+00	.2934E+00	.2934E+00	.2934E+00	.2934E+00	.2934E+00
V	-.6251E-05	-.5646E-05	-.4785E-05	-.3735E-05	-.2556E-05	-.1297E-05
T	703.356	704.230	704.817	705.199	705.434	705.560
Q	.2757E+00	.2757E+00	.2757E+00	.2757E+00	.2757E+00	.2757E+00

J	19	20	21	22	23	24
U	.2934E+00	.2934E+00	.2934E+00	.2934E+00	.2934E+00	.2934E+00
V	.2769E-13	.1297E-05	.2556E-05	.3735E-05	.4785E-05	.5646E-05
T	705.599	705.560	705.434	705.199	704.817	704.230
Q	.2757E+00	.2757E+00	.2757E+00	.2757E+00	.2757E+00	.2757E+00

J	25	26	27	28	29	30
U	.2934E+00	.2933E+00	.2933E+00	.2932E+00	.2931E+00	.2929E+00
V	.6251E-05	.6522E-05	.6381E-05	.5768E-05	.4661E-05	.3121E-05
T	703.356	702.086	700.285	697.791	694.429	690.032
Q	.2757E+00	.2757E+00	.2757E+00	.2757E+00	.2757E+00	.2757E+00

J	31	32	33	34	35	36
U	.2928E+00	.2927E+00	.4413E+00	.6130E+00	.8054E+00	0.
V	.1347E-05	-.3164E-06	-.1564E-05	-.1741E-05	-.7102E-06	0.
T	684.484	677.784	670.143	662.857	658.000	658.000
Q	.2757E+00	.2757E+00	.2757E+00	.2757E+00	.2757E+00	0.

J	37
U	0.
V	0.
T	658.000
Q	0.

********** TIME = 5.0000 .0156
RE = .12675E+05

INLET TEMPERATURE = 588.000
AVERAGE TEMPERATURE RISE = 103.260
AVERAGE EXIT TEMPERATURE = 691.260
AVERAGE POWER DENSITY = .33690E+08

IN ROW 20 AVER TEMP = 691.2598 MASS FLOW IN = .290411E+03 MASS FLOW OUT = .282262E+03

J	1	2	3	4	5	6
U	0.	0.	.4733E+00	.4430E+00	.3964E+00	.3274E+00
V	0.	0.	.4842E-06	.1088E-05	.6929E-06	-.6402E-06
T	658.011	658.090	658.417	663.140	670.221	677.678
Q	0.	0.	.2757E+00	.2757E+00	.2757E+00	.2757E+00

J	7	8	9	10	11	12
U	.3274E+00	.3275E+00	.3276E+00	.3276E+00	.3276E+00	.3277E+00
V	-.2643E-05	-.4994E-05	-.7084E-05	-.8601E-05	-.9435E-05	-.9603E-05
T	684.229	689.646	693.932	697.202	699.623	701.367
Q	.2757E+00	.2757E+00	.2757E+00	.2757E+00	.2757E+00	.2757E+00

J	13	14	15	16	17	18
U	.3277E+00	.3277E+00	.3277E+00	.3277E+00	.3277E+00	.3277E+00
V	-.9186E-05	-.8289E-05	-.7020E-05	-.5479E-05	-.3749E-05	-.1915

T	702.593	703.435	703.999	704.365	704.589	704.709
Q	.2757E+00	.2757E+00	.2757E+00	.2757E+00	.2757E+00	.2757E+00

J	19	20	21	22	23	24
U	.3277E+00	.3277E+00	.3277E+00	.3277E+00	.3277E+00	.3277E+00
V	.3321E-13	.1903E-05	.3749E-05	.5479E-05	.7020E-05	.8289E-05
T	704.747	704.709	704.589	704.365	703.999	703.435
Q	.2757E+00	.2757E+00	.2757E+00	.2757E+00	.2757E+00	.2757E+00

J	25	26	27	28	29	30
U	.3277E+00	.3277E+00	.3276E+00	.3276E+00	.3276E+00	.3275E+00
V	.9186E-05	.9603E-05	.9435E-05	.8601E-05	.7084E-05	.4994E-05
T	702.593	701.367	699.623	697.202	693.932	689.646
Q	.2757E+00	.2757E+00	.2757E+00	.2757E+00	.2757E+00	.2757E+00

J	31	32	33	34	35	36
U	.3274E+00	.3274E+00	.3964E+00	.4430E+00	.4733E+00	0.
V	.2643E-05	.6402E-06	-.6929E-06	-.1088E-05	-.4842E-06	0.
T	684.229	677.678	670.221	663.140	658.417	658.090
Q	.2757E+00	.2757E+00	.2757E+00	.2757E+00	.2757E+00	0.

J	37
U	0.
V	0.
T	658.011
Q	0.

********** TIME = 10.0000 .0313
RE = .12482E+05

INLET TEMPERATURE = 588.000
AVERAGE TEMPERATURE RISE = 90.472
AVERAGE EXIT TEMPERATURE = 678.472
AVERAGE POWER DENSITY = .23224E+08

IN ROW 20 AVER TEMP = 678.4716 MASS FLOW IN = .285988E+03 MASS FLOW OUT = .278961E+03

J	1	2	3	4	5	6
U	0.	0.	.5346E+00	.4782E+00	.4039E+00	.3116E+00
V	0.	0.	-.2223E-05	-.5863E-05	-.8323E-05	-.1001E-04
T	657.972	656.557	653.138	654.994	660.094	666.241
Q	0.	0.	.2757E+00	.2757E+00	.2757E+00	.2757E+00

J	7	8	9	10	11	12
U	.3117E+00	.3118E+00	.3118E+00	.3119E+00	.3119E+00	.3120E+00
V	-.1143E-04	-.1287E-04	-.1394E-04	-.1446E-04	-.1437E-04	-.1371E-04
T	671.791	676.469	680.228	683.136	685.313	686.897
Q	.2757E+00	.2757E+00	.2757E+00	.2757E+00	.2757E+00	.2757E+00

J	13	14	15	16	17	18
U	.3120E+00	.3120E+00	.3120E+00	.3120E+00	.3120E+00	.3120E+00
V	-.1255E-04	-.1099E-04	-.9117E-05	-.7016E-05	-.4758E-05	-.2402E-05
T	688.021	688.799	689.324	689.666	689.877	689.990
Q	.2757E+00	.2757E+00	.2757E+00	.2757E+00	.2757E+00	.2757E+00

J	19	20	21	22	23	24
U	.3120E+00	.3120E+00	.3120E+00	.3120E+00	.3120E+00	.3120E+00
V	.2754E-13	.2402E-05	.4758E-05	.7016E-05	.9117E-05	.1099E-04
T	690.026	689.990	689.877	689.666	689.324	688.799
Q	.2757E+00	.2757E+00	.2757E+00	.2757E+00	.2757E+00	.2757E+00

J	25	26	27	28	29	30
U	.3120E+00	.3120E+00	.3119E+00	.3119E+00	.3118E+00	.3118E+00
V	.1255E-04	.1371E-04	.1437E-04	.1446E-04	.1394E-04	.1287E-04
T	688.021	686.897	685.313	683.136	680.228	676.469
Q	.2757E+00	.2757E+00	.2757E+00	.2757E+00	.2757E+00	.2757E+00

J	31	32	33	34	35	36
U	.3117E+00	.3116E+00	.4039E+00	.4782E+00	.5346E+00	0.
V	.1143E-04	.1001E-04	.8323E-05	.5863E-05	.2223E-05	0.
T	671.791	666.241	660.094	654.994	653.138	656.557
Q	.2757E+00	.2757E+00	.2757E+00	.2757E+00	.2757E+00	0.

J	37
U	0.
V	0.
T	657.972
Q	0.

********** TIME = 560.0000 1.0000
RE = .90076E+03

INLET TEMPERATURE = 588.000
AVERAGE TEMPERATURE RISE = 97.571
AVERAGE EXIT TEMPERATURE = 685.571
AVERAGE POWER DENSITY = .23942E+07

IN ROW 20 AVER TEMP = 685.5714 MASS FLOW IN = .206383E+02 MASS FLOW OUT = .200912E+02

J	1	2	3	4	5	6
U	0.	0.	.5027E-01	.4090E-01	.2993E-01	.1829E-01
V	0.	0.	-.1338E-04	-.3505E-04	-.4632E-04	-.4918E-04
T	664.662	665.529	667.488	670.235	673.434	676.709
Q	0.	0.	.2757E+00	.2757E+00	.2757E+00	.2757E+00

J	7	8	9	10	11	12
U	.1899E-01	.1964E-01	.2022E-01	.2073E-01	.2117E-01	.2154E-01
V	-.4768E-04	-.4415E-04	-.3947E-04	-.3428E-04	-.2903E-04	-.2401E-04
T	679.753	682.529	685.018	687.213	689.120	690.749
Q	.2757E+00	.2757E+00	.2757E+00	.2757E+00	.2757E+00	.2757E+00

J	13	14	15	16	17	18
U	.2185E-01	.2210E-01	.2230E-01	.2246E-01	.2256E-01	.2263E-01
V	-.1937E-04	-.1520E-04	-.1149E-04	-.8208E-05	-.5270E-05	-.2573E-05
T	692.115	693.233	694.122	694.796	695.267	695.546
Q	.2757E+00	.2757E+00	.2757E+00	.2757E+00	.2757E+00	.2757E+00

J	19	20	21	22	23	24
U	.2265E-01	.2263E-01	.2256E-01	.2246E-01	.2230E-01	.2210E-01
V	.2468E-14	.2573E-05	.5270E-05	.8208E-05	.1149E-04	.1520E-04
T	695.639	695.546	695.267	694.796	694.122	693.233
Q	.2757E+00	.2757E+00	.2757E+00	.2757E+00	.2757E+00	.2757E+00

J	25	26	27	28	29	30
U	.2185E-01	.2154E-01	.2117E-01	.2073E-01	.2022E-01	.1964E-01
V	.1937E-04	.2401E-04	.2903E-04	.3428E-04	.3947E-04	.4415E-04
T	692.115	690.749	689.120	687.213	685.018	682.529
Q	.2757E+00	.2757E+00	.2757E+00	.2757E+00	.2757E+00	.2757E+00

J	31	32	33	34	35	36
U	.1899E-01	.1829E-01	.2993E-01	.4090E-01	.5027E-01	0.
V	.4768E-04	.4918E-04	.4632E-04	.3505E-04	.1338E-04	0.
T	679.753	676.709	673.434	670.235	667.488	665.529
Q	.2757E+00	.2757E+00	.2757E+00	.2757E+00	.2757E+00	0.

J	37
U	0.
V	0.
T	664.662
Q	0.

********** TIME = 565.0000 1.0000
RE = .90076E+03

INLET TEMPERATURE = 588.000
AVERAGE TEMPERATURE RISE = 97.601
AVERAGE EXIT TEMPERATURE = 685.601
AVERAGE POWER DENSITY = .23942E+07

IN ROW 20 AVER TEMP = 685.6006 MASS FLOW IN = .206383E+02 MASS FLOW OUT = .200911E+02

J	1	2	3	4	5	6
U	0.	0.	.5029E-01	.4091E-01	.2993E-01	.1829E-01
V	0.	0.	-.1340E-04	-.3509E-04	-.4638E-04	-.4926E-04
T	664.750	665.611	667.557	670.293	673.484	676.752
Q	0.	0.	.2757E+00	.2757E+00	.2757E+00	.2757E+00

J	7	8	9	10	11	12
U	.1899E-01	.1964E-01	.2022E-01	.2073E-01	.2116E-01	.2154E-01
V	-.4777E-04	-.4425E-04	-.3957E-04	-.3438E-04	-.2913E-04	-.2410E-04
T	679.791	682.562	685.046	687.238	689.142	690.768
Q	.2757E+00	.2757E+00	.2757E+00	.2757E+00	.2757E+00	.2757E+00

J	13	14	15	16	17	18
U	.2185E-01	.2210E-01	.2230E-01	.2245E-01	.2256E-01	.2262E-01
V	-.1946E-04	-.1527E-04	-.1155E-04	-.8256E-05	-.5302E-05	-.2 05
T	692.132	693.249	694.136	694.809	695.280	695.5
Q	.2757E+00	.2757E+00	.2757E+00	.2757E+00	.2757E+00	.2. 00

J	19	20	21	22	23	24
U	.2264E-01	.2262E-01	.2256E-01	.2245E-01	.2230E-01	.2210E-01
V	.3751E-14	.2589E-05	.5302E-05	.8256E-05	.1155E-04	.1527E-04
T	695.651	695.558	695.280	694.809	694.136	693.249
Q	.2757E+00	.2757E+00	.2757E+00	.2757E+00	.2757E+00	.2757E+00

J	25	26	27	28	29	30
U	.2185E-01	.2154E-01	.2116E-01	.2073E-01	.2022E-01	.1964E-01
V	.1946E-04	.2410E-04	.2913E-04	.3438E-04	.3957E-04	.4425E-04
T	692.132	690.768	689.142	687.238	685.046	682.562
Q	.2757E+00	.2757E+00	.2757E+00	.2757E+00	.2757E+00	.2757E+00

J	31	32	33	34	35	36
U	.1899E-01	.1829E-01	.2993E-01	.4091E-01	.5029E-01	0.
V	.4777E-04	.4926E-04	.4638E-04	.3509E-04	.1340E-04	0.
T	679.791	676.752	673.484	670.293	667.557	665.611
Q	.2757E+00	.2757E+00	.2757E+00	.2757E+00	.2757E+00	0.

J	37
U	0.
V	0.
T	664.750
Q	0.

********** TIME = 570.0000 1.0000
RE = .90076E+03

INLET TEMPERATURE = 588.000
AVERAGE TEMPERATURE RISE = 97.630
AVERAGE EXIT TEMPERATURE = 685.630
AVERAGE POWER DENSITY = .23942E+07

IN ROW 20 AVER TEMP = 685.6296 MASS FLOW IN = .206383E+02 MASS FLOW OUT = .200909E+02

J	1	2	3	4	5	6
U	0.	0.	.5032E-01	.4092E-01	.2994E-01	.1830E-01
V	0.	0.	-.1341E-04	-.3513E-04	-.4645E-04	-.4935E-04
T	664.837	665.692	667.625	670.351	673.534	676.795
Q	0.	0.	.2757E+00	.2757E+00	.2757E+00	.2757E+00

J	7	8	9	10	11	12
U	.1899E-01	.1964E-01	.2022E-01	.2072E-01	.2116E-01	.2153E-01
V	-.4786E-04	-.4435E-04	-.3967E-04	-.3449E-04	-.2923E-04	-.2419E-04
T	679.828	682.594	685.074	687.263	689.164	690.787
Q	.2757E+00	.2757E+00	.2757E+00	.2757E+00	.2757E+00	.2757E+00

J	13	14	15	16	17	18
U	.2184E-01	.2210E-01	.2230E-01	.2245E-01	.2255E-01	.2262E-01
V	-.1954E-04	-.1535E-04	-.1161E-04	-.8303E-05	-.5334E-05	-.2605E-05
T	692.149	693.264	694.150	694.822	695.292	695.570
Q	.2757E+00	.2757E+00	.2757E+00	.2757E+00	.2757E+00	.2757E+00

J	19	20	21	22	23	24
U	.2264E-01	.2262E-01	.2256E-01	.2245E-01	.2230E-01	.2210E-01
V	.2070E-14	.2605E-05	.5334E-05	.8303E-05	.1161E-04	.1535E-04
T	695.662	695.570	695.292	694.822	694.150	693.264
Q	.2757E+00	.2757E+00	.2757E+00	.2757E+00	.2757E+00	.2757E+00

J	25	26	27	28	29	30
U	.2184E-01	.2153E-01	.2116E-01	.2072E-01	.2022E-01	.1964E-01
V	.1954E-04	.2419E-04	.2923E-04	.3449E-04	.3967E-04	.4435E-04
T	692.149	690.787	689.164	687.263	685.074	682.594
Q	.2757E+00	.2757E+00	.2757E+00	.2757E+00	.2757E+00	.2757E+00

J	31	32	33	34	35	36
U	.1899E-01	.1830E-01	.2994E-01	.4092E-01	.5032E-01	0.
V	.4786E-04	.4935E-04	.4645E-04	.3513E-04	.1341E-04	0.
T	679.828	676.795	673.534	670.351	667.625	665.692
Q	.2757E+00	.2757E+00	.2757E+00	.2757E+00	.2757E+00	0.

J	37
U	0.
V	0.
T	664.837
Q	0.

********** TIME = 575.0000 1.0000
= .90076E+03

INLET TEMPERATURE = 588.000
AVERAGE TEMPERATURE RISE = 97.658
AVERAGE EXIT TEMPERATURE = 685.658

AVERAGE POWER DENSITY = .23942E+07

IN ROW 20 AVER TEMP = 685.6583 MASS FLOW IN = .206383E+02 MASS FLOW OUT = .200907E+02

J	1	2	3	4	5	6
U	0.	0.	.5034E-01	.4093E-01	.2995E-01	.1830E-01
V	0.	0.	-.1342E-04	-.3517E-04	-.4651E-04	-.4943E-04
T	664.923	665.772	667.692	670.408	673.583	676.838
Q	0.	0.	.2757E+00	.2757E+00	.2757E+00	.2757E+00

J	7	8	9	10	11	12
U	.1899E-01	.1964E-01	.2022E-01	.2072E-01	.2116E-01	.2153E-01
V	-.4796E-04	-.4445E-04	-.3978E-04	-.3459E-04	-.2933E-04	-.2429E-04
T	679.865	682.626	685.102	687.287	689.185	690.806
Q	.2757E+00	.2757E+00	.2757E+00	.2757E+00	.2757E+00	.2757E+00

J	13	14	15	16	17	18
U	.2184E-01	.2209E-01	.2229E-01	.2244E-01	.2255E-01	.2261E-01
V	-.1963E-04	-.1542E-04	-.1168E-04	-.8351E-05	-.5366E-05	-.2622E-05
T	692.165	693.279	694.164	694.835	695.304	695.582
Q	.2757E+00	.2757E+00	.2757E+00	.2757E+00	.2757E+00	.2757E+00

J	19	20	21	22	23	24
U	.2263E-01	.2261E-01	.2255E-01	.2244E-01	.2229E-01	.2209E-01
V	.3958E-14	.2622E-05	.5366E-05	.8351E-05	.1168E-04	.1542E-04
T	695.674	695.582	695.304	694.835	694.164	693.279
Q	.2757E+00	.2757E+00	.2757E+00	.2757E+00	.2757E+00	.2757E+00

J	25	26	27	28	29	30
U	.2184E-01	.2153E-01	.2116E-01	.2072E-01	.2022E-01	.1964E-01
V	.1963E-04	.2429E-04	.2933E-04	.3459E-04	.3978E-04	.4445E-04
T	692.165	690.806	689.185	687.287	685.102	682.626
Q	.2757E+00	.2757E+00	.2757E+00	.2757E+00	.2757E+00	.2757E+00

J	31	32	33	34	35	36
U	.1899E-01	.1830E-01	.2995E-01	.4093E-01	.5034E-01	0.
V	.4796E-04	.4943E-04	.4651E-04	.3517E-04	.1342E-04	0.
T	679.865	676.838	673.583	670.408	667.692	665.772
Q	.2757E+00	.2757E+00	.2757E+00	.2757E+00	.2757E+00	0.

J	37
U	0.
V	0.
T	664.923
Q	0.

********** TIME = 580.0000 1.0000
RE = .90076E+03

INLET TEMPERATURE = 588.000
AVERAGE TEMPERATURE RISE = 97.687
AVERAGE EXIT TEMPERATURE = 685.687
AVERAGE POWER DENSITY = .23942E+07

IN ROW 20 AVER TEMP = 685.6867 MASS FLOW IN = .206383E+02 MASS FLOW OUT = .200906E+02

J	1	2	3	4	5	6
U	0.	0.	.5036E-01	.4094E-01	.2995E-01	.1830E-01
V	0.	0.	-.1343E-04	-.3521E-04	-.4658E-04	-.4951E-04
T	665.009	665.853	667.759	670.465	673.632	676.880
Q	0.	0.	.2757E+00	.2757E+00	.2757E+00	.2757E+00

J	7	8	9	10	11	12
U	.1899E-01	.1964E-01	.2021E-01	.2072E-01	.2116E-01	.2153E-01
V	-.4805E-04	-.4455E-04	-.3988E-04	-.3469E-04	-.2943E-04	-.2438E-04
T	679.902	682.658	685.130	687.311	689.206	690.825
Q	.2757E+00	.2757E+00	.2757E+00	.2757E+00	.2757E+00	.2757E+00

J	13	14	15	16	17	18
U	.2183E-01	.2209E-01	.2229E-01	.2244E-01	.2254E-01	.2261E-01
V	-.1971E-04	-.1550E-04	-.1174E-04	-.8399E-05	-.5399E-05	-.2638E-05
T	692.182	693.294	694.178	694.848	695.316	695.594
Q	.2757E+00	.2757E+00	.2757E+00	.2757E+00	.2757E+00	.2757E+00

J	19	20	21	22	23	24
U	.2263E-01	.2261E-01	.2254E-01	.2244E-01	.2229E-01	.2209E-01
V	.4107E-14	.2638E-05	.5399E-05	.8399E-05	.1174E-04	.1550E-04
T	695.686	695.594	695.316	694.848	694.178	693.294
Q	.2757E+00	.2757E+00	.2757E+00	.2757E+00	.2757E+00	.2757E+00

J	25	26	27	28	29	30
U	.2183E-01	.2153E-01	.2116E-01	.2072E-01	.2021E-01	.1964E-01

V	.1971E-04	.2438E-04	.2943E-04	.3469E-04	.3988E-04	.4455E-04
T	692.182	690.825	689.206	687.311	685.130	682.658
Q	.2757E+00	.2757E+00	.2757E+00	.2757E+00	.2757E+00	.2757E+00

J	31	32	33	34	35	36
U	.1899E-01	.1830E-01	.2995E-01	.4094E-01	.5036E-01	0.
V	.4805E-04	.4951E-04	.4658E-04	.3521E-04	.1343E-04	0.
T	679.902	676.880	673.632	670.465	667.759	665.853
Q	.2757E+00	.2757E+00	.2757E+00	.2757E+00	.2757E+00	0.

J	37
U	0.
V	0.
T	665.009
Q	0.

********** TIME = 585.0000 1.0000
RE = .90076E+03

INLET TEMPERATURE = 588.000
AVERAGE TEMPERATURE RISE = 97.715
AVERAGE EXIT TEMPERATURE = 685.715
AVERAGE POWER DENSITY = .23942E+07

IN ROW 20 AVER TEMP = 685.7149 MASS FLOW IN = .206383E+02 MASS FLOW OUT = .200904E+02

J	1	2	3	4	5	6
U	0.	0.	.5039E-01	.4096E-01	.2996E-01	.1830E-01
V	0.	0.	-.1344E-04	-.3525E-04	-.4664E-04	-.4960E-04
T	665.095	665.932	667.826	670.521	673.680	676.922
Q	0.	0.	.2757E+00	.2757E+00	.2757E+00	.2757E+00

J	7	8	9	10	11	12
U	.1899E-01	.1964E-01	.2021E-01	.2072E-01	.2115E-01	.2152E-01
V	-.4814E-04	-.4465E-04	-.3999E-04	-.3480E-04	-.2953E-04	-.2448E-04
T	679.938	682.689	685.157	687.335	689.227	690.843
Q	.2757E+00	.2757E+00	.2757E+00	.2757E+00	.2757E+00	.2757E+00

J	13	14	15	16	17	18
U	.2183E-01	.2208E-01	.2228E-01	.2243E-01	.2254E-01	.2260E-01
V	-.1980E-04	-.1557E-04	-.1180E-04	-.8447E-05	-.5431E-05	-.2654E-05
T	692.198	693.309	694.191	694.860	695.328	695.605
Q	.2757E+00	.2757E+00	.2757E+00	.2757E+00	.2757E+00	.2757E+00

J	19	20	21	22	23	24
U	.2262E-01	.2260E-01	.2254E-01	.2243E-01	.2228E-01	.2208E-01
V	.4610E-14	.2654E-05	.5431E-05	.8447E-05	.1180E-04	.1557E-04
T	695.697	695.605	695.328	694.860	694.191	693.309
Q	.2757E+00	.2757E+00	.2757E+00	.2757E+00	.2757E+00	.2757E+00

J	25	26	27	28	29	30
U	.2183E-01	.2152E-01	.2115E-01	.2072E-01	.2021E-01	.1964E-01
V	.1980E-04	.2448E-04	.2953E-04	.3480E-04	.3999E-04	.4465E-04
T	692.198	690.843	689.227	687.335	685.157	682.689
Q	.2757E+00	.2757E+00	.2757E+00	.2757E+00	.2757E+00	.2757E+00

J	31	32	33	34	35	36
U	.1899E-01	.1830E-01	.2996E-01	.4096E-01	.5039E-01	0.
V	.4814E-04	.4960E-04	.4664E-04	.3525E-04	.1344E-04	0.
T	679.938	676.922	673.680	670.521	667.826	665.932
Q	.2757E+00	.2757E+00	.2757E+00	.2757E+00	.2757E+00	0.

J	37
U	0.
V	0.
T	665.095
Q	0.

********** TIME = 590.0000 1.0000
RE = .90076E+03

INLET TEMPERATURE = 588.000
AVERAGE TEMPERATURE RISE = 97.743
AVERAGE EXIT TEMPERATURE = 685.743
AVERAGE POWER DENSITY = .23942E+07

IN 20 AVER TEMP = 685.7428 MASS FLOW IN = .206383E+02 MASS FLOW OUT = .200903E+02

J	1	2	3	4	5	6
U	0.	0.	.5041E-01	.4097E-01	.2996E-01	.1831E-01
V	0.	0.	-.1346E-04	-.3529E-04	-.4671E-04	-.4968E-04

T	665.180	666.011	667.892	670.577	673.728	676.964
Q	0.	0.	.2757E+00	.2757E+00	.2757E+00	.2757E+00

J	7	8	9	10	11	12
U	.1899E-01	.1964E-01	.2021E-01	.2072E-01	.2115E-01	.2 -01
V	-.4824E-04	-.4475E-04	-.4009E-04	-.3490E-04	-.2963E-04	-. 04
T	679.974	682.721	685.184	687.359	689.247	690.8[illegible]
Q	.2757E+00	.2757E+00	.2757E+00	.2757E+00	.2757E+00	.2757E+00

J	13	14	15	16	17	18
U	.2183E-01	.2208E-01	.2228E-01	.2243E-01	.2253E-01	.2260E-01
V	-.1989E-04	-.1565E-04	-.1186E-04	-.8494E-05	-.5464E-05	-.2671E-05
T	692.214	693.323	694.205	694.873	695.340	695.617
Q	.2757E+00	.2757E+00	.2757E+00	.2757E+00	.2757E+00	.2757E+00

J	19	20	21	22	23	24
U	.2262E-01	.2260E-01	.2253E-01	.2243E-01	.2228E-01	.2208E-01
V	.2629E-14	.2671E-05	.5464E-05	.8494E-05	.1186E-04	.1565E-04
T	695.708	695.617	695.340	694.873	694.205	693.323
Q	.2757E+00	.2757E+00	.2757E+00	.2757E+00	.2757E+00	.2757E+00

J	25	26	27	28	29	30
U	.2183E-01	.2152E-01	.2115E-01	.2072E-01	.2021E-01	.1964E-01
V	.1989E-04	.2457E-04	.2963E-04	.3490E-04	.4009E-04	.4475E-04
T	692.214	690.861	689.247	687.359	685.184	682.721
Q	.2757E+00	.2757E+00	.2757E+00	.2757E+00	.2757E+00	.2757E+00

J	31	32	33	34	35	36
U	.1899E-01	.1831E-01	.2996E-01	.4097E-01	.5041E-01	0.
V	.4824E-04	.4988E-04	.4671E-04	.3529E-04	.1346E-04	0.
T	679.974	676.964	673.728	670.577	667.892	666.011
Q	.2757E+00	.2757E+00	.2757E+00	.2757E+00	.2757E+00	0.

J	37
U	0.
V	0.
T	665.180
Q	0.

********** TIME = 595.0000 1.0000
RE = .90076E+03

INLET TEMPERATURE = 588.000
AVERAGE TEMPERATURE RISE = 97.770
AVERAGE EXIT TEMPERATURE = 685.770
AVERAGE POWER DENSITY = .23942E+07

IN ROW 20 AVER TEMP = 685.7704 MASS FLOW IN = .206383E+02 MASS FLOW OUT = .200901E+02

J	1	2	3	4	5	6
U	0.	0.	.5043E-01	.4098E-01	.2997E-01	.1831E-01
V	0.	0.	-.1347E-04	-.3533E-04	-.4678E-04	-.4977E-04
T	665.264	666.089	667.957	670.632	673.775	677.005
Q	0.	0.	.2757E+00	.2757E+00	.2757E+00	.2757E+00

J	7	8	9	10	11	12
U	.1899E-01	.1964E-01	.2021E-01	.2071E-01	.2115E-01	.2152E-01
V	-.4834E-04	-.4486E-04	-.4020E-04	-.3501E-04	-.2974E-04	-.2467E-04
T	680.009	682.751	685.211	687.382	689.268	690.879
Q	.2757E+00	.2757E+00	.2757E+00	.2757E+00	.2757E+00	.2757E+00

J	13	14	15	16	17	18
U	.2182E-01	.2207E-01	.2227E-01	.2242E-01	.2253E-01	.2259E-01
V	-.1997E-04	-.1572E-04	-.1193E-04	-.8543E-05	-.5497E-05	-.2687E-05
T	692.230	693.338	694.218	694.885	695.352	695.628
Q	.2757E+00	.2757E+00	.2757E+00	.2757E+00	.2757E+00	.2757E+00

J	19	20	21	22	23	24
U	.2261E-01	.2259E-01	.2253E-01	.2242E-01	.2227E-01	.2207E-01
V	.4439E-14	.2687E-05	.5497E-05	.8543E-05	.1193E-04	.1572E-04
T	695.720	695.628	695.352	694.885	694.218	693.338
Q	.2757E+00	.2757E+00	.2757E+00	.2757E+00	.2757E+00	.2757E+00

J	25	26	27	28	29	30
U	.2182E-01	.2152E-01	.2115E-01	.2071E-01	.2021E-01	.1964E-01
V	.1997E-04	.2467E-04	.2974E-04	.3501E-04	.4020E-04	.4486E-04
T	692.230	690.879	689.268	687.382	685.211	682.751
Q	.2757E+00	.2757E+00	.2757E+00	.2757E+00	.2757E+00	.2757E+00

J	31	32	33	34	35	36
U	.1899E-01	.1831E-01	.2997E-01	.4098E-01	.5043E-01	0.
V	.4834E-04	.4977E-04	.4678E-04	.3533E-04	.1347E-04	0.
T	680.009	677.005	673.775	670.632	667.957	666.089
Q	.2757E+00	.2757E+00	.2757E+00	.2757E+00	.2757E+00	0.

J	37
U	0.
V	0.
T	665.264
Q	0.

********** TIME = 600.0000 1.0000
RE = .90076E+03

INLET TEMPERATURE = 588.000
AVERAGE TEMPERATURE RISE = 97.798
AVERAGE EXIT TEMPERATURE = 685.798
AVERAGE POWER DENSITY = .23942E+07

IN ROW 20 AVER TEMP = 685.7978 MASS FLOW IN = .206383E+02 MASS FLOW OUT = .200900E+02

J	1	2	3	4	5	6
U	0.	0.	.5045E-01	.4099E-01	.2998E-01	.1831E-01
V	0.	0.	-.1348E-04	-.3537E-04	-.4685E-04	-.4985E-04
T	665.348	666.167	668.022	670.686	673.822	677.045
Q	0.	0.	.2757E+00	.2757E+00	.2757E+00	.2757E+00

J	7	8	9	10	11	12
U	.1899E-01	.1964E-01	.2021E-01	.2071E-01	.2114E-01	.2151E-01
V	-.4843E-04	-.4496E-04	-.4030E-04	-.3511E-04	-.2984E-04	-.2476E-04
T	680.045	682.782	685.237	687.405	689.288	690.897
Q	.2757E+00	.2757E+00	.2757E+00	.2757E+00	.2757E+00	.2757E+00

J	13	14	15	16	17	18
U	.2182E-01	.2207E-01	.2227E-01	.2242E-01	.2252E-01	.2259E-01
V	-.2006E-04	-.1580E-04	-.1199E-04	-.8591E-05	-.5529E-05	-.2704E-05
T	692.246	693.352	694.231	694.897	695.363	695.639
Q	.2757E+00	.2757E+00	.2757E+00	.2757E+00	.2757E+00	.2757E+00

J	19	20	21	22	23	24
U	.2261E-01	.2259E-01	.2252E-01	.2242E-01	.2227E-01	.2207E-01
V	.3256E-14	.2704E-05	.5529E-05	.8591E-05	.1199E-04	.1580E-04
T	695.731	695.639	695.363	694.897	694.231	693.352
Q	.2757E+00	.2757E+00	.2757E+00	.2757E+00	.2757E+00	.2757E+00

J	25	26	27	28	29	30
U	.2182E-01	.2151E-01	.2114E-01	.2071E-01	.2021E-01	.1964E-01
V	.2006E-04	.2476E-04	.2984E-04	.3511E-04	.4030E-04	.4496E-04
T	692.246	690.897	689.288	687.405	685.237	682.782
Q	.2757E+00	.2757E+00	.2757E+00	.2757E+00	.2757E+00	.2757E+00

J	31	32	33	34	35	36
U	.1899E-01	.1831E-01	.2998E-01	.4099E-01	.5045E-01	0.
V	.4843E-04	.4985E-04	.4685E-04	.3537E-04	.1348E-04	0.
T	680.045	677.045	673.822	670.686	668.022	666.167
Q	.2757E+00	.2757E+00	.2757E+00	.2757E+00	.2757E+00	0.

J	37
U	0.
V	0.
T	665.348
Q	0.

```
B N L   SCOPE 2.1.5  512AR                          02/06/84       84037

SYS DEVICES 844/15/PF FLS=200K FLL=1747K MXS=160K MXL=1321K MXB=1321B

HH.MM.SS CPU SECOND ORIGIN
          10.19.41.MFB. QL    NOS/BE 1.4 MFB 518CK 02/06/84
10.33.13 00000.004 MFZ.      -ERIK,STMFZ,T477.
10.33.13 00000.005 JOB.      -ACCOUNT,EGC,1530,*.:
10.33.17 00000.026 JOB.      -ATTACH,P,TWODNEW,ID=EGC,ST=MFB.
10.33.17 00000.027 JOB.      -FILE,P,RT=Z,FL=80.
10.33.17 00000.028 JOB.      -ATTACH,TAPE1,FLATDISTRIB,ID=EGC,ST=STP.
10.33.17 00000.029 JOB.      -FILE,TAPE1,RT=Z,FL=80.
10.33.17 00000.030 LOD.      -FTN,I=P,R=3.
10.33.18 00000.038 MFZ.        JM262 - STAGE PF ST=MFB LFN=P
          10.33.33 MFB.       10.31.30.Z0005RJ    02/06/84
          10.33.33 MFB.       10.31.31.-SP- ATTACHING  PFN=TWODNEW
          10.33.33 MFB.       10.31.35.AT CY= 035 SN=SHARE
          10.33.33 MFB.       10.31.38.NO. WORDS=      11424  NO. OF EOR =      0
          10.33.34 MFB.        JM511 - WORDS  READ-        26240B
10.36.19 00002.912 USR.          2.879 CP SECONDS COMPILATION TIME
10.36.19 00002.912 LOD.      -LGO,PL=77777.
10.36.20 00003.113 MFZ.        LD610 - FLS REQUIRED TO LOAD - 0015624 OU.COG
10.36.20 00003.114 MFZ.        LD603 - EXECUTION INITIATED OS.EXP
10.36.20 00003.114 USR.       FORTRAN LIBRARY 552           05/02/83
10.36.20 00003.118 MFZ.        JM262 - STAGE PF ST=STP LFN=TAPE1
          10.36.29 MFA.       10.34.34.Z00055G    02/06/84
          10.36.29 MFA.       10.34.34.-SP- ATTACHING  PFN=FLATDISTRIB
          10.36.30 MFA.       10.34.34.AT CY= 010 SN=SHARE
          10.36.30 MFA.       10.34.35.NO. WORDS=        149  NO. OF EOR =      0
          10.36.31 STP.        JM511 - WORDS  READ-          225B
10.43.32 00161.407 USR.          STOP
10.43.32 00161.407 USR.          043000   FINAL EXECUTION FL.
10.43.32 00161.407 USR.        158.292 CP SECONDS EXECUTION TIME.
10.43.32 00161.409 MFZ.        JM166 - MAXIMUM USER SCM          47000B WORDS
10.43.32 00161.409 MFZ.        JM167 - MAXIMUM USER LCM              0B WORDS
10.43.32 00161.410 MFZ.        JM170 - MAXIMUM JS+IO LCM           110B BUFFERS
10.43.32 00161.410 MFZ.        RM770 - MAXIMUM ACTIVE FILES                      5
10.43.32 00161.410 MFZ.        RM771 - OPEN/CLOSE CALLS                         26
10.43.32 00161.410 MFZ.        RM772 - DATA TRANSFER CALLS                  42,217
10.43.32 00161.410 MFZ.        RM773 - CONTROL/POSITIONING CALLS               150
10.43.32 00161.410 MFZ.        RM774 - BM DATA TRANSFER CALLS                2,865
10.43.32 00161.410 MFZ.        RM775 - BM CONTROL/POSITIONING CALLS            227
10.43.32 00161.411 MFZ.        RM776 - QUEUE MANAGER CALLS                     528
10.43.32 00161.411 MFZ.        RM777 - RECALL CALLS                            437
10.43.32 00161.411 MFZ.        SCM               3 019.224  KWS
10.43.32 00161.411 MFZ.        I/O                   0.266  MW
10.43.32 00161.412 MFZ.        RMS                  27.073  MWS
10.43.32 00161.412 MFZ.        USER                157.465  SEC
10.43.32 00161.412 MFZ.        JOB                 161.414  SEC
10.43.32 00161.412 MFZ.        DIO               1 605.577  KW
10.43.32 00161.412 MFZ.        SIO                  11.573  KW
10.43.32 00161.412 MFZ.        RU                  348.351
10.43.32 00161.413 MFZ.        BNL CCUS             11.950
10.43.32 00161.413 MFZ.        SC050 - 007420 SC/LC SWAPS
10.43.32 00161.413 MFZ.        EJ  END OF JOB  -  PN001530
```

B.5 CODE LIMITATIONS

1. The present version of the code limits the total number of axial and radial nodes to 40 each; if a larger number of nodes is desired in the analysis, all arrays of the form $X(M_{axial}, N_{radial})$ and $Y(N_{radial})$ should be properly redimensioned, bearing in mind that the number of radial nodes, for computational reasons, should be odd in input.

2. Due to the presence of discontinuity in the slope of the friction factor vs. Re for blanket assemblies, inaccuracies in computed velocities may be present in the vicinity of $4500 < Re \leq 5500$.

3. Flow-reversal in channel has not been considered; hence, if axial velocity becomes negative, a message is printed to this effect, giving time and position of occurrence, and axial velocity is reset to $10^{-5} \times \hat{U}$; a similar message is displayed when velocity recovers to positive values.

4. There is no restart capability at present.

5. Axial power distribution is in the shape of a chopped cosine, with peak to average value at 1.4 while the upper and lower fission gas plena have no heat fluxes associated with them.

6. At present, friction factors for radial blankets are included as default, for fuel assembly calculations appropriate friction factors must be provided.

7. Porosity and hydraulic diameters are assigned as follows:

radial node number	j = 1,2,3; and N,N-1,N-2	are External
	$6 \leq j \leq N-5$	are Internal
	others	linearly interpolate

8. The number of radial nodes, N, must be greater or equal to 11 (N must be an odd number).

NRC FORM 335 (11 81)

U.S. NUCLEAR REGULATORY COMMISSION

BIBLIOGRAPHIC DATA SHEET

1. REPORT NUMBER (Assigned by DDC)
NUREG/CR-3498
BNL-NUREG-51713

4. TITLE AND SUBTITLE (Add Volume No., if appropriate)
Two-Dimensional Modeling of Intra-Subassembly Heat Transfer and Buoyancy-Induced Flow Redistribution in LMFBRs

2. (Leave blank)

3. RECIPIENT'S ACCESSION NO.

7. AUTHOR(S)
Mohsen Khatib-Rahbar and Erik G. Cazzoli

5. DATE REPORT COMPLETED
MONTH: May YEAR: 1984

9. PERFORMING ORGANIZATION NAME AND MAILING ADDRESS (Include Zip Code)
Department of Nuclear Energy
Brookhaven National Laboratory
Upton, Long Island, New York 11973

DATE REPORT ISSUED
MONTH YEAR

6. (Leave blank)

8. (Leave blank)

12. SPONSORING ORGANIZATION NAME AND MAILING ADDRESS (Include Zip Code)
Division of Accident Evaluation
Office of Nuclear Regulatory Research
U.S. Nuclear Regulatory Commission
Washington, D.C. 20555

10. PROJECT/TASK/WORK UNIT NO.

11. FIN NO.
A-3015

13. TYPE OF REPORT
Technical Report

PERIOD COVERED (Inclusive dates)

15. SUPPLEMENTARY NOTES

14. (Leave blank)

16. ABSTRACT (200 words or less)

Phenomenological models and numerical techniques for prediction of coolant flow and temperature fields during forced, mixed, and free convection regimes of operation in LMFBR subassemblies are addressed. It is shown that, simplified integral solutions provide an excellent approach to assessing the importance of the intra-subassembly buoyancy induced flow redistribution, and the transverse thermal conduction and mixing effects on the assembly wide peak coolant temperatures. Furthermore, a more detailed steady-state and transient parabolic two-dimensional porous-body model, resulting in the TWIST computer code is developed. Comparison of calculated results and out-of-pile sodium and water test data indicate generally good agreement in cross-assembly temperature profiles. However, the impact of fuel pin distortion and bowing, caused by large transverse power gradients on transverse temperature distributions are found to be significant.

17. KEY WORDS AND DOCUMENT ANALYSIS

17a. DESCRIPTORS

LMFBR
TWIST Code
Heat Transfer
Forced, Mixed and Free Convection
Flow Redistribution, Conduction and Turbulent Mixing
Experimental Data

17b. IDENTIFIERS/OPEN-ENDED TERMS

18. AVAILABILITY STATEMENT
UNLIMITED

19. SECURITY CLASS (This report)
unclassified

20. SECURITY CLASS (This page)
unclassified

21. NO. OF PAGES

22. PRICE
$

NRC FORM 335 (11 81)